

UNIVERSIDAD AUTÓNOMA DE MADRID
DEPARTMENT OF MOLECULAR BIOLOGY
FACULTY OF SCIENCE



The role of PTEN in synaptic and cognitive function and in social behavior.

Cristina Sánchez-Puelles Peñaranda

Madrid, 2017



FACULTAD DE
CIENCIAS
UNIVERSIDAD AUTÓNOMA DE MADRID

**UNIVERSIDAD AUTÓNOMA DE MADRID
MOLECULAR BIOLOGY DEPARTMENT
FACULTY OF SCIENCE**

The role of PTEN in synaptic and cognitive function and in social behavior.

Doctoral thesis submitted to the Universidad Autónoma de Madrid for the degree of Doctor of Philosophy by M.Sci. in Molecular Biosciences.

Cristina Sánchez-Puelles

Thesis Directors:
Dr. Shira Knafo
Dr. José A. Esteban

Thesis Tutor:
Dr. Javier Díez-Guerra

Centro de Biología Molecular “Severo Ochoa” (CBMSO – UAM/CSIC)



La realización de esta tesis doctoral ha sido posible gracias a la concesión de una ayuda predoctoral de formación de personal investigador (Subprograma de Formación de Personal Investigador, convocatoria 2011) del extinto Ministerio de Ciencia e Innovación, ahora Ministerio de Economía y Competitividad (Ayuda BES-2011-043464, Proyecto SAF2010-15676). El desarrollo de esta tesis ha tenido lugar en laboratorio del Doctor José A. Esteban García, bajo su dirección y de la Dra. Shira Knafo, en el Centro de Biología Molecular “Severo Ochoa”, centro mixto de la Universidad Autónoma de Madrid y del Consejo Superior de Investigaciones Científicas (CBMSO – UAM/CSIC).

"Not explaining science seems to me perverse. When you're in love, you want to tell the world."

— Carl Sagan.

Here you have my lifelong love affair with science.

Y como tal aquí os la describo, bienvenidos a mi tesis. Prestad atención, pues no habrá bises ni segundas partes. Espero que disfrutéis de ella como yo lo he hecho, pues la intensidad con la que la he vivido merece que así la describa, como una historia de amor: con lágrimas y carcajadas entremezcladas durante años. Pues la ciencia es un sentimiento que, como el arte, nace en lo más profundo.

A vosotros, mi familia, tanto la de sangre como la elegida.

Agradecimientos

En primer lugar, me gustaría expresar mi agradecimiento a mis directores de tesis, Shira y José, por darme la oportunidad de desarrollar este trabajo. Gracias por haberme aportado las ideas y las herramientas necesarias para esta tesis, formándome profesionalmente de cara al futuro. Como no puede ser de otra manera, debo agradecer también a mi director ficticio, César, su dedicación a este proyecto y su inestimable ayuda. En segundo lugar, agradecer la ayuda y los materiales brindados por los diferentes colaboradores, gracias a los cuales ha sido posible realizar un trabajo tan completo. Gracias a los doctores Manuel Serrano, Andrew Chan, Rafael Luján, Jesús Cortés, Yann Humeau y Miguel López Pérez.

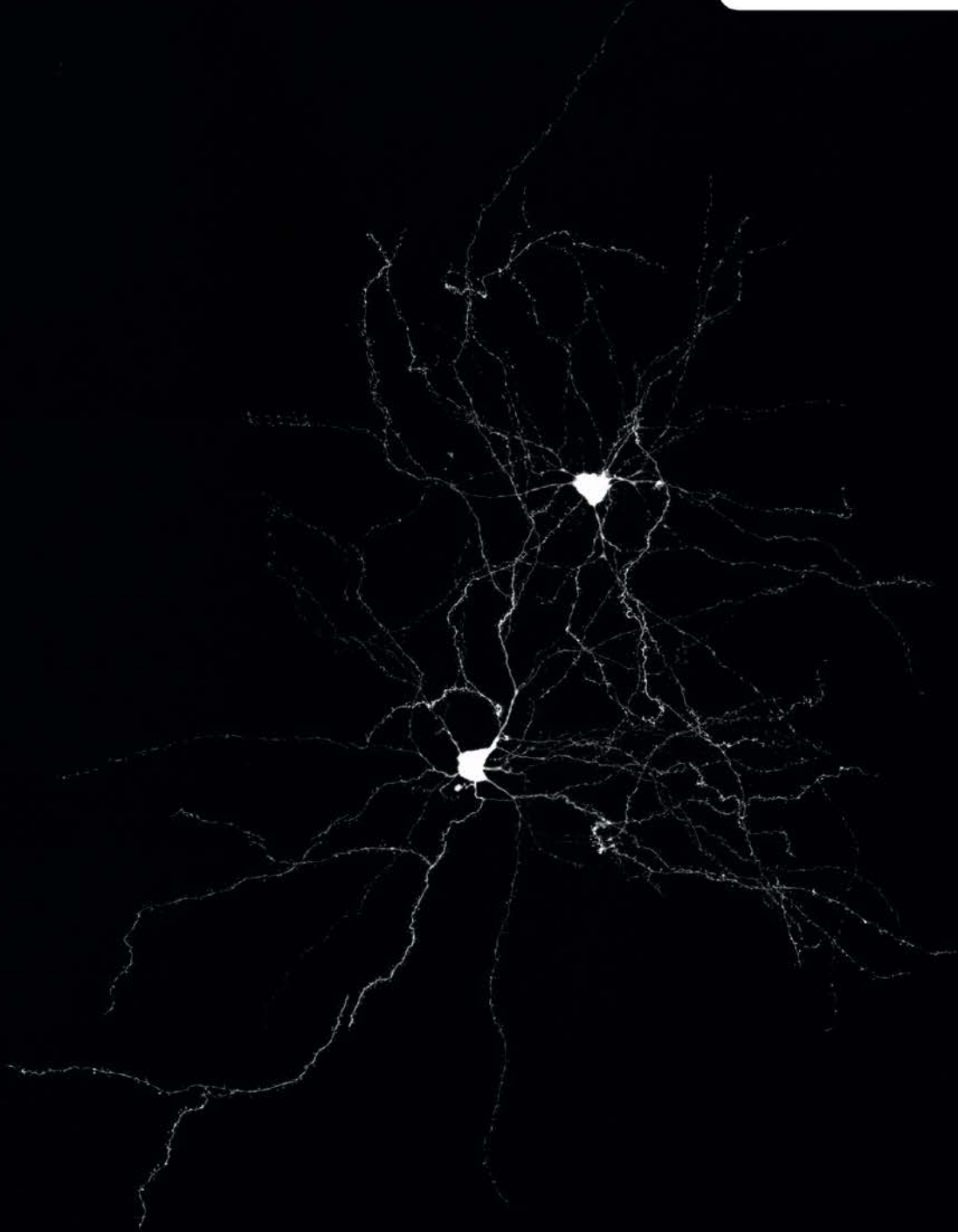
Gracias, muchas gracias a mis labos, sí, en plural, han sido varios y todos buenos. He tenido el estebanlab antiguo y el nuevo, con gente que me ha ayudado mucho y de los cuales me llevo muy buenas amigas; el de la UNED (que a su vez son dos) donde he encontrado grandes personas y un gran apoyo; y a los vasquitos, que aunque hemos compartido pocos momentos han sido muy buenos.


Y por último, pero no por ello menos importante, a todas las personas que a nivel personal han estado a mi lado durante estos años, que por suerte no son pocas, soy muy afortunada de teneros.

Siento no ser más explícita, esto no es lo mío, pero sabéis que os quiero y os lo agradeceré personalmente cada día.

GRACIAS

Abstract





The establishment of functional brain circuits depends on the correct formation of synaptic connections among neurons, followed by an intense activity-dependent remodeling during postnatal development and adulthood. This process, known as synaptic plasticity, is highly regulated by phosphatidylinositol-3 kinase (PI3K) pathway, which also regulates cell growth, proliferation and cell survival. PTEN (*phosphatase and tensin homologue deleted on chromosome 10*) is a negative regulator of this pathway and is highly expressed in brain, where it controls synaptogenesis and synaptic plasticity. PTEN activity is required for NMDA receptor-dependent long-term depression (LTD), and its anchoring to the postsynaptic terminal requires the C-terminal PDZ binding motif of PTEN.

PTEN has been linked to Autism Spectrum Disorders (ASD), since mutations in this gene are associated with a form of autism that is accompanied by macrocephaly (PTEN-ASD). These patients show poorly developed communication skills, altered social behavior, stereotypic movements and higher anxiety. The neuronal control of these complex behaviors is still being elucidated, and appears to involve multiple brain regions, such as the amygdala and the hippocampus. Thus, in this work I have evaluated the role of PTEN in these brain areas and its implication in synaptic plasticity, cognitive processes and social behavior.

To explore the importance of PTEN for synaptic organization and cognitive function, I have employed two transgenic mice. *Pten^{tg}*, presenting moderate overexpression of PTEN, and *PTEN-ΔPDZ*, in which PTEN lacks the last four amino acids, therefore removing the PDZ binding motif. I found that *Pten^{tg}* mice present microcephaly, with reduced hippocampal volume and neuron number. These parameters are normal in the lateral amygdala (LA), although LA neurons display reduced dendritic complexity and spine density. Ultrastructure analysis revealed decreased synapse density in both brain regions and reduced PSD length in the LA. Conversely, *PTEN-ΔPDZ* mice present macrocephaly, similar to the phenotype found in patients with PTEN-ASD, suggesting a bidirectional modulation of brain anatomy by PTEN in a region- and PDZ-dependent manner.

These anatomical changes were correlated with alterations in synaptic function using electrophysiological recordings. Thus *Pten^{tg}* mice present depressed excitatory basal synaptic transmission in the hippocampus and in the thalamic input to the LA, impaired long-term potentiation (LTP) in the hippocampus and in the cortical input to the LA and enhanced long-term depression (LTD) in the cortical input to the LA. On the other hand, *PTEN-ΔPDZ* mice present normal basal synaptic transmission and deficient LTD in the hippocampus and the cortical input to the LA. These findings revealed an input-specific modulation of synaptic plasticity by PTEN and its implication in hippocampal and cortico-LA pathway LTD in a PDZ-dependent manner.

To further study whether these synaptic alterations have an impact on behavior, I carried out several tests related to hippocampal and LA function, as well as those behaviors related to ASD. *Pten^{tg}* mice present impaired spatial and fear memory, which could be related to alterations in LTP in the hippocampus and the LA, respectively. With respect to ASD related behaviors, impaired communication skills, normal stereotyped behavior, decreased anxiety and prosocial behavior were found in *Pten^{tg}* mice. Conversely, *PTEN-ΔPDZ* mice present normal communication skills, normal anxiety-like behavior and impaired social behavior. Thus, PTEN is involved in the modulation of several behaviors, but only social behavior seems to require PTEN PDZ interactions. These findings suggest a relationship between a specific form of synaptic plasticity in the cortical input to the LA and social behaviour under PTEN regulation.



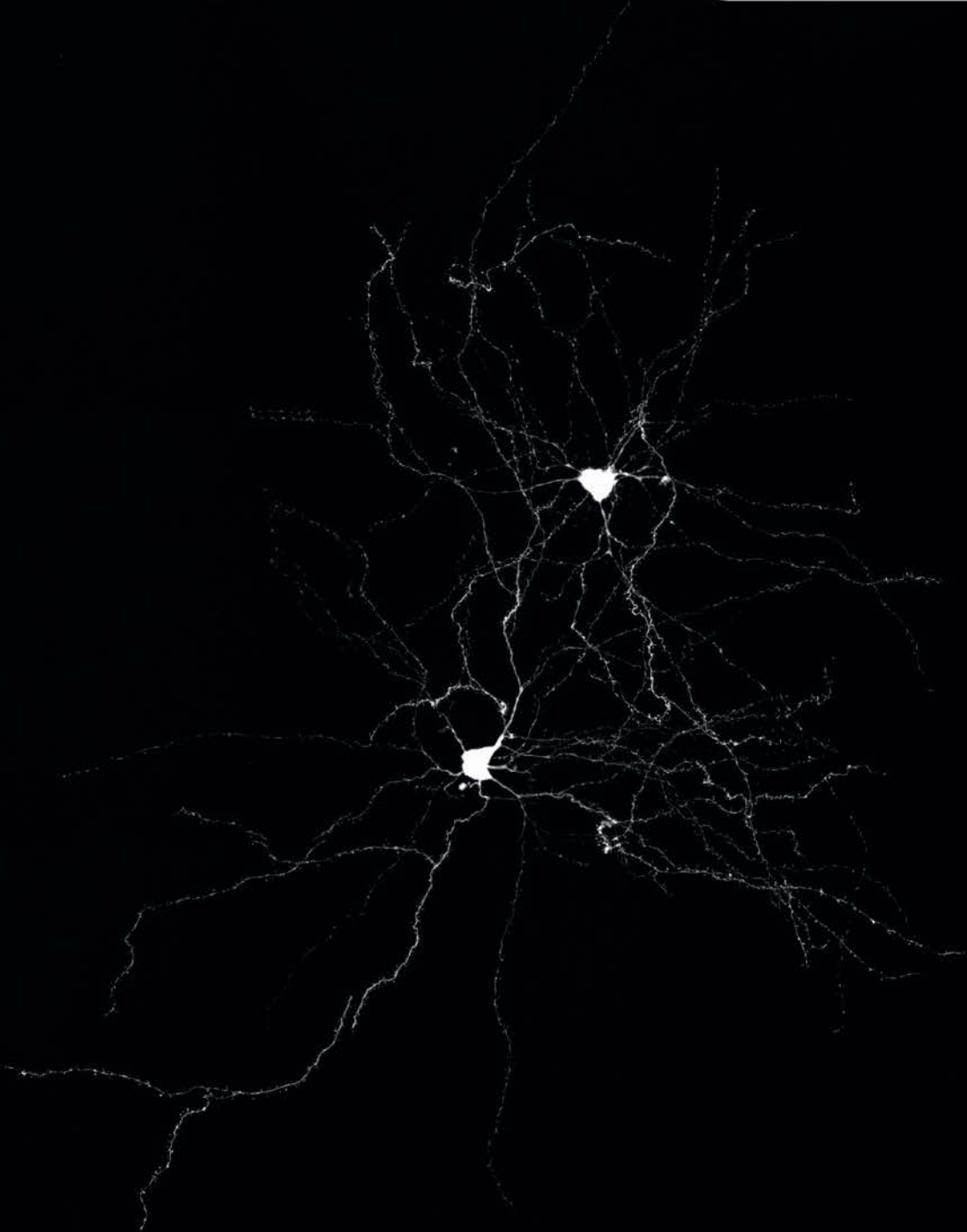
El establecimiento de los circuitos funcionales en el cerebro depende de la correcta formación de conexiones sinápticas entre neuronas, seguida de un intenso remodelado dependiente de actividad durante el desarrollo postnatal y la vida adulta. Este proceso, conocido como plasticidad sináptica, está regulado por la ruta de señalización de fosfatidilinositol-3 quinasa (PI3K), regulada a su vez negativamente por PTEN (*phosphatase and tensin homologue deleted on chromosome 10*). Esta vía de señalización modula el crecimiento, la proliferación y la supervivencia celular. PTEN se expresa en el cerebro, donde controla la sinaptogénesis y la plasticidad sináptica. Concretamente, la actividad de PTEN es necesaria para la depresión a largo plazo dependiente de receptores NMDA (*LTD*), para lo cual necesita ser anclada a la densidad postsináptica a través de la interacción del motivo PDZ, presente en el carboxilo terminal, con la proteína PSD-95.

PTEN se ha asociado a los Trastornos del Espectro Autista (TEA), ya que mutaciones en este gen producen una forma de autismo acompañada de macrocefalia (PTEN-TEA). Los pacientes con estos trastornos muestran una alteración en la comunicación y en el comportamiento social, además de presentar movimientos corporales estereotípicos y una mayor ansiedad. Los circuitos neuronales encargados de estos comportamientos complejos no están del todo claros, aunque se han observado alteraciones en diferentes regiones del cerebro, como la amígdala y el hipocampo. Por ello, el objetivo de este trabajo ha sido evaluar el papel de PTEN en estas regiones cerebrales, tanto su implicación en la plasticidad sináptica como en procesos cognitivos asociados y el comportamiento social. Con este fin utilicé ratones *Pten^{tg}*, que sobreexpresan PTEN, y ratones PTEN- Δ PDZ, con una mutación que resulta en la delección de los cuatro últimos aminoácidos de PTEN, lo que elimina las interacciones tipo PDZ de la proteína.

Los ratones *Pten^{tg}* cursan con microcefalia, con una reducción en el volumen y el número de células del hipocampo. Estos parámetros son normales en la amígdala lateral (AL), aunque las neuronas de esta región presentan una menor complejidad del árbol dendrítico y menor densidad de espinas. En ambas regiones se observó una reducción en la densidad de sinapsis excitatorias, siendo además más pequeñas en la AL. Por otro lado, los ratones PTEN- Δ PDZ cursan con macrocefalia, similar a la observada en los pacientes de PTEN-TEA, sugiriendo una modulación bidireccional de la anatomía cerebral por parte de PTEN, dependiendo de la región cerebral y de las interacciones PDZ. Para evaluar si estos cambios anatómicos afectan a la función sináptica realicé registros electrofisiológicos en el hipocampo (sinapsis CA3-CA1) y en la AL (sinapsis talámico-AL y cortico-AL). En los ratones *Pten^{tg}* se obtuvo una depresión de la transmisión excitatoria basal tanto en el hipocampo como en la vía talámica de la AL, así como una reducción en la potenciación a largo plazo (*LTP*) en el hipocampo y en la vía cortical de la AL y un aumento de la *LTD* en la vía cortical de la AL. Por otro lado, los ratones PTEN- Δ PDZ presentaron transmisión basal excitatoria normal y *LTD* alterada tanto en el hipocampo como en la vía cortical de la AL. Estos resultados revelan que PTEN modula la plasticidad sináptica de forma específica en las diferentes vías analizadas y que las interacciones a través del motivo PDZ son necesarias para la *LTD* tanto en el hipocampo como en la vía cortical de la AL.

Finalmente, para estudiar si las alteraciones en la plasticidad sináptica pudieran tener un efecto funcional realicé varios experimentos de comportamiento. Primeramente analicé la función de ambas estructuras, observando que los ratones *Pten^{tg}* tenían problemas de aprendizaje espacial (hipocampo) y de condicionamiento del miedo (AL), lo cual se relaciona con la alteración en la *LTP* observada en ambas estructuras. Relativo a los comportamientos asociados a los TEA, los ratones *Pten^{tg}* presentan alteraciones en la comunicación, menor ansiedad y mayor sociabilidad que los controles. Por otro lado, los ratones PTEN- Δ PDZ no presentaron problemas de comunicación ni ansiedad, pero sí una alteración en la sociabilidad. Estos resultados sugieren una relación entre una forma específica de plasticidad sináptica controlada por el motivo PDZ de PTEN, la *LTD* en la vía cortical de la AL, y el comportamiento social, siendo modulados bidireccionalmente por PTEN.

Contents



- **Introduction [23]**

- 1. **The limbic system and its contribution to cognitive and emotional processes. [25]**

- 1.1 The hippocampus. [25]

- 1.2 The amygdala. [25]

- 2. **Mechanisms of memory formation. [28]**

- 2.1 The neuron as the basic unit of the brain. [29]

- 2.2 The synapse. [29]

- 2.3 Synaptic plasticity. [30]

- 3. **Autism spectrum disorders (ASD). [32]**

- 3.1 Neuroanatomy of autism. [32]

- 3.2 ASD is an environmental and genetic disorder. [34]

- 4. **PTEN. [35]**

- 4.1 PTEN is a negative regulator of PI3K pathway. [36]

- 4.2 PTEN structure. [37]

- 4.3 PTEN regulation. [38]

- 4.4 PTEN in the CNS. [40]

- 5. **PTEN in autism spectrum disorder. [42]**

- 5.1 PTEN mutations related to ASD. [43]

- 5.2 Pten mouse models of ASD. [43]

- **Objectives. [47]**

- **Material and methods. [51]**

- **Chapter 1: [63]**

- **Chapter 2: [79]**

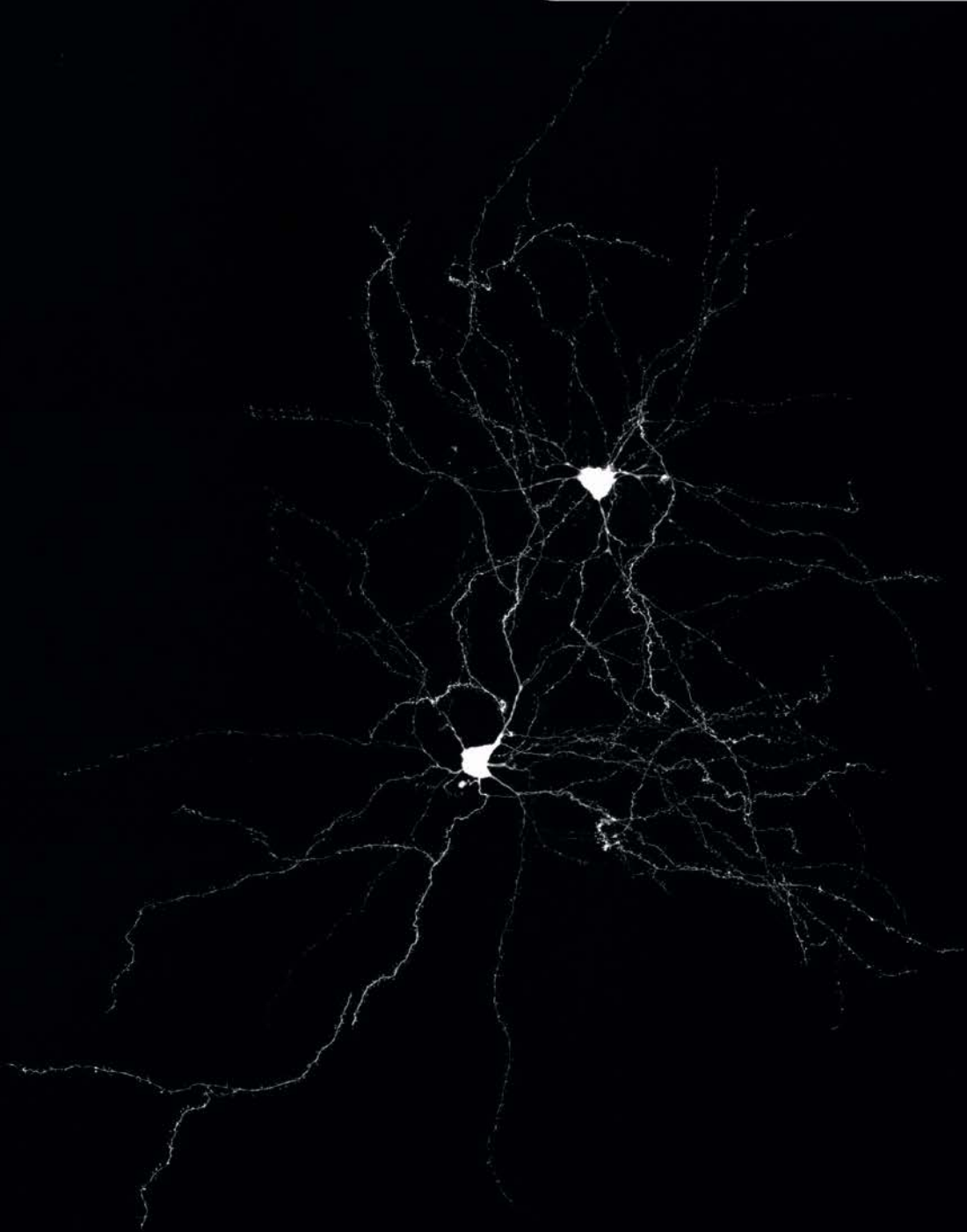
- **Discussion. [89]**

- **Conclusions. [101]**

- **Bibliography. [105]**

- **Annex I. [123]**

Abbreviations



Abbreviations

aCFS: Artificial cerebrospinal fluid.

AEP: Autism epilepsy phenotype.

AMPA: Alfa-amino-3-hydroxy-5-methyl-4-isoxazolepropionic acid.

ASD: Autism spectrum disorders.

BA: Basal amygdala.

BLA: Basolateral amygdala.

BM: Basomedial nucleus.

BNST: Bed nuclei of the stria terminalis.

CA: *Cornus ammonis*.

CBP: CREB-binding protein.

CE: Coefficient of error.

CeA: Central nucleus of the amygdala.

CeL: Lateral central nucleus of the amygdala.

CeM: Medial central nucleus of the amygdala.

CK2: casein kinase 2.

CNS: Central nervous system.

CNV: Copy number variations.

CS: Conditioned stimulus.

DG: Dentate Gyrus.

dHPC: Dorsal hippocampus.

DMS: Diagnostic and statistical manual.

EC: Entorhinal cortex.

EDTA: Ethylenediaminetetraacetic acid.

EGR1: Early Growth Response 1.

EGTA: Ethylene glycol-bis(2-aminoethylether)-*N,N,N',N'*-tetraacetic acid.

E-LTP: Early long-term potentiation.

fEPSP: Field excitatory postsynaptic potential.

FMR: Fragile X mental retardation.

FRK: Fyn-related kinase.

GABA: *Gamma*- γ Aminobutyric acid.

GSK3: Glycogen Synthase Kinase-3

HAUSP: Herpesvirus-associated ubiquitin-specific protease.

HDAC6: Histone deacetylase.

HEPES: 2-[4-(2-hydroxyethyl)piperazin-1-yl]ethanesulfonic acid.

HFS: High frequency stimulation.

HRP: Horseradish peroxidase.

HRSS: High-risk siblings.

IGF2. Insulin-like Growth Factor-II.

IQ: Intelligence quotient.

KO: Knock-out.

LA: Lateral amygdala.

LFS: Low Frequency stimulation.

L-LTP: Late long-term potentiation.

LTD: Long-term depression.

LTP: Long-term potentiation.

MAGI: Membrane-associated guanylate kinase, WW and PDZ domain-containing protein.

MAST: Microtubule-associated serine/threonine-protein kinase .

mEPSCs: Miniature excitatory postsynaptic currents.

mGluR: Metabotropic glutamate receptor.

MKK4: Mitogen-activated protein kinase kinase-4.

mPFC: Medial prefrontal cortex.

mTOR: Mechanistic target of rapamycin.

NAc: Nucleus accumbens.

NEDD4: Neural precursor cell expressed developmentally down-regulated protein 4.

NF-1: Neurofibromin.

NFκB : Nuclear factor kappa-light-chain-enhancer of activated B cells.

NLGN: Neuroligin.

NMDA: *N*-Methyl-D-aspartic acid or *N*-Methyl-D-aspartate.

NRXN: Neurexin.

OCD: Obsessive compulsive disorder.

OFC: Occipital frontal circumference.

PBD: Phosphatidylinositol-4,5-bisphosphate-binding domain.

PBS: Phosphate buffer saline.

PCAF: p300/CPB-associated factor.

PCC: Posterior cingulate cortex.

PCR: Polymerase Chain Reaction.

PDK1: 3-phosphoinositide-dependent protein kinase-1.

PDZ: PSD-95, Disc-large, ZO-1.

PEST: Peptide sequence rich in proline (P), glutamic acid (E), serine (S), and threonine (T).

PHG: Parahippocampal gyrus.

PHTS: Hamman-Richards-Turner Syndrome.

PI3K: Phosphatidylinositol-3-kinase.

PIKKs: PI3K-related kinase family.

PIP₂: Phosphatidylinositol-(4,5)-biphosphate.

PIP₃: Phosphatidylinositol-(3,4,5)-trisphosphate.

PKB/AKT: Serine/threonine protein kinase B.

PKC: Protein kinase C.

PLC: Phospholipase C.

PML: Promyelocytic leukaemia protein.

PREX2a: PIP₃-dependent RAC exchange factor 2a.

PSD: Postsynaptic density.

PSD-95: Postsynaptic density protein 95.

PTEN: Phosphatase and tensin homologue deleted on chromosome 10.

PVDF: Polyvinylidene difluoride.

RFP: Ret finger protein.

ROCK1: Rho-associated, coiled-coil-containing protein kinase.

RPM: Revolutions per minute.

SDS-PAGE: Sodium dodecyl sulfate polyacrylamide gel electrophoresis.

SFG: Superior frontal gyrus.

SHANK: SH3 And Multiple Ankyrin Repeat Domains.

SNPs: Single nucleotide polymorphisms.

SUMO: Small ubiquitin-like modifiers.

TBS: Theta-burst stimulation.

TBS-T: Tween-Tris buffer saline.

TSC: Tuberous sclerosis complex.

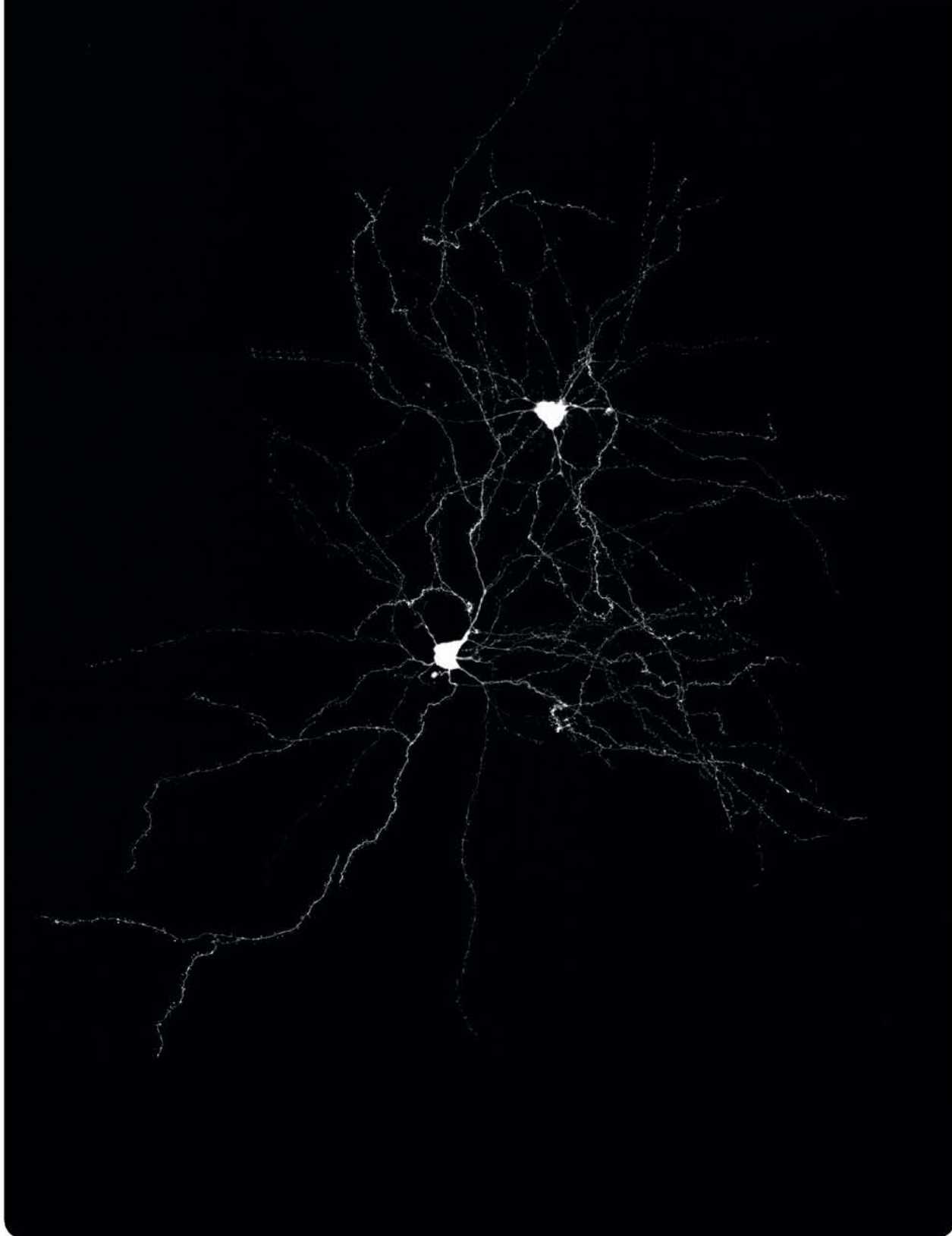
US: Unconditioned stimulus.

USV: Ultrasonic vocalization.

vHPC: Ventral hippocampus.

VTA: Ventral tegmental area.

Introduction



1 The limbic system and its contribution to cognitive and emotional processes

Cognitive processes include brain mechanisms of perception, attention, problem solving and memory (LeDoux, 2000). These type of processes are well developed in mammals, especially in primates, suggesting initially an important implication of the neocortex in cognitive processes (LeDoux, 2000). But, in the mid-1950s the importance of the hippocampus for cognitive function was clearly defined, as hippocampal lesions results in dramatic memory impairments (Scoville and Milner, 1957). The hippocampus is included in the limbic system, which encompasses a series of contiguous cortical and subcortical structures, such as the amygdala, the septal nuclei, and midbrain (Andersen et al., 2007).

Emotional behavior is defined as behavioral responses to attractive (food, sex) or aversive (danger, pain) stimuli (Janak and Tye, 2015). Emotional cognition is under intense investigation, because of its relevance for the survival of animals and species. However, cognitive research in this field is complicated by the fact that subjectivity experience is part of the emotion concept (LeDoux, 2000). The limbic system concept was proposed in the early 1950s, as an initial interpretation of the brain circuit of emotion (Maclean, 1952). Further studies targeting the brain circuits in response to danger, focusing in the fear system, revealed that the amygdala plays a critical role in the transmission of information for emotional behaviors and the control of fear reactions (LeDoux, 2000).

1.1 The hippocampus.

The hippocampus is a vastly studied brain region, especially due to its relevance for cognitive function and its unique neuroanatomy. It is formed late in development in rodents, pyramidal cells are generated during the second half of the embryonic period (E10-E18), with field specific markers found at E14.5-E15.5; and granule cell formation starts only a few days before birth and continues long in postnatal period and, in a reduced level, in adulthood. In contrast, hippocampal neurogenesis in humans takes place relatively early in development, the different subfields are discernable between E70 and E80 and dentate granule layer appears around E90. Cells differentiation continues for a relatively long period, as total dendritic length is reached at P90 in rats and spine density increases until the time of sexual maturation; whereas in humans spine density and total dendritic length of CA1 pyramidal neurons increase until the age of three. The hippocampus is considered a cortical region and is buried within the medial temporal lobe with its cell layers in a highly organized laminar distribution (Andersen et al., 2007).

The hippocampus is known to play a prominent role in the processes of learning and memory formation; particularly, in the formation of declarative memories and in the integration of time and space. Historically, memories were believed to be encoded through a two-phase process: first acquired and stored for a limited period in the hippocampus, and then restructured and transferred to the neocortex for long-term storage (Zola-Morgan and Squire, 1990). But recent studies have shown that the hippocampus is also involved in long-term memory and memory recall (Goshen et al., 2011). Additionally, the hippocampus is implicated in emotional processes, such as responses to stress (Moser and Moser, 1998), anxiety (Felix-Ortiz et al., 2013) and sociability (Felix-Ortiz and Tye, 2014; Hitti and Siegelbaum, 2014a; Okuyama et al., 2016).

This complexity of the cognitive functions of the hippocampus is supported by anatomical and functional differentiation along its dorso-ventral axis. Thus, connections to dorsal and ventral hippocampus are different (Moser and Moser, 1998), leading to a subregional specificity. The dorsal hippocampus (posterior in primates)

appears to be important for encoding spatial learning; whereas the ventral hippocampus (anterior in primates) seems to be involved in emotion, sociability, anxiety and stress responses (Fanselow and Dong, 2010; Felix-Ortiz and Tye, 2014; Felix-Ortiz et al., 2013; Okuyama et al., 2016). However, and very importantly, these two hippocampal areas are not isolated, but they show a significant extent of interconnectivity (Fanselow and Dong, 2010).

1.1.1 Hippocampus anatomy.

Anatomically, the hippocampus formation includes the entorhinal cortex (EC); the dentate gyrus (DG); the proper hippocampus or *cornus ammonis* (CA), which is subdivided into CA3, CA2 and CA1; and the subicular complex, composed of the subiculum, the presubiculum and the parasubiculum (Andersen et al., 2007). This anatomical subdivision of the hippocampus formation can be appreciated in figure 1. The DG presents a characteristic V or U shape and it is formed mostly by granule neurons. One portion of the DG is located between the CA3 and the CA1, as it surrounds the proximal part of CA3. Definition of the three hippocampal sub-fields is based on cell size and input/output network. CA2 is a narrow region between CA3 and CA1, with large pyramidal neurons soma size, like neurons in CA3, but is not innervated by mossy fibers from DG, as the CA1 sub-field. Besides that, laminar organization is similar for the three CA fields of the hippocampus.

The hippocampus is distributed in different layers:

- i) The cell layer is called stratum pyramidale and contains pyramidal cells somas; it is quite compact in CA1 and more lightly packed in CA2 and CA3.
- ii) The stratum oriens is the layer located deep to the pyramidal one and contains the basal dendrites from pyramidal cells and interneurons.
- iii) Deep to the stratum oriens is the alveus, which contains the axons from pyramidal cells, resulting one of the major outputs from the hippocampus.
- iv) In the CA3 field there is a thin layer of mossy fibers called the stratum lucidum and is located above the pyramidal cell layer.
- v) The stratum radiatum appears beyond the pyramidal cell layer of CA2 and CA1, and superficial to the stratum lucidum in CA3. In this region are located the CA3-CA3 connections and the CA3-CA1 connections. In the CA1, these are formed by the apical dendrites of pyramidal cells innervated by CA3 Schaffer collaterals axons, surrounded by a variety of interneurons and glial cells.
- vi) The most superficial region is called the stratum lacunosum-moleculare, which contains fibers from the entorhinal cortex and afferents from other regions.

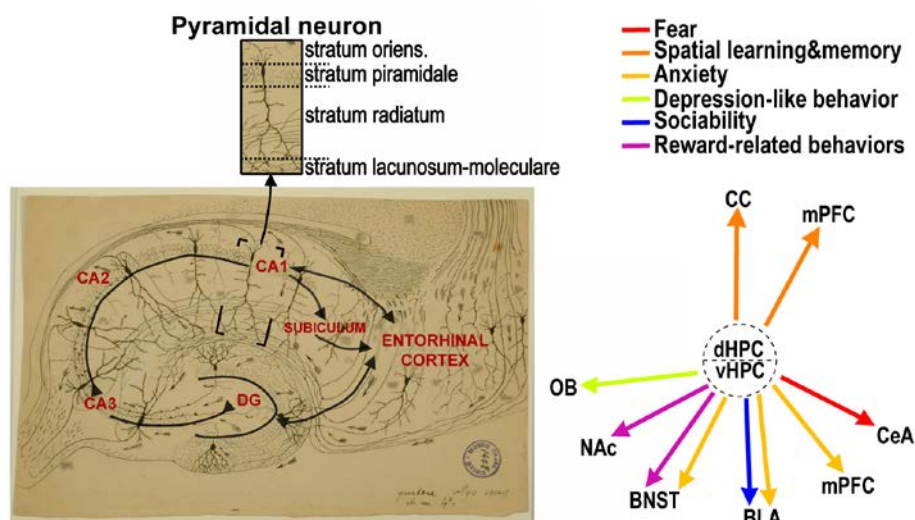


[Figure 1] Left, basic anatomy of the hippocampal formation. Hippocampal draw from Ramon y Cajal. Right, hippocampus connectivity. dHPC: dorsal hippocampus, vHPC: ventral hippocampus, CC: cingulate cortex, mPFC: medial prefrontal cortex, OB: olfactory bulb, NAc: nucleus accumbens, BNST: bed nuclei of the stria terminalis, BLA: basolateral amygdala, mPFC: medial prefrontal cortex, CeA: central nucleus amygdala.

1.1.2 Hippocampal connectivity.

Within the hippocampus, sensory information from neocortical sources is processed through unidirectional connectivity between individual components (Fig. 1). EC, through the perforant pathway, connects to DG principal neurons. Axons from these neurons, called mossy fibers, project to CA3 pyramidal neurons. The CA3 subfield is the major input to CA1 pyramidal neurons, through Schaffer collateral axons. Finally, CA1 neurons project to the subiculum and back to EC neurons (Andersen et al., 2007).

Hippocampal output resides in the subiculum, which is connected to infralimbic and prelimbic cortices, the nucleus accumbens, the hypothalamus, the amygdala, the thalamus and the retrosplenial portion of the cingulate cortex. Hippocampal connections are differently distributed along the dorso-ventral axis, as it can be seen in figure 1. Dorsal hippocampus projects to cortical structures, specifically, with the retrosplenial and anterior cingulate cortical areas and the medial prefrontal cortex (mPFC), that mediates processes of learning, memory formation, navigation and exploration (Fanselow and Dong, 2010; Griffin, 2015). Ventral hippocampus projects to areas involved in emotion, sociability, anxiety and stress responses, through outputs to the bed nuclei of the stria terminalis (BNST), the nucleus accumbens (NAc), the amygdala and the prefrontal cortex (PFC) (Adhikari, 2014; Fanselow and Dong, 2010; Felix-Ortiz and Tye, 2014; Felix-Ortiz et al., 2013; Okuyama et al., 2016).

In this thesis, I have focused on the synapses formed between the Schaffer collateral coming from CA3 and the apical dendrites of the CA1 pyramidal neurons. These synapses are excitatory glutamatergic synapses that occur at specialized structures called dendritic spines. Dendritic spines are small protrusions on the dendritic surface that contain organelles, neurotransmitter receptors and all the subcellular machinery needed to transduce the signals received from the excitatory pre-synaptic input (Nimchinsky et al., 2002).

1.2 The amygdala.

The amygdala is believed to be the brain region responsible for emotional processing, a vital function that is well conserved across evolution (Janak and Tye, 2015). The amygdala is located in the temporal lobes and it is one of the neuronal substrates proposed to mediate both anxiety and social behavior, as well as reward-based behaviors (Janak and Tye, 2015). It also controls the acquisition, storage and expression of fear memory (Allsop et al., 2014). The study of the amygdala has intensified during the past years, as it has been found to be implicated in a wide range of physiological and pathological conditions, such as in anxiety or autism spectrum disorders (ASD) (Janak and Tye, 2015).

Amygdala function is typically studied in rodents through fear conditioning behavioral experiments. This is a type of associative learning known as Pavlovian conditioning, in which neutral conditioned stimuli (CS) (for example, a tone), is paired with an aversive unconditioned stimulus (US) (typically an electric footshock). The acquisition of this associative learning is thought to occur at the lateral nucleus of the amygdala (LA, detailed below), leading to fear responses. Indeed, electrophysiological recordings revealed experience-dependent synaptic strengthening in LA neurons associated with fear conditioning (Janak and Tye, 2015).

1.2.1 Amygdala anatomy.

The amygdala develops early in gestation, but the separate nuclei are not differentiated until postnatal life (Baron-Cohen et al., 2000), originated from the centro-medial cortex and the striatum (LeDoux, 2000). The developed amygdala complex is composed of two main nucleus: basolateral amygdala (BLA), which is thought to have the clearest role in social cognition and fear memories, subdivided into the lateral (LA), the basal (BA) and the basomedial (BM) nucleus; and the central nucleus of the amygdala (CeA), further subdivided into medial (CeM) and lateral (CeL) subnuclei, also important for fear behavior (Allsop et al., 2014; Baron-Cohen et al., 2000; Janak and Tye, 2015)

The BLA complex contains glutamatergic principal neurons, which are pyramidal-like neurons (as those described before for the hippocampus), and inhibitory interneurons. The CeA neurons are predominantly inhibitory interneurons, GABAergic neurons (GABA: γ -aminobutyric acid, the principal inhibitory neurotransmitter), with the CeL projecting to the CeM and a high interconnection between the BLA and the CeA (Janak and Tye, 2015).

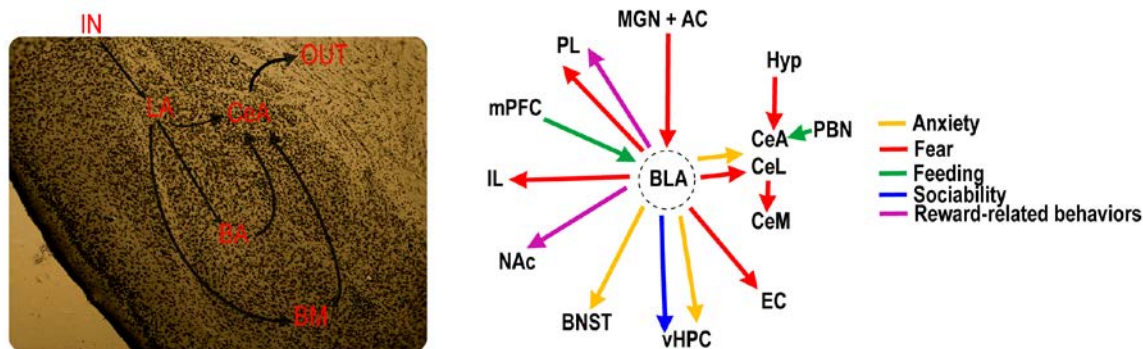


[Figure 2] Left, basic anatomy of the amygdala. Right, amygdala connectivity. AC: auditory cortex, BNST: bed nucleus of the stria terminalis, CeA: central nucleus of the amygdala, CeL: lateral CeA, CeM: medial CeA, EC: entorhinal cortex, Hyp: hypothalamus, IL: infralimbic, MGN: medial geniculate nucleus, mPFC: medial prefrontal cortex, NAc: nucleus accumbens, PBN: parabrachial nucleus, PL: prelimbic, vHPC: ventral hippocampus. Modified from (Janak and Tye, 2015).

1.2.2 Amygdala connectivity.

The amygdala subnuclei have differentiated functions and they are intricately connected (Allsop et al., 2014). The amygdala receives auditory inputs to the LA from both the auditory thalamus and the auditory cortex, further transmitted to the BA, the BM and the CeA (Janak and Tye, 2015; LeDoux, 2000) (Fig.2). Contextual information reaches the amygdala through the projections from ventral hippocampus to the BLA. Cortical areas that process somatosensory stimuli, including nociception, project to the LA, but also the BM nucleus receives this nociceptive input through the posterior thalamus, and the CeA from the parabrachial area or directly from the spinal cord. The amygdala complex is interconnected with many brain areas, as for example the hypothalamus, the hippocampus, the basal forebrain and the neocortex; implicated in behaviors related to emotion, aggressiveness or fear (Baron-Cohen et al., 2000). The BLA is reciprocally connected with cortical regions, principally with the PFC and the hippocampus. On the other hand, unidirectional outputs from the BLA projects to the striatum, especially the NAc, the BNST and the CeA (Janak and Tye, 2015). The main output pathway occurs through the CeA nucleus, that projects to brainstem areas (LeDoux, 2000). I detailed in figure 2 the different connections of the BLA, representing a simplify description of the circuits proposed for each behavior.

For this work, I have focused on the study of the BLA complex, specifically on pyramidal neuron morphology and functionality from the LA nucleus, as it is well known that this is the initial region for processing sensory information (Janak and Tye, 2015).

2 Mechanisms of memory formation.

Memory is defined as the storage, retention and retrieval of information acquired through learning. It has mainly two temporal stages: short-term memory (minutes to hours) and long-term memory (days, weeks or longer)(Kandel, 1997). There are at least two types of memories: declarative (explicit) and non-declarative (implicit). Declarative memory refers to events and facts that are consciously recollected and reproduced, as information about people, places and objects. Non-declarative memories refer to non-conscious procedures, such as learning motor skills or perceptual strategies. These two forms of learning are localized in different brain areas. Thus, declarative memories require regions within the temporal lobe of the cerebral cortex, including the hippocampus, while non-declarative memories involve specific motor and sensory systems (Kandel, 1997).

2.1 The neuron as the basic unit of the brain.

The Central Nervous System (CNS) is mainly composed of two cell types: neurons and glial cells. In this work I am going to focus on neurons, described by Ramon y Cajal as the basic unit of the brain (Ramón y Cajal, 1909). Neurons are highly polarized cells that could be divided into three major morphological and functionally different compartments: the soma, or cell body, from which one axon and the dendritic arbor emerge. The axon is the output emitting part of the cell and the dendrites constitute the input receiving one. From the dendritic surface of some type of neurons arise membranous protrusions called spines, the basic functional unit of neuronal integration, where most excitatory synaptic connections occur (Yuste et al., 1995). The complexity of the dendritic tree is reflected in the number of dendrites and their ramifications. Additionally, neuronal connectivity is determined by the number of synapses, which may increase or decrease in response to activity (Harris and Kirov, 1999).

2.2 The synapse.

A synapse occurs when an axon contacts with a dendrite or dendritic spine of other neuron, being the presynaptic component the axonal bouton and the postsynaptic element the dendritic shaft or the spine. The presynaptic compartment contains the active zone, where key scaffold molecules are located for the release of neurotransmitter. The postsynaptic compartment contains ligand-gated ionic channels, other receptors, and a complex network of signaling molecules. There are two types of synapses depending on their molecular components and ultrastructure (Harris and Weinberg, 2012):

- i. Type I or asymmetric synapses, with a prominent postsynaptic density (PSD). These are the excitatory glutamatergic synapses, found mainly on dendrites and dendritic spines.
- ii. Type II or symmetric synapses, with less dense presynaptic and postsynaptic specializations. These are the inhibitory synapses, found mainly on the cell soma and axonal initial segment, with a sparse distribution along both spiny and nonspiny dendritic shafts.

Of special interest for this work are the excitatory synapses that will be explained in more detail below. These synapses operate with the neurotransmitter glutamate, which is released from the presynaptic terminal in response to an action potential and reaches the postsynaptic terminal, binding there to glutamate receptors and activating different signaling events. These receptors are divided into:

- Ionotropic receptors, which mediate fast excitatory synaptic transmission. Ionotropic receptors subunits are known as iGluRs, which forms tetramers, concretely, dimers of dimers.
 - i) Alfa-amino-3-hydroxy-5-methyl-4-isoxazolepropionic acid receptors (AMPA)s: They are formed by different combinations of four subunits, GluA1-GluA4 (Madden, 2002). Usually, AMPARs are presented as dimers of dimers of GluA2/GluA3, which are in rapid constitutively cycling to maintain synaptic transmission; or GluA1/GluA2, whose trafficking is regulated upon synaptic activity (Passafaro et al., 2001). AMPARs are permeable to Na^+ and impermeable to Ca^{2+} , with the exception of GluA2-lacking receptors, which are also permeable to Ca^{2+} .
 - ii) N-methyl-D-aspartate receptors (NMDAR)s: The subunits that form the NMDAR are GluN1, GluN2A to GluN2D, and GluN3A to 3B. These receptors are formed as tetramers that contain both GluN1 and GluN2 subunits, and in some cases GluN3 subunits (Madden, 2002). An important feature of the NMDAR is that under resting membrane potentials it is blocked by Mg^{2+} . This block is released by depolarization of the membrane allowing the activation of the receptor (Madden, 2002). NMDAR are permeable to Ca^{2+} and Na^+ .
 - iii) Kainate receptors: They are compound by GluR5–GluR7, KA1 and KA2 subunits. They are present presynaptically and postsynaptically. Kainate receptors can mediate excitatory synaptic transmission, but they are also implicated in the modulation of neurotransmitter release (Madden, 2002).

- Metabotropic glutamate receptors (mGluR) that mediates synaptic signaling through G proteins and their second messenger systems. There are three types of mGluR, classify on their localization and mechanism of action: I (mGluR1,5), II (mGluR2,3) and III (mGluR4,6,7,8) (Niswender and Conn, 2010).

Glutamate acts primarily on AMPARs and NMDARs (Bredt and Nicoll, 2003) (fig. 3). Indeed, most excitatory transmission is mediated by AMPA receptors. Therefore, correct neuronal communication is critically dependent on the synaptic expression of AMPARs (Esteban, 2003). Whereas NMDARs are fairly immobile, AMPARs display a dynamic behavior, with a continuous cycling in and out of the synaptic membrane in response to neuronal activity. This dynamic behavior is important for maintaining synaptic transmission in resting conditions. Furthermore, the control of AMPAR trafficking is crucial to modify synaptic strength during brain development or during experience-dependent plasticity, which underlie essential aspects of learning and memory (Bredt and Nicoll, 2003; Esteban, 2003).

2.3 Synaptic plasticity.

Santiago Ramón y Cajal, one of the promoters of modern neuroscience, defined the neuron as the basic unit of the brain, describing its functional and histological individuality (Ramón y Cajal, 1909). Later, it was demonstrated that the connections between the neurons are strongly specialized active areas, which we know today as synapses (Sherrington, 1906). However, it was not until 1948 that Donald Hebb formalized the concept that learning is produced by formation of synaptic contacts between neurons that are synchronously activated forming neural networks. Donald Hebb was the first to examine the mechanisms by which environment and experience can influence brain structure and function, proposing that pre-post synaptic changes are the basis for the memory trace (Hebb, 2002). Indeed, much of our current understanding of functional neural connections is based on Hebb's neural theory of perception (Brown and Milner, 2003) and Hebbian plasticity is a widely accepted concept, in which learning and memory involves modifications of synaptic strength by specific patterns of activity (Kandel, 1997). However, synaptic plasticity not only involves changes in synaptic function, but also structural changes, leading to the concept of structural plasticity, in which dendritic spines appear and disappear, accompanied by formation and elimination of synapses (Holtmaat and Svoboda, 2009). Structural plasticity has been conclusively related to processes of learning and memory in animals (Caroni et al., 2012). In the past decade the “Synaptic Plasticity and Memory” hypothesis has been proposed by Dr. Richard Morris and collaborators (2003):

“Activity-dependent synaptic plasticity is induced at appropriate synapses during memory formation, and is both necessary and sufficient for the information storage underlying the type of memory mediated by the brain area in which that plasticity is observed”.

The investigations of Morris have been of high relevance in the field, as he developed the “Morris Water Maze”, the experimental approach more widely used to study hippocampal-dependent learning and memory, where animals have to swim to a hidden platform using landmarks placed outside the pool (de Bruin et al., 1994). The best characterized cellular substrates of learning and memory-dependent synaptic plasticity are the long-term potentiation (LTP) and long-term depression (LTD), which are common phenomena expressed at possibly every excitatory synapse in the mammalian brain (Malenka and Bear, 2004). Particularly, in this thesis, I have focused my research on the excitatory glutamatergic synapses between CA3-CA1 in the hippocampus and the cortical and thalamic inputs to the LA.

2.3.1 Long-term potentiation (LTP).

LTP mechanisms have been extensively studied, particularly in the hippocampus, due to its unique anatomy and unidirectional connectivity (Andersen et al., 2007). But LTP also occurs in other brain regions, as the PFC (Auclair et al., 2000) or the amygdala (LeDoux, 2000). In 1973, Tim Bliss and Terje Lømo described for the first time a phenomenon of synaptic plasticity in the rabbit hippocampus that seemed to match the specifications previously described by Hebb. With electrophysiological recordings they showed that neuron population responses, known as field excitatory post-synaptic potentials (fEPSPs), were increased after repetitive stimulation, resulting in long-lasting potentiation. It was proposed that neurons could generate new connections or undergo metabolic changes that gave rise to a better communication between them

(Bliss and Lomo, 1973). This event, caused by the induction of activity, could last for hours and even days and is now known as LTP (Bliss and Lomo, 1973).

Later, in 1988, it was proposed that the mechanism mediating the activity-dependent increase in synaptic efficiency involves the NMDARs. When glutamate binds to NMDARs, receptor opening allows calcium influx, leading to an increase in the intracellular calcium concentration and activation of signaling cascades that would enhance postsynaptic conductance (Brown et al., 1988). Thus, this form of synaptic plasticity was called NMDAR-dependent LTP (referred to as LTP). Some years later it was proposed that this form of LTP involves postsynaptic enhancement of AMPAR function (Nicoll and Malenka, 1995), with a rapid redistribution and synaptic delivery after NMDAR activation (Shi et al., 1999). In this manner, NMDARs are necessary for LTP induction, whereas AMPARs mediate the expression and maintenance of synaptic potentiation.

This form of synaptic plasticity is typically elicited by delivering high frequency stimulation (HFS) or theta-burst stimulation (TBS) to the presynaptic fibers, leading to the release of glutamate and subsequent activation of AMPARs. AMPAR opening will produce sufficient depolarization of the postsynaptic membrane for the activation of NMDAR, then allowing the flow of Na^+ and Ca^{2+} into the cell (Blitzer, 2005). The increase of intracellular calcium drives the activation of signaling cascades that mediate the delivery of AMPAR to the synaptic membrane, which results in the enhancement in postsynaptic conductance. Dependent on the persistence of the potentiation, LTP has been classified in two types: early LTP (E-LTP), which requires posttranslational modifications and AMPAR trafficking, and late LTP (L-LTP), which involves new protein synthesis (Blitzer, 2005).

2.3.2 Long-term depression (LTD).

Long-term depression is another long-lasting change in synaptic function that mediates learning and memory. NMDAR-dependent LTD is typically induced by low-frequency stimulation (LFS) that produces the removal of AMPARs from synapses, leading to a persistent decrease in synaptic transmission (Malinow and Malenka, 2002). The first evidence for synaptic depression comes from the study of the cellular mechanisms of habituation and dishabituation performed in *Aplysia*. Kandel and colleagues suggested that changes in the efficacy of excitatory synapses could explained habituation and dishabituation processes (Castellucci et al., 1970). Later, in 1978, studies in hippocampal CA1 subfield showed that prolonged low frequency stimulation of Schaffer collateral afferents leads to a decrease in the synaptically evoked responses (Dunwiddie and Lynch, 1978). Mechanistically, it was established that LTD induced by LFS required the activation of NMDARs and a rise in postsynaptic Ca^{2+} intracellular concentration (although this is being recently debated (Babiec et al., 2014; Nabavi et al., 2013)). Subsequently, activation of the corresponding signaling cascades triggers AMPAR dephosphorylation and internalization, leading to a reduction in synaptic AMPAR currents (Malenka and Bear, 2004).

In this thesis I am interested in synaptic plasticity processes, LTP and LTD, in both the hippocampus and the amygdala. In particular, I have studied the regulation of these processes by PTEN function, and its implication for memory formation as well as for cognitive pathologies such as autism.

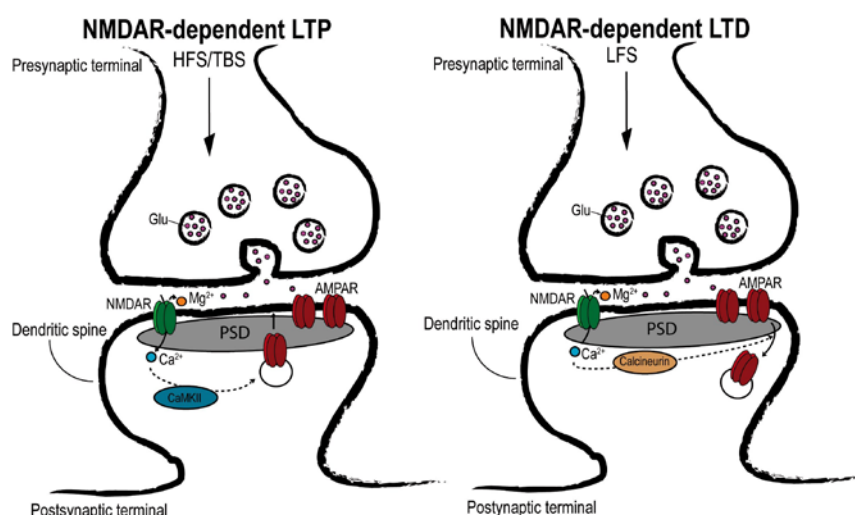


[Figure 3] Simplified representation of the NMDA-dependent LTP (left) and NMDA-dependent LTD (right). Modified from (Kauer and Malenka, 2007).

3 Autism spectrum disorders (ASD).

Autism spectrum disorders (ASD) are phenotypically and etiologically heterogeneous complex neurodevelopmental disorders, characterized by deficits in social interaction, language and restricted and repetitive behaviors (Frazier et al., 2015), often accompanied by one or more comorbidities, such as anxiety, intellectual disability, seizures, motor problems or hyperactivity (Lázaro and Golshani, 2015). The prevalence of the disease is high, around 1% of the population, with an approximately 4:1 bias towards males (Fields and Glazebrook, 2017), presenting gender-specific thresholds, with a higher genetic loading required for females to meet ASD diagnosis (Frazier et al., 2015).

The term autism is derived from the Greek “autos”, which means “self”. This term was firstly introduced by the psychiatrist Eugen Bleuler in 1911. He used it to refer to a classical schizophrenic symptom, “the dominance of inner life with an active isolation from the external world”, observing different degrees of social withdrawal (Bleuler, 1951). Later, Leo Kanner refined the term in 1943 to refer to a specific syndrome observed in children with disrupted affective relationships, which appear from the very beginning of life, in contrast to schizophrenia, in which first manifestations appear after, at least, two years of life (Kanner, 1943). Kanner observed individual differences between children, but there was a remarkable number of essential common characteristics that form a unique syndrome, as the inability to interact with other people or with the environment or the altered communicative functions of speech (Kanner, 1943).

Nowadays, in spite of the great number of studies related to autism, there is no clear etiological model or biomarker of the disease. Autism is defined by the Diagnostic and Statistical Manual (DMS) as a disorder with three main characteristics: social impairment, communication impairment and repetitive behaviors (London, 2014); which appears during the first three years of life (Tordjman et al., 2017). Usually, these three given symptoms are not developed together, only 20-40% have two of these symptoms (London, 2014).

The limit between patients with ASD and part of the population with discrete symptoms of the disease is not strictly clear. In fact, the families of autistic patients usually present autistic phenotypes (London, 2014). This leads to the hypothesis that ASD represent the extreme of a distribution of traits in the population (London, 2014). Additionally, the variability in IQ (Intelligence quotient) scores in autism patients ranges from profoundly cognitively impaired to brilliance. Therefore, because of the clinical heterogeneity, including many etiologies and presentations of autism, the authors use the term 'autisms' or ASD, which implies multiple disorders and looser limits, accepting both the range and the severity of impairments seen in ASD (London, 2014).

Comorbidities are usual in ASD patients. For example, the co-occurrence of one or more non-ASD developmental diagnoses is 83% or one or more neurologic diagnoses is 16% (Levy et al., 2010). One comorbid neurological disorder is the appearance of mental retardation, seen in around 30% of ASD patients (Amaral et al., 2008). Schizophrenia is a psychiatric disorder that shares many symptoms with autism. In fact, there is a subgroup of schizophrenia patients whose diagnosis is preceded by, and comorbid with, ASD in 30-50% of the patients (London, 2014). Also, epilepsy is found in ASD patients, within a range of 5-40% of seizure disorder comorbid with ASD (Amaral et al., 2008). Another common comorbidity is the alteration in motor performance, found in high-risk siblings (HRs) autistic probands when compared to low-risk controls (London, 2014). Anxiety alterations have been consistently found in autism patients. Because of this, many times it has been intermingled with the core symptoms (London, 2014). Anxiety disorders have been reported in around 84% of individuals with autism. Furthermore, up to 50% of ASD children have comorbid obsessive compulsive disorder (OCD), together with repetitive behaviors (London, 2014).

3.1 Neuroanatomy of autism.

Despite several attempts to elucidate the brain areas implicated in the pathology of autism, the heterogeneity of the autism phenotype, including the core features and the comorbidities, makes this definition a complicated task. Attending to the large amount of information available, it seems that the

components of the neural systems underlying ASD are the frontotemporal and front parietal regions, amygdala-hippocampal complex, the cerebellum, basal ganglia and anterior and posterior cingulate regions (Ecker et al., 2015). More specifically, the areas described to be implicated in socio-emotional behaviors are the frontal lobe, the parietal cortex, the superior temporal cortex and the amygdala (Amaral et al., 2008), together known as “social brain” (Baron-Cohen et al., 2000). The language function is settled in the Broca’s area, the superior temporal sulcus, supplementary motor cortex, basal ganglia, substantia nigra, thalamus and the pontine nuclei cerebellum (Amaral et al., 2008). Repetitive or stereotyped behaviors are controlled by the orbitofrontal cortex, the anterior cingulate cortex, the basal ganglia and the thalamus (Amaral et al., 2008).

3.1.1 Macrocephaly.

Macrocephaly refers to abnormal large head, including the scalp, cranial bone and intracranial contents. It is clinically defined as an occipital frontal circumference (OFC) higher than 2 standard deviations or more above the mean (Williams et al., 2008). Macrocephaly occurs in 15-35 % of autistic children (Williams et al., 2008), with greater increases in white matter than in gray matter volume (Amaral et al., 2008). In many cases, the increased brain volume disappears around the age of 6-8 years of age; these changes in brain volume could imply altered neurodevelopmental trajectories of brain maturation (Ecker et al., 2015).

It seems that these variations in neurodevelopment occurs differentially in different brain areas, being more affected the frontal and temporal lobes than the parietal and occipital lobes (Ecker et al., 2015). Specific areas with abnormal grown pattern have been identified. For example, in postmortem studies cortical dysgenesis was described, with increased cortical thickness, including high neuronal density (Bailey et al., 1998) and increasing growth rate (Ecker et al., 2015). Other studies have described abnormal enlargement of the amygdala, which has been associated with more severe anxiety (Juraneck et al., 2006) and social and communication impairments (Munson et al., 2006). In contrast, other studies in postmortem cases of autism reported a significantly decreased number of neurons in the amygdala (Schumann and Amaral, 2006). In addition, enlargement of the caudate nucleus and the hippocampus has been found (Amaral et al., 2008).

3.1.2 Brain connectivity in ASD.

Anomalous functioning has been described for the cerebellum, the hippocampus, the amygdala or the fronto-limbic connections (Baron-Cohen et al., 2000). Differences in age, gender and clinical severity between studies make it difficult to define a clear pattern of brain connectivity related to ASD, although differences in connectivity are well established. However, it is still unclear whether the cause of ASD relies on a failure to generate connections, an inappropriate pruning or alterations in the formation of new connections (Hull et al., 2017). Structural abnormalities of several brain regions have been related with functional alterations in ASD patients (Ecker et al., 2015).

Studies of brain connectivity have been performed, analyzing the correlation of fMRI activation changes between different regions (global connectivity) or within a brain region (local connectivity)(Hull et al., 2017); but the heterogeneity of emerging results bring high controversy regarding the nature of connectivity impairment in ASD (Ecker et al., 2015). Hypoconnectivity in regions responsible for social behavior, including the mPFC, the posterior cingulate cortex (PCC) and in the limbic-related brain regions has been described; as well as hyperconnectivity, including the frontostriatal connections or the primary sensory and subcortical networks in basal ganglia and thalamic, correlating the degree of hyperconnectivity in these areas to the severity of ASD(Hull et al., 2017). Recent findings propose the contribution to ASD of connectivity changes in both directions: hypoconnectivity of the PCC and the superior frontal gyrus (SFG) (correlated with poor social functioning), and hyperconnectivity of the PCC with the right-PHG (parahippocampal gyrus) (associated with more severe repetitive behaviors)(Hull et al., 2017). These findings support the existence of local over-connectivity and long-distance under-connectivity in the brains from ASD patients when compared to typical developing subjects, emerging the theory of less segregated functional networks with more diffused pattern of connectivity between them (Hull et al., 2017).

To establish a relationship between specific symptoms with a precise brain mechanism in humans is not easy due to technical limitations; it will require invasive techniques that are not suitable for human individuals. Recently, researchers have developed novel techniques to discern brain regions and circuits

underlying sociability using animal models, which enable more invasive technologies. For example, fiber photometry can measure directly the activity of a specific neuronal population projecting to its downstream target. This approach suggested the implication of VTA activation and projection to the NAc as a key element in modulation of social behavior (Gunaydin et al., 2014).

3.1.3 Amygdala and hippocampal implication in ASD.

The amygdala is one of the regions proposed as a neuronal substrate that mediates both anxiety and social behavior (Allsop et al., 2014). The “amygdala theory of autism” suggests that the amygdala is one of the regions that is necessarily abnormal in ASD (Baron-Cohen et al., 2000). This region is activated in humans when decoding social signals, and patients with autism show similar phenotypes compared to those with amygdala lesions (Baron-Cohen et al., 2000). Studies in monkeys revealed that amygdala-lesioned individuals present socio-emotional deficits (Baron-Cohen et al., 2000).

In many cases, social deficits are presented with anxiety disorders, and it has been shown that patients with anxiety show a greater activation of the amygdala in response to emotional face stimuli in comparison with control individuals, and that the degree of activation correlates with the severity of the pathology. Moreover, high anxiety has been shown to be associated with increased volume and connectivity of amygdala (Allsop et al., 2014). As in humans, amygdala lesions in animals result in reduced anxiety-related behaviors and social behavior (Allsop et al., 2014).

The amygdala complex is interconnected with many brain areas implicated in behaviors related to emotion, aggressiveness or fear (Baron-Cohen et al., 2000). BLA projections to the mPFC control bidirectionally both anxiety and social behavior, while activating BLA-mPFC projections increase anxiety-like behavior and reduce social interaction. The opposite result is obtained by inhibiting this circuit (Felix-Ortiz et al., 2015). Similar results were found regarding the reciprocal connections between the amygdala and the ventral hippocampus (vHPC): BLA inputs to the vHPC control bidirectionally both anxiety and social behaviors (Felix-Ortiz and Tye, 2014; Felix-Ortiz et al., 2013). Thus, suggesting that anxiety and sociability are mechanistically linked, providing good evidence for the neural circuit that could be underneath the co-morbidity of anxiety disorders and ASD (Allsop et al., 2014).

Hippocampus has also been related to ASD pathology; both amygdala and hippocampus have been found to be enlarged in children with autism with and without mental retardation (Schumann, 2004). Additionally, several ASD mouse models present alterations in hippocampal function, in both CA1 (Takeuchi et al., 2013; Wang et al., 2006) and CA2 subfields (Hitti and Siegelbaum, 2014a), highlighting the importance of hippocampus in social behavior.

3.2 ASD is an environmental and genetic disorder.

There is great heterogeneity in the literature on the causes of ASD, including environmental and genetic factors. Environmental factors can be prenatal, as the serotonin-melatonin-oxidative stress-placental insertion (Anderson, 2015), perinatal and postnatal, as for example social (Hoksbergen et al., 2005; Rutter et al., 1999, 2007) and/or sensory (Mukaddes et al., 2007; Rosenhall et al., 1999) deprivation or epigenetics (Tordjman et al., 2017). Genes implicated in syndromic forms of autism were firstly identified in the 1990s (Ey et al., 2011), and at present more than 200 autism susceptibility genes have been reported (Tordjman et al., 2017). There is a high genetic heterogeneity causing ASD, including chromosomal alterations, copy number variations (CNV), or single nucleotide polymorphisms (SNPs) (Hull et al., 2017). Most recently, rare *de novo* and inherited sequence variants in ASD patients have been identified, emerging new genes related to autism due to *de novo* loss-of-function and likely-gene-disrupting mutations found in affected patients (Ey et al., 2011).

ASD are diagnosed before the age of three, a period characterized by intense synaptogenesis in human brain (Bourgeron, 2009). Moreover, brain overgrowth in ASD patients is observed before 2 years of age, associated with the emergence of behavioral core alterations of ASD (Hazlett et al., 2017). Thus, it has been shown that the products of many ASD-associated genes are implicated in neuronal growth and synaptic regulation and that they are active in early- or mid-fetal development (Fields and Glazebrook, 2017).

The evidence that macrocephaly occurs in 15-35% of ASD patients (Williams et al., 2008) led to the study of susceptibility genes for autism implicated in neuronal growth, finding that mutations in tumor suppressor

genes as Neurofibromin (NF-1), TSC1/TSC2 (Tuberous complex) and PTEN (phosphatase and tensin homologue deleted on chromosome 10) result in neuronal hypertrophy and susceptibility to ASD (Williams et al., 2008). Moreover, all of them are negative regulators of the mechanistic target of rapamycin (mTOR) pathway, implicated in cellular growth, as well as in synaptic function controlling protein synthesis at synapses, leading to the abnormal cellular growth and synaptic alterations reported in ASD (Bourgeron, 2009).

De novo mutations enriched in a gene set implicated in synaptic networks have been described (Ram Venkataraman et al., 2016). Moreover, transcriptome analysis in postmortem ASD brains have revealed downregulation of several genes involved in synaptic function (Chen et al., 2014). There are synaptic adhesion molecules implicated in autism, such as the presynaptic NRXN (Neurexin) or the postsynaptic Neuroligin (NLGN); scaffolding proteins, as Shank family or PSD-95 (postsynaptic density protein-95); or alterations in synaptic receptors associated with autism, such as GABA or glutamate receptors (Chen et al., 2014).

Recent studies have pointed to the hypothesis of synaptic elimination as a potential pathogenic mechanism for ASD, altering the synaptic homeostasis mechanism produced during development (Ram Venkataraman et al., 2016). This is based on *de novo* mutations found in genes involved in synaptic elimination or synaptic pruning, a process that occurs during neurodevelopment parallel with synaptic formation (Ram Venkataraman et al., 2016). The rate of synaptic formation and pruning goes through different phases throughout development, where most dramatic changes occur during perinatal period. The selection process is crucial for the correct cognitive development of the child (Bourgeron, 2009). Among the genes implicated in synaptic elimination network are SHANK2 (SH3 And Multiple Ankyrin Repeat Domains 2), NLGN3, NRX and PTEN, all of which have already been confirmed as genes associated with autism risk (Bourgeron, 2009; Sanders et al., 2015). Investigation of the different ASD susceptibility genes highlights the heterogeneity of genetic etiologies, supporting the hypothesis of the existence of common biological pathways or brain circuits that give rise to ASD.

Overgrowth during early brain development has been suggested to be a key factor for the development of ASD. Meanwhile other studies have demonstrated the role of synaptic proteins in social behavior, proposing synaptic function as a key factor in the pathogenesis of ASD. Recently, there is a hypothesis that combines both proposals, the “multi-hint” model, arguing that possible mutations in multiple autism-related genes could be acting synergistically to contribute to ASD phenotype (Zhou and Parada, 2012). This “multi-hint” model could better explain the phenotypic diversity among autistic patients.

Several ASD models have been developed to study the mechanistic causes of the disease. Most of them are mouse models, taking advantage of a controllable biological system that could help to understand the interaction of a genetic alteration with other proteins and signaling pathways, suggesting potential treatments (Lázaro and Golshani, 2015). Early models tried to deeply study the primary symptomatic presentations, focusing on behavioral deficits, such as social cognition (Baron-Cohen, 2002). Lately, second generation ASD-models have been proposed to further study the neurodevelopmental and neurocognitive mechanisms that underlie ASD (Fields and Glazebrook, 2017). It has been found that several mouse models reach to convergent signaling pathways, as it is the case of ASD models with mutations in TSC1/2, NF1, PTEN or FMR1 (fragile X mental retardation 1), all of them upregulating the mTOR signaling, suggesting that mTOR-dependent activity could be a common pathway of some ASD-related molecular cascades (Lázaro and Golshani, 2015). On the other hand, mouse models with mutations in the NRX-NGL-SHANK pathway have been related to abnormal synaptogenesis (Ey et al., 2011), also observed in PTEN mouse models (Williams et al., 2015). Altogether, these studies propose that abnormal brain development and synaptic homeostasis represent risk factors of ASD (Ey et al., 2011)

4 PTEN.

The Phosphatase and tensin homolog deleted on chromosome ten (PTEN) is a tumor suppressor, found to be frequently mutated or deleted in several neoplastic diseases (Boosani and Agrawal, 2013). PTEN is thought to be expressed constitutively in all cells during the whole life (Boosani and Agrawal, 2013). In most tissues, including the brain, PTEN acts as a general break for cell proliferation and growth, both during embryo development (Kwon et al., 2006; Stiles et al., 2004) and also in the adult (Chow et al., 2009; Gregorian et al., 2009). In addition, PTEN is involved in neuronal synaptic plasticity (Tilot et al., 2015).

Pten gene mutations have been attributed to hereditary diseases, clinically referred as Hamman-Richards Syndrome (PHTS) (Boosani and Agrawal, 2013). PHTS are a family of related tumor syndromes with autosomal inheritance and highly variable expression, including Cowden syndrome, Bannayan-Riley-Rubalcaba syndrome and Proteus syndrome (Buxbaum et al., 2007). These disorders are characterized by the presence of benign hamartomas of the skin, intestinal tract, central nervous system and by an increased incidence of thyroid and breast cancers (Vazquez et al., 2000). Furthermore, mutations in Pten gene lead to neurodevelopmental alterations that end up with autism and macrocephaly, combined usually with mental retardation and epilepsy (Garcia-Junco-Clemente and Golshani, 2014). This specific type of ASD, termed PTEN-ASD (Frazier et al., 2015; Tilot et al., 2015) is characterized by lower amounts of functional PTEN protein in association with macrocephaly, cognitive deficits and impaired social interaction (Frazier et al., 2015). Several PTEN knockout (KO) mouse models further link changes in neural function to autism-like behavioral abnormalities (Table 1, Annex I) (Tilot et al., 2015). However, the exact molecular, synaptic and cellular mechanisms linking PTEN to social behavior and cognitive functions are not fully understood.

4.1 PTEN is a negative regulator of PI3K pathway.

PTEN and Phosphatidylinositol-3-kinase (PI3K) are opposite regulators of the PI3K pathway. There are three major classes of PI3K (I, II, III), according to their molecular structure and substrate specificity (Domin and Waterfield, 1997). PIP₃ (phosphatidylinositol-(3,4,5)-trisphosphate) is synthesized by class I PI3Ks, activating the pathway. PTEN catalyzes the opposite reaction, dephosphorylating PIP₃ into phosphatidylinositol-(4,5)-biphosphate (PIP₂), therefore antagonizing PI3K activity (Stambolic et al., 1998) (fig. 4).

PIP₃ and PIP₂ are two of the seven phosphoinositides present in the cells. These are phosphorylated derivatives of phosphatidylinositol and represent only a small fraction of the lipid membrane (Di Paolo and De Camilli, 2006). Phosphoinositides play a role in nearly all aspects of cell physiology, including signal transduction, vesicle trafficking, membrane receptor localization and activity, and determination of membrane identity (Di Paolo and De Camilli, 2006). In neurons, phosphoinositide turnover is essential for neurotransmitter vesicle cycling in presynaptic terminals (Wenk and De Camilli, 2004) and for synaptic plasticity in postsynaptic terminals (Arendt et al., 2010, 2014). Phosphoinositides are located at the cytosolic layer of membranes and their functions depend on their dynamic and highly regulated metabolism (Di Paolo and De Camilli, 2006). This high and constant turnover in basal conditions and its activity-dependent regulation have also been shown to happen in dendritic spines (Arendt et al., 2014).

Signaling effects of phosphoinositides are achieved through the binding of their head groups to cytosolic proteins or cytosolic domains of membrane proteins, typically through electrostatic interactions (Di Paolo and De Camilli, 2006). By doing so, they can recruit and regulate the function of different signaling components (Di Paolo and De Camilli, 2006). The PIP₂-PIP₃ balance controls signal transduction at the plasma membrane (Di Paolo and De Camilli, 2006), and has major relevance for several diseases, such as diabetes and cancer, where PI3K and PTEN appear to be frequently mutated (Gross, 2016).

PIP₂ is the precursor for two second messengers obtained upon the action of Phospholipase C (PLC): Diacylglycerol and Inositol-triphosphate, which activate the protein kinase C (PKC) and intracellular calcium release (Berridge, 2009; Bishop et al., 1992). PIP₃ is present in negligible amounts in resting cells, but can transiently and dramatically increase in response to activity, such as growth factor stimulation (Cantley, 2002) or synaptic plasticity (Arendt et al., 2014). PIP₃ acts by recruiting important signaling effectors, such as the 3-phosphoinositide-dependent protein kinase-1 (PDK1) and the serine/threonine protein kinase B (PKB), also known as AKT (Di Paolo and De Camilli, 2006).

Activation of AKT occurs after membrane-targeting through the pleckstrin homology (PH) domain interaction with PIP₃ (Stephens et al., 1998), being 10-fold stronger than the interaction with PIP₂ (Cohen et al., 1997). Co-localization of AKT and PDK1 leads to the phosphorylation of AKT at the threonine 308, by PDK1 (Cohen et al., 1997), and at serine 473, by members of the PI3K-related kinase family (PIKKs). Both phosphorylation events are needed for the synergistic full activation of the enzyme (Alessi et al., 1996; Cohen et al., 1997). The phosphorylation of T308 induces catalytic active conformation, which is stabilized upon the phosphorylation of S473 (Fayard et al., 2010). AKT is a major mediator of the PIP₃ pathway (Fayard

et al., 2010). Upon its activation, AKT phosphorylates a wide range of substrates with different roles in the cell, including cell cycle progression, cell growth, cell differentiation, cell survival/suppression of apoptosis, metabolism, angiogenesis and motility (Fayard et al., 2010). A schematic revision of AKT downstream effectors, such as GSK3 (Glycogen Synthase Kinase-3) or mTOR, can be found in figure 4.

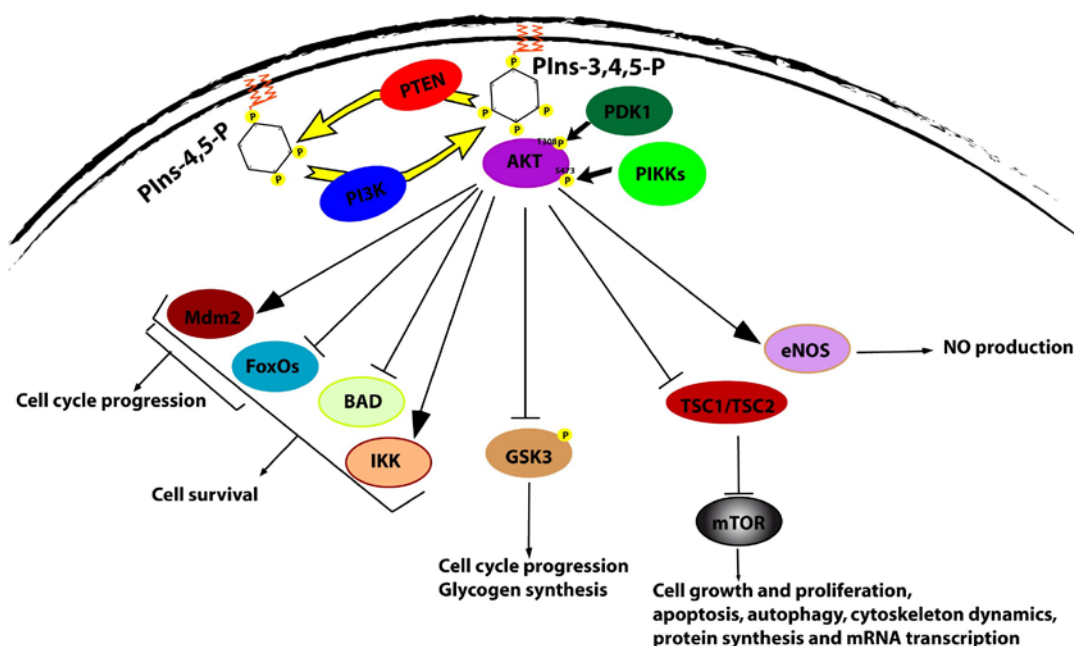


[Figure 4] Schematic representation of the PI3K pathway. BAD: Bcl-2-antagonist of dead, IKK: NF- κ B kinase, Mdm2: E3 ubiquitin ligase mouse double minute 2, FoxOs: Forkhead family of transcription factors, eNOS: endothelial nitric oxide synthase, TSC2: tuberous sclerosis 2, mTOR: mechanistic target of

4.2 PTEN structure.

PTEN gene (NCBI Acc # NM_000314.4, also known as BZS; DEC; GLM2; MHAM; TEP1; MMAC1; PTEN1; 10q23del) was originally identified as a tumor suppressor gene frequently mutated in chromosome 10q23 (Hopkins et al., 2014). The PTEN gene contains 9 exons and encodes a 403 amino acid protein (47.17 kDa) (Li et al., 1997). A schematic representation of PTEN structure can be found in figure 5.

Sequence analysis of the protein has revealed a protein tyrosine phosphatase (PTP) domain, a dual-specificity phosphatase catalytic domain and a large region of homology (\approx 175 aa) to chicken tensin and bovine auxilin, giving these characteristics the name for the gene (Li et al., 1997). Crystal structure of amino acids 7-351 of PTEN revealed that the N-terminal domain contains the signature motif present in active sites of protein tyrosine phosphatase (HCXXGXXES/T) (Lee et al., 1999). This domain contains a deep and wide catalytic active site pocket with positive charge, capable of accommodating phospholipid substrates, and to dephosphorylate serine/threonine substrates in addition to phosphotyrosine (Lee et al., 1999). The protein contains a C2-domain (residues 186-351) with positive charges that binds to phospholipid membranes in a Ca^{2+} -independent manner and it is implicated in the regulation of cell migration (Lee et al., 1999). The interface between the phosphatase and the C2 domains is important for PTEN function, as mutations in its residues have frequently been found in cancer (Lee et al., 1999).

The PBD (phosphatidylinositol-4,5-bisphosphate-binding domain) contains the first 15 amino acids of the N terminus and constitutes the consensus sequence for the PIP₂ binding motif (Campbell et al., 2003). This domain is particularly important for membrane localization and PTEN catalytic activity (Lee et al., 1999), with both nuclear and cytoplasmic localization sequences (Tilot et al., 2015). Binding of PIP₂ to PTEN induces an allosteric conformational change that activates PTEN, leading to a positive feedback loop between PTEN product, PIP₂, and PTEN substrate, PIP₃ (Campbell et al., 2003).

The last 50 amino acids of the protein are known as "the tail" (residues 354-403), which is rich in serine and threonine (28% of the residues) and contains consensus phosphorylation sites for several kinases (Vazquez et al., 2000), which modulate PTEN functions (Boosani and Agrawal, 2013). Deletion of the tail

results in a more unstable protein, but with increased activity, due to phosphorylation sites present on it, which regulate both PTEN stability and activity (Vazquez et al., 2000). Two PEST sequence (peptide sequence rich in proline (P), glutamic acid (E), serine (S), and threonine (T)) were found between the amino acids 350-375 and 379-396, being essential for the degradation rate of the protein, which has a relatively long half-life, more than 2 hours (Georgescu et al., 1999).

The last 3 aa of PTEN form the consensus (Thr401-Lys402-Val403-COOH, T-X-V-COOH) for binding PDZ (PSD-95, Disc-large, ZO-1) domains (Georgescu et al., 1999). Mutations on this sequence do not affect the expression level of the protein or tumor suppressor function (Georgescu et al., 1999), as it has been shown that AKT activation is not affected upon mutation in the PDZ motif (Leslie et al., 2001). PDZ domains are modular protein interaction domains often found in multi-domain scaffolding proteins (Valiente et al., 2005). These domains usually recognize C-terminal motifs in their target proteins, playing important roles in protein targeting and/or protein complex assembly to perform a specialized local functions (Valiente et al., 2005). PTEN-PDZ binding is important for the specificity of interaction with different PDZ containing proteins, and it has a regulatory role on PTEN function by controlling its stability and phosphorylation status (Valiente et al., 2005), regulating the inhibition of cell spreading modulated by PTEN (Leslie et al., 2001).

Recently, it has been identified another isoform of PTEN known as PTEN-long, with additional 179 amino acids placed at the N-terminus (Tilot et al., 2015). This translational variant of PTEN is transferred from one cell to another by vesicles, but it is also secreted, as it can be detected in human serum and plasma (Hopkins et al., 2014).

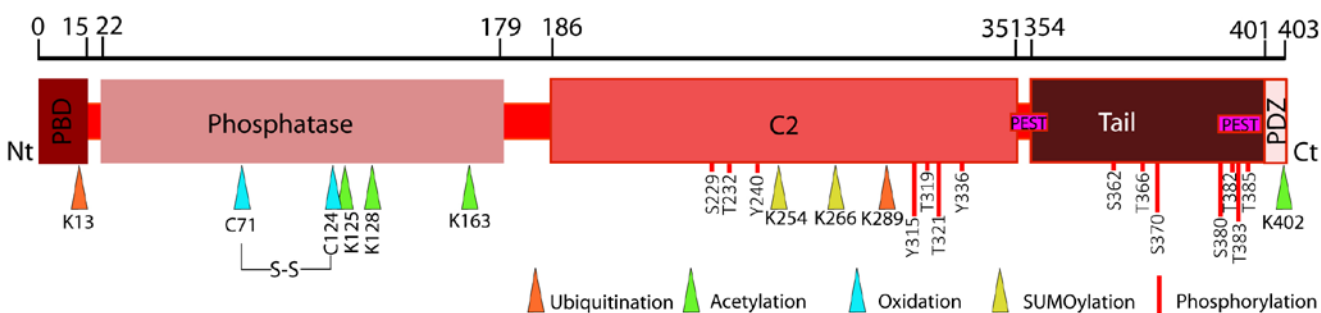


[Figure 5] Schematical representation of PTEN structure and regulation. Modified form (Hopkins et al., 2014)

4.3 PTEN regulation.

The functional activity of PTEN is highly regulated by transcriptional regulation, post-translational modifications (fig. 5), and through protein-protein interactions (Boosani and Agrawal, 2013).

4.3.1 Transcriptional regulation of PTEN.

There are several transcription factors that bind directly to the PTEN promoter and regulate its expression positively, such as the immediate early gene EGR1 (Early Growth Response 1) (Virolle et al., 2001) induced by the IGF2 (Patel et al., 2001) (Insulin-like Growth Factor-II) (Moorehead et al., 2003), or negatively (Tamguney and Stokoe, 2007), as the NFκB (nuclear factor kappa-light-chain-enhancer of activated B cells), which downregulates PTEN expression upon the activation of MKK4 (Mitogen-activated protein kinase kinase-4) (Xia et al., 2007).

4.3.2 PTEN regulation by post-translational modifications.

Oxidation. Oxidants, including those produced by cells, can inactivate the PTEN phosphatase activity. Through this mechanism, oxidative stress increases cellular levels of PIP₃ and the consequent activation of downstream signaling pathways (Leslie et al., 2003). PTEN could be reversibly inactivated through oxidation predominantly by thioredoxin in the Cys124, which leads to the formation of a disulfide bond with the Cys71 (Lee et al., 2002).

Acetylation. PTEN is acetylated by the CREB-binding protein (CBP) on Lys402, within the PDZ domain-binding motif (Hopkins et al., 2014). Lys402 acetylation enhances its interaction with PDZ domain-containing

proteins (Ikenoue et al., 2008). PTEN interacts with PCAF (p300/CPB-associated factor), a histone acetyltransferase that acetylates the residues Lys125 and Lys128 (Hopkins et al., 2014). These residues are within the catalytic cleft of PTEN, a structure essential for PIP₃ specificity, resulting in a decreased catalytic activity upon acetylation (Okumura et al., 2006). Deacetylation by the HDAC6 (Histone deacetylase) activates PTEN (Meng et al., 2016), inhibiting the interaction between the C-terminal tail with the remaining part of PTEN, resulting in PTEN membrane translocation and activation of the protein (Meng et al., 2016).

Ubiquitylation. Ubiquitylation regulates PTEN by promoting protein degradation, nuclear localization and inhibition of phosphatase activity (Hopkins et al., 2014). PTEN has at least two possible ubiquitination sites, Lysine13 and Lysine289, and NEDD4-1 (neural precursor cell expressed developmentally down-regulated protein 4) has been identified as an efficient E3 ubiquitin ligase for PTEN (Trotman et al., 2007; Wang et al., 2007). While PTEN polyubiquitylation correlates with proteasome-mediated degradation, monoubiquitylation of PTEN has been shown to promote the nuclear accumulation of the protein (Wang et al., 2007). For example, ubiquitylation by PML (promyelocytic leukaemia protein) allows PTEN to be accumulated in the nucleus, whereas PTEN deubiquitylation by HAUSP (herpesvirus-associated ubiquitin-specific protease) favors PTEN accumulation in the cytoplasm (Song et al., 2008). Within the ubiquitins that regulates catalytic activity we can find the E3 ubiquitin ligase Ret finger protein (RFP), which significantly inhibits PTEN phosphatase activity (Lee et al., 2013). Addition of small ubiquitin-like modifiers (SUMO) or SUMOylation of PTEN has also been implicated in the regulation of PTEN cellular localization. Particularly, PTEN is covalently modified by SUMO1 at both Lys266 and Lys254 sites in the C2 domain, enhancing PTEN plasma membrane binding (Huang et al., 2012).

Phosphorylation. The C-terminal tail has multiple phosphorylation sites, which regulate PTEN activity. The residues identified for such phosphorylation are Ser366, Ser370 and the cluster Ser380-Thr382-Thr383-Ser385 (Miller et al., 2002; Vazquez et al., 2000). The phosphorylation status of the Ser380-Ser385 residue group positively regulates the half-life of PTEN, but significantly decreases enzyme activity (Vazquez et al., 2000). In contrast, phosphorylation of Thr366 results in a decrease of PTEN stability (Tibarewal et al., 2012). Additionally, phosphorylation of PTEN in the C-terminal tail is critical for protein-protein interactions.

Several kinases have been described to be capable of phosphorylating these residues, such as the casein kinase 2 (CK2) or the GSK3. CK2 can phosphorylate PTEN in the Ser370 and the Ser380-Ser385 group, regulating positively protein stability and negatively PTEN activity (Miller et al., 2002; Torres and Pulido, 2001). PTEN can be cleaved at multiple sites of the C-terminal tail by caspase-3, event blocked by phosphorylation by CK2 at the Ser370 and Ser385. When PTEN is cleaved it becomes less stable and reduces its binding to interacting proteins (Torres and Pulido, 2001). The kinase GSK3 phosphorylates PTEN at Ser362 and Thr366 and it has been shown that this occurs in a synergistic manner with CK2 phosphorylation (Al-Khouri et al., 2005). Phosphorylation at the Ser370 residue by CK2 primes the phosphorylation of Thr366 by GSK3 (Odriozola et al., 2007). The involvement of GSK3 could be part of a negative-feedback loop present in the PIP₃ pathway (Al-Khouri et al., 2005).

In addition, PTEN can activate itself through dephosphorylation at multiple serine and threonine residues in the C-terminal domain through its protein phosphatase activity, regulating PTEN localization and controlling cell invasion and morphology (Tibarewal et al., 2012), as for example, it was described to regulate spine density in hippocampal cultures (Zhang et al., 2012). The phosphorylation of the Ser380-Ser385 group determines the intramolecular interaction that occurs between the C-terminal tail and the PTEN catalytic region, being a "closed" conformation of PTEN that constrains the recruitment of PTEN to the plasma membrane, thus negatively regulating the PTEN function (Rahdar et al., 2009). Additionally, this "closed" conformation appears to conceal the PDZ binding domain, thereby blocking PTEN binding to proteins that contain PDZ domain. Thus this conformational change blocks the activity of PTEN by controlling the recruitment of PTEN into the PTEN-associated complex (Vazquez et al., 2001).

4.3.3 PTEN regulation by protein-protein interaction.

PTEN functions can also be regulated through interaction with other proteins. These may play important roles in the regulation of PTEN activity during development, as key factor in alterations such as cancer (Hopkins et al., 2014) and neurodevelopmental disorders like ASD (Orrico et al., 2009). PTEN interaction with other proteins can regulate its function, including the cellular localization, as the kinase ROCK1 (rho-associated,

coiled-coil-containing protein kinase), which regulates the recruitment of PTEN to the membrane (Li et al., 2005); PTEN stability, as the FRK (Fyn-related kinase) through ubiquitination (Hopkins et al., 2014); PTEN conformation or regulation of phosphatase activity (Hopkins et al., 2014), as PREX2a (PIP₃-dependent RAC exchange factor 2a) that binds to PTEN in the PDZ-binding domain, the catalytic phosphatase and the C2 domain, inhibiting lipid phosphatase activity (Hodakoski et al., 2014).

A relevant interaction for the cellular location control of PTEN is that performed through PDZ binding domains, regulating membrane ruffling and cell spreading (Leslie et al., 2000, 2001; Tolkacheva and Chan, 2000). The molecular basis of protein-protein interaction mediated by PDZ domains has been extensively investigated, but its implication in some diseases remains unclear. PDZ domain may contribute to stabilize PTEN at particular subcellular localizations, where regulation of its function takes place (Valiente et al., 2005). In this context, several PDZ-domain containing proteins are scaffolding proteins enriched at cell junctions, which are involved in the assembling and maintenance of multimolecular signaling complexes in the postsynaptic densities of neurons and in tight junctions of cells (Valiente et al., 2005). By doing so, PTEN is able to bind to numerous scaffolding proteins, such as MAGI-1/2/3 (Membrane-associated guanylate kinase, WW and PDZ domain-containing protein 1/2/3), the human homolog of the *Drosophila* Dlg (hDlg/SAP97) or PSD95 (postsynaptic density protein-95), and the Ser/Thr kinase MAST205 (Microtubule-associated serine/threonine-protein kinase). In the postsynaptic density of excitatory synapses, PDZ proteins like PSD-95 organize glutamate receptors and their accompanying signaling proteins, determining the size and strength of synapses (Kim and Sheng, 2004) and modulating synaptic plasticity (Jurado et al., 2010). Particularly, PTEN is implicated in the modulation of NMDAR-dependent LTD through the interaction of the PDZ binding motif and PSD-95 (Jurado et al., 2010).

4.4 PTEN in the CNS.

The PI3K pathway is crucial for an appropriate function of the CNS. Specifically, PTEN modulates neuronal cytoarchitecture, and synaptic number and size. At the functional level, PTEN is recruited to the postsynaptic terminal upon LTD induction (Jurado et al., 2010). Thus, opposing the function of PI3K in maintaining PIP₃ at the postsynaptic terminal to sustain basal synaptic transmission and LTP expression (Arendt et al., 2010).

4.4.1 PTEN function in neuron morphology.

In the central nervous system, PTEN is essential for development and maintenance of the structure and function of the circuit. PTEN is widely expressed in the brain, where it controls cell proliferations and growth, leading to brain overgrowth upon *Pten* haploinsufficiency (*Pten*^{+/-}) (Clipperton-Allen and Page, 2014), through β -catenin signaling (Chen et al., 2015); or upon *Pten* conditional deletion (Groszer et al., 2001).

In the brain, PTEN negatively regulates neural stem cell proliferation during embryonic development (Groszer et al., 2001), as well as in adult neural stem cells from dentate gyrus (Amiri et al., 2012). Ablating PTEN results in higher proliferation rates and accelerated differentiation, thus *Pten*-deleted progenitor cells develop into hypertrophied neurons with abnormal polarity, resulting in macrocephaly and abnormal social behavior (Amiri et al., 2012).

Studies in post-mitotic neurons highlight PTEN importance in controlling neuronal development at different stages. One of the most used mouse model with *Pten* deletion, specifically in differentiated cortical and hippocampal neurons, present macrocephaly, somatic and dendritic hypertrophy, accompanied by growth of ectopic dendritic branches with increased spine density and altered neuronal polarity (Kwon et al., 2006). In addition, ectopic and hypertrophic axons were observed, accompanied by an increased size of presynaptic terminals containing more vesicles (Kwon et al., 2006). It has been shown that some of these effects, derived from deletion of *Pten* in post-mitotic neurons, can be reversed by rapamycin, the inhibitor of mTOR (Zhou et al., 2009). In fact, rapamycin can prevent or reverse macrocephaly, neuronal hypertrophy and altered neuronal polarity in *Pten* mutant mice, depending on the age in which the treatment has been administered (Zhou et al., 2009).

Recent studies examining the effect of shRNA knockdown of PTEN in the basolateral amygdala and dentate gyrus of adult animals have led to some controversy in the field, claiming that *Pten* deletion does not alter overall spine density, but induces changes in spine morphology, from thin protrusions to mushroom spines, a

more mature form of spines (Haws et al., 2014). As previously described in others Pten-deleted mice, these neurons are hypertrophic, with increased soma size and dendritic diameter, but not length (Haws et al., 2014).

Overall, PTEN controls cell proliferation, growth and morphology in the CNS, as alterations in PTEN function or levels generally result in aberrant brain growth and neuron hypertrophy.

4.4.2 PTEN's role in synaptic function.

i. Synaptic transmission.

Structural changes derived from the deletion of PTEN (Kwon et al., 2006), could be accompanied by profound alterations in synaptic transmission due to hyperconnectivity. For example, excessive axonal branching and connectivity between the mPFC and the BLA is observed in germ-line heterozygous Pten mutant mice (Huang et al., 2016). Moreover, in the BLA, the deletion of PTEN causes increased frequency and amplitude of miniature excitatory postsynaptic currents (mEPSCs), accompanied by an increase of the mushroom-shaped spines density (Haws et al., 2014). Similar functional results were observed in DG granule cells (Luikart et al., 2011). Additionally, deletion of PTEN in striatal and DG cells results in an increase of the magnitude of glutamatergic and GABAergic evoked synaptic responses, accompanied by an increase in the number of vesicles available for release (Kwon et al., 2006; Weston et al., 2012).

Deletion of Pten in postnatally generated DG neurons are sufficient to cause seizures (Pun et al., 2012). Such hyperexcitability may be a physiological basis for epilepsy accompanying ASD. Indeed, PTEN mutations were documented in patients with an autism epilepsy phenotype (AEP)(Marchese et al., 2014). This suggests that epilepsy may be due to the loss of PTEN function and the consequent increase of neuronal activity reaching pathological levels. It seems that the appearance of seizures depends on the stage at which PTEN is removed. PTEN deletion in developing DG neurons are hyperexcitable, as a consequence of increased excitatory synaptogenesis, inducing seizures (Williams et al., 2015). On the other hand, conditional deletion of PTEN in auditory cortical neurons of young adult mice enhances synaptic inputs from the cortex and thalamus, but only subtly alters the firing patterns (Xiong et al., 2012).

ii. Synaptic plasticity.

Alterations in PTEN function or protein levels results in macrocephaly and hyperconnectivity; however, it is also involved in the mechanisms underlying synaptic plasticity.

Electrophysiological recordings from CA1 neurons from adult Pten^{+/-} mice revealed that basal synaptic transmission remained normal, while LTP was decreased and LTD is completely blocked(Wang et al., 2006). Suggesting that PTEN is directly involved in both forms of synaptic plasticity, but it is essential for LTD induction (Wang et al., 2006).

Consequences of postnatal deletion of Pten on synaptic transmission outcome are quite variable, depending on the area and the age where deletion took place. Basal synaptic transmission remains normal in the CA1 in all ages (Sperow et al., 2012; Takeuchi et al., 2013), while it is altered in middle aged DG neurons. LTP is decreased in DG and CA1 in adult and old mice (Sperow et al., 2012; Takeuchi et al., 2013) , but increased in the DG and remained normal in the CA1 from young animals (Takeuchi et al., 2013). Attending to synaptic depression, NMDA-dependent LTD results absent in CA1 from adult Pten deleted animals (Sperow et al., 2012), meanwhile mGluR-dependent LTD, another form of LTD dependent on glutamatergic metabotropic receptors, remained normal, but is decreased in the DG (Takeuchi et al., 2013). Postnatal deletion of Pten results in changes in synaptic plasticity without affecting morphology of excitatory synapses (Sperow et al., 2012). Indeed, synaptic deficits upon Pten deletion precedes morphological abnormalities (Takeuchi et al., 2013). These results suggests that Pten independently controls the functional and structural properties of the synapses (Sperow et al., 2012).

The exact mechanism by which PTEN controls synaptic plasticity is not fully understood, specially taking into account the pleiotropic effect observed in Pten deleted mice studies. In contrast, altering PTEN function acutely with a PTEN specific inhibitor in organotypic hippocampal slices blocks only NMDAR-dependent LTD, while basal synaptic transmission, LTP or mGluR-dependent LTD remains unaltered (Jurado et al., 2010). Thus, PTEN lipid phosphatase activity is needed specifically for NMDAR-dependent LTD, while it is not needed for LTP or mGluR-LTD (Jurado et al., 2010). This reflects certain consistency with previous studies in which, in

most cases, LTD is abolished upon Pten deletion, but LTP results altered in different ways depending on the brain region and on the age of the mice that are considered (Sperow et al., 2012; Takeuchi et al., 2013).

Mechanistically, activation of NMDA receptors during LTD induces the association between PTEN and the PSD-95, a scaffolding protein that drives the recruitment and anchoring of PTEN at the PSD (Jurado et al., 2010), through the interaction of the PTEN PDZ binding domain with the PDZ domains 1-2 of PSD-95 (Knafo et al., 2016). This increased in the interaction is specific for PSD-95, as MAGI-2 association with PTEN was not altered upon NMDAR activation (Jurado et al., 2010). Indeed, the importance of the PDZ motif for NMDAR-dependent LTD was confirmed using a knock-in mouse lacking the PDZ motif (PTEN- Δ PDZ), which has normal basal synaptic transmission and LTP, but impaired NMDAR-dependent LTD in the hippocampus. Hence, PDZ binding motif is essential for the maintenance of the NMDA-dependent LTD in the hippocampus (Knafo et al., 2016).

The mechanism by which PTEN modulates NMDAR-dependent LTD modulation is not completely clear. The downregulation of PIP₃ in the synaptic membrane leads to increased mobility of AMPARs, which elicits a decrease of synaptic AMPARs and leads to synaptic depression (Arendt et al., 2010), so the modulation of the PIP₂-PIP₃ balance in the synaptic membrane could be of vital importance for synaptic plasticity. Additionally, PTEN is able to bind to NMDARs, modulating its surface expression and functionality through its protein phosphatase activity (Ning et al., 2004). On the other hand, PTEN activity during LTD could be important for downstream regulation of PIP₃ pathway, given that GSK3 is required for LTD (Peineau et al., 2009a) and PTEN causes the pathway inactivation and dephosphorylation of GSK3, activating it (Cohen et al., 1997).

To summarize, PTEN seems to be essential for NMDAR-dependent LTD and this function requires the lipid phosphatase activity and the PDZ binding domain. On the other hand, when PTEN is altered in vivo, major forms of synaptic plasticity are altered, especially those leading to synaptic depression, which probably contributes to the cognitive impairment seen in PTEN associated diseases, as autism with macrocephaly.

5 PTEN in autism spectrum disorder.

Individuals with germline heterozygous mutations in PTEN develop a specific type of ASD named PTEN-ASD (Frazier et al., 2015). During the last decade it has been reported a prevalence of 7% of PTEN mutations in ASD patients (Tilot et al., 2015). Prevalence of PTEN mutations could be underestimated because they are found through screening of genomic DNA from blood or saliva, mostly limited to the coding region, while very few studies have examined the promoter and exon-flanking sequences, which could influence PTEN levels (Zhou and Parada, 2012). Additionally, PTEN could be regulated within specific brain regions, for example, through epigenetically mechanisms, which would not be detected analysing peripheral blood (Zhou and Parada, 2012).

Compared with patients with idiopathic (non-PTEN) ASD and healthy controls, PTEN-ASD patients express less PTEN protein, which is associated with macrocephaly, significant white-matter abnormalities, enlarged perivascular spaces and impaired cognition (Frazier et al., 2015; Vanderver et al., 2014). Indeed, most children with PTEN mutations have macrocephaly, making it a predominant aspect of the clinical presentation of PTEN-ASD (Williams et al., 2008). Generally, the degree of macrocephaly in PTEN-ASD patients is more severe than in other genetic autism syndromes (Tilot et al., 2015).

Combined with ASD core features and macrocephaly, PTEN-ASD patients suffer from other alterations or comorbidities, as motor difficulties, including delays in independent walking and alterations in usual motor patterns (Tilot et al., 2015). Abnormal language development have also been found in patients with PTEN-ASD, with delays in the beginning of verbal communication and reduced scores in verbal ability (Tilot et al., 2015). Recently, cases of epileptic seizures have been reported in PTEN mutation-positive individuals, frequently linked to cortical dysplasia (Tilot et al., 2015). Another comorbidity is intellectual disability that appears in 47% of the cases and, additionally, borderline-to-low average intellectual functioning in 29% of the PTEN-ASD patients (Tilot et al., 2015). Slow processing speed and important deficits in working memory have also been observed (Frazier et al., 2015).

5.1 PTEN mutations related to ASD.

Most germline PTEN-ASD related mutations are point mutations, including nonsense mutations, missense mutations and single base pair insertion (Zhou and Parada, 2012). It is not easy to correlate PTEN mutations with specific phenotypes, due to the high heterogeneity observed, and since the phenotype of PTEN mutation carriers is strongly affected by other factors, such as genetic background or environmental factors (Leslie and Longy, 2016).

A higher dominance of missense mutations has been related to macrocephaly (Leslie and Longy, 2016). One example is the missense mutation found in the exon 8 of Pten gene (Buxbaum et al., 2007), which is located within the C2 domain important for phospholipid membrane binding (Lee et al., 1999). This *de novo* mutation was identified in a patient with macrocephaly, mental retardation, and with motor, language and speech delay (Buxbaum et al., 2007). Another *de novo* mutation, a nucleotide substitution in the exon 5, was found in a macrocephalic child with abnormal white matter and developmental delay, including communication, social interaction and motor skills delayed (Orrico et al., 2009). In the same study, another nucleotide change was found in the exon 6, which leads to a phenotype of severe autism, speech delay and absence of social interaction, with macrocephaly and mental disability (Orrico et al., 2009). The functional relevance of these mutations relies in the position with respect to the catalytic domain of PTEN.

It seems that ASD-associated PTEN mutations affect differently to AKT inhibition than those with more severe cancer phenotypes (Tilot et al., 2015). The PTEN autism-associated mutations retain the ability to suppress PIP₃-AKT signalling, but most of them are highly unstable, which leads to a considerable reduction in protein abundance, decreasing PTEN biological activity (Spinelli et al., 2015). Opposite to the mutations usually found in PHTS patients, characterized by the accumulation of stable inactive protein, leading to more severe functional impairment (Tilot et al., 2015).

Regardless the high number of clinical and laboratory based studies evidences reported during the last decade, phenotypic effect of germline PTEN mutations are extremely variable, even within a single mutation (Tilot et al., 2015). The exact molecular, synaptic and cellular mechanisms leading to this disorder are not fully understood. Hence, more studies are needed to relate connectivity failures seen in PTEN-ASD patients (Hull et al., 2017) and the molecular processes involved.

5.2 Pten mouse models of ASD.

During the past years many PTEN disrupted mice have been generated with macrocephaly and abnormal social behavior, generally combined with other behavioral deficits (Tilot et al., 2015). The detailed information of the phenotype of PTEN mouse models can be found in table 1 (Annex I).

PTEN homozygous deletion is lethal by embryonic day 7.5. Therefore, heterozygous and conditional Pten deleted mice have been developed to obtain models for Pten loss in the CNS (Tilot et al., 2015). The first mouse model developed was the Nse-Cre Pten^{loxP/loxP}, with conditional Pten deletion from differentiated cortical and hippocampal neurons (Kwon et al., 2006). These mice, which morphological and electrophysiological phenotypes were described before, present behavioral phenotypes reminiscent of human ASD, including reduced sociability, combined with higher anxiety-like behavior, seizures, learning deficits and increased nociception (Kwon et al., 2006; Lugo et al., 2014).

Gfap-Cre; Pten^{loxP/loxP} mice, in which the deletion is restricted to the cortex, cerebellum and hippocampus, develop altered social and repetitive behaviors with lower anxiety-like behavior, decreased contextual fear conditioning and hyperactivity (Lugo et al., 2013, 2014). In addition, Gfap-Cre; Pten^{loxP/loxP} mice present a decrease in the synaptic scaffolding proteins PSD-95 and SAP102, as well as mGluR signaling, suggesting a relationship between social behavior regulated by PTEN and synapses (Lugo et al., 2014).

Another mouse model of PTEN-related ASD is the Pten^{m3m4}, a knock-in mice with decreased amount of nuclear PTEN and protein dosage, which presents macrocephaly and neuronal hypertrophy, but increased sociability in males; suggesting the importance of Pten subcellular localization in regulation of proliferation, cell size and behavior (Tilot et al., 2014). Despite the social behavior observed in these animals, PTEN misslocalization produces alterations in the expression of genes related to ASD, placing PTEN upstream in the pathogenesis

(Tilot et al., 2016). Particularly, PTEN misslocalization leads to a downregulation of synaptic pathways genes expression (Tilot et al., 2016), reinforcing the hypothesis of synaptic alteration as ASD causative mechanism (Sperow et al., 2012).

Often, Pten mutations found in peripheral blood samples from ASD patients are heterozygous mutations (Zhou and Parada, 2012). A mouse model with Pten haploinsufficiency ($Pten^{+/-}$) shows macrocephaly, social deficits and increased repetitive behaviors; combined with decreased anxiety, aggressive behavior and impaired fear conditioning (Clipperton-Allen and Page, 2014, 2015; Page et al., 2009). $Pten^{+/-}$ phenotype is exacerbated when it is combined with *Serotonin transporter* haploinsufficiency ($Slc6a4^{+/-}$) (Page et al., 2009). Thus, it seems that both Pten and *Serotonin transporter* cooperatively contribute to brain size and social behavior, reinforcing the “multi-hint” model of cooperation of different signaling pathways to social behavior (Zhou and Parada, 2012).

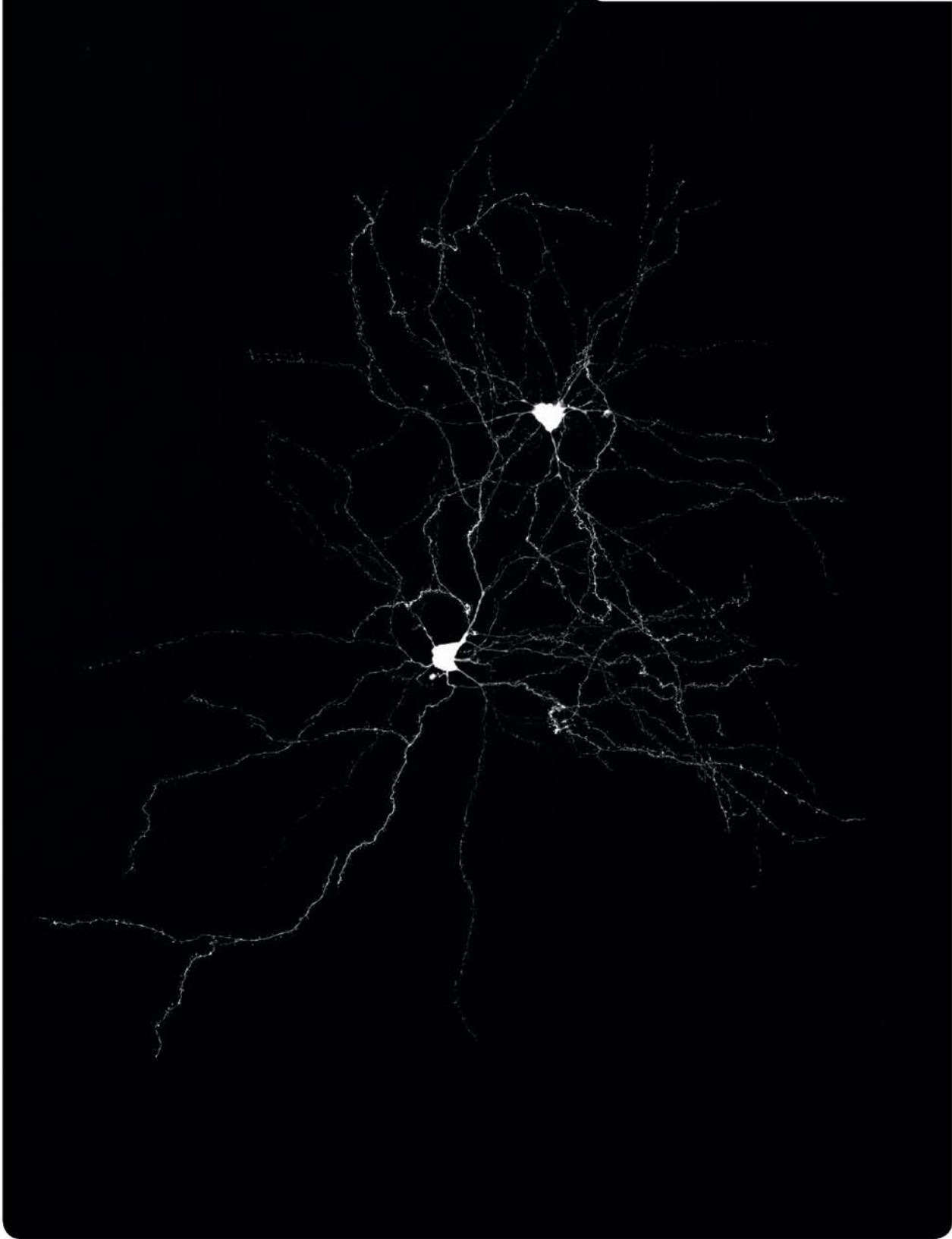
Finally, the ASD-model resulting from prenatal exposure to valproic acid (VPA) results of special interest, it is not a Pten-mutated model, but presents alterations in PTEN protein levels in multiple brain areas. VPA treated animals present ASD-related behavior, such as social impairments and developmental delays, and increased spine density (Yang et al., 2016). VPA-exposed offspring exhibited other alterations in behavior, in addition to impaired sociability and increased repetitive behaviors, that have been described as comorbidities in ASD patients, including anxiety, depression-like behavior and abnormal nociception (Wu et al., 2016). These animals showed lack of NMDAR-dependent LTD and altered depotentiation (DPT), a distinct type of long-lasting synaptic depression that consist in a reversion of pre-established LTP (Peineau et al., 2009b), in the cortico-lateral amygdala electrophysiological recordings, emphasizing the amygdala complex role in socio-emotional behavior (Baron-Cohen et al., 2000; Gallagher and Chiba, 1996), and increased GSK-3 β phosphorylation (Wu et al., 2016). Both social behavior impairment and GSK-3 β phosphorylation were recovered treating the animals with the PI3K inhibitor wortmanin (Wu et al., 2016). This data suggests that NMDAR-synaptic plasticity in the LA and the PIP₃ pathway are crucial in core-ASD behaviors, pointing to the hypothesis of ASD as a synaptic pathology (Brose et al., 2010; Wu et al., 2016).

Although neurological consequences of PTEN loss have been extensively studied, the consequences and potential benefits of elevating PTEN in the brain remain unknown. In this PhD dissertation, I describe the role of PTEN in cognition, a term that includes the processes of memory and learning; and emotion, including sociability and emotional memories. I aim to take advantage of two transgenic mouse lines with PTEN abnormalities to explore the relationship between PTEN activity and socio-emotional and cognitive behaviour. Using a variety of approaches I could explore these phenomena at multiple levels. The in-depth study of these features upon PTEN modification could lead to a better understanding of the behavioural and cognitive abnormalities observed in human PTEN-ASD patients in a way that will serve to define new targets for possible future treatments.

The first chapter is focused on the effect of PTEN overexpression on cognitive function and on emotional memory. To this end, I analysed a *Pten* transgenic (*Pten^{tg}*) mice carrying additional genomic copies of *Pten* and thus expresses ~2-fold levels of *Pten* over normal levels across their body, accompanied by a downregulation of PIP₃ pathway (Ortega-Molina et al., 2012). Apart from being particularly small, these mice present a significant extension of life span, lower cancer incidence, increased energy expenditure and protection from metabolic pathologies (Ortega-Molina et al., 2012). During this thesis, I have investigated the morphological, behavioral and synaptic consequences of PTEN overexpression. Specifically, I have observed in these mice a significant microcephaly together with neuron dystrophy and hypoconnectivity, complemented by a decrease in the activity of multiple brain areas. These alterations are accompanied by severe cognitive impairment as well as a plasticity shift towards depression in hippocampus and amygdala. Nevertheless, overexpression of PTEN results also in beneficial consequences as *Pten^{tg}* mice present a prosocial behavior and lower levels of anxiety, an interesting fact attending to PTEN-ASD, as these phenotypes results opposite to those observed in most of *Pten* deleted mice (Kwon et al., 2001; Page et al., 2009; Tilot et al., 2014).

In the second chapter, to further understand the regulation of PIP₃ pathway by PTEN, I used PTEN-ΔPDZ animals (Knafo et al., 2016), a knock-in mouse model in which PTEN lacks the last five amino acids (-QITKV, the PDZ binding motif). The effect of genetically preventing PDZ-dependent PTEN interactions enhance the understanding of the function and specificity of this modulation, exploring whether PTEN alteration effects depend on canonical functions of the protein, cell growth and proliferation, or if they are PDZ-dependent, as for example synapse-specific functions of PTEN (Jurado et al., 2010). The importance of the PDZ motif for hippocampal NMDA-dependent LTD has previously been analyzed, observing that PTEN-ΔPDZ mice have normal basal synaptic transmission and LTP when compared to WT mice, but impaired NMDA-dependent LTD in the hippocampus (Knafo et al., 2016). Regardless of PTEN-ΔPDZ mice do not present differences in body size or in PIP₃ pathway modulation, significant macrocephaly has been found. Interestingly, despite of the fact that there were no differences in anxiety or spatial and emotional memories, PTEN-ΔPDZ animals showed impaired sociability. Compromised sociability is accompanied by alterations in synaptic physiology, resulting crucial the role of PTEN in LTD, specifically in the cortical input of the lateral amygdala, pointing to a relation between synaptic plasticity in the lateral amygdala and social behavior. These data offer important information about the role of PTEN in social behavior and demonstrate that sociability can be modulated bi-directionally.

Objectives

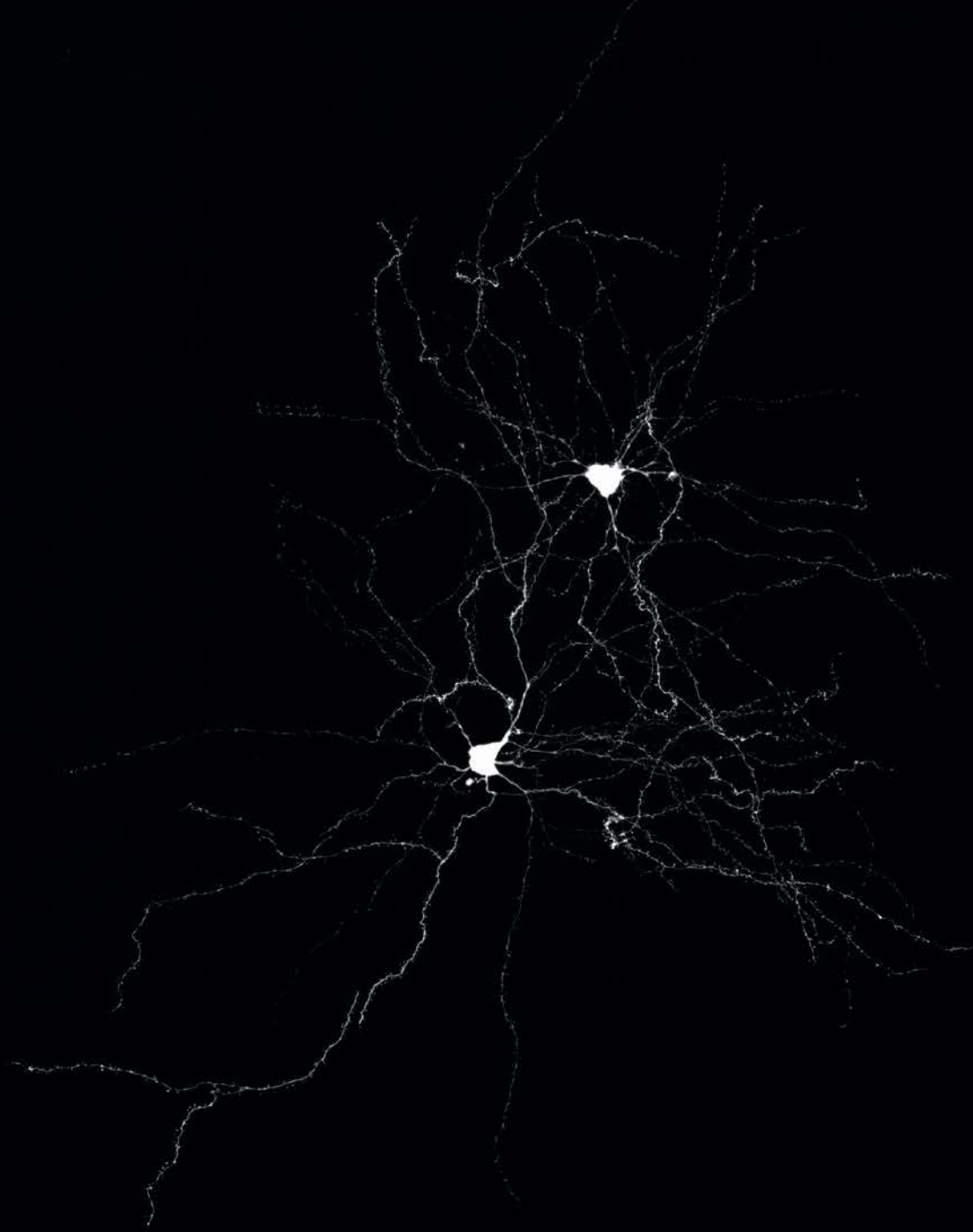


Changes in PTEN expression and function predict alterations of the PI3K pathway, which, for reasons that remain unclear, are associated to PTEN-ASD. The wide range of social behaviours that we find in the normal population could also be the result of variable activation of this pathway within physiological levels. Thus, finding the mechanisms by which PTEN governs social behaviour and cognition is important for both physiological and pathological conditions. In order to test whether the PI3K pathway controls social cognition, and the role of PTEN in this process, I have evaluated the consequences of up- or down-regulating the PTEN function, using genetic approaches, coupled to behavioural and electrophysiological functional assays. These studies were focused on the hippocampus and the amygdala, known as key brain regions for the pathology of ASD(Ecker et al., 2015).

To address this issue, the aims of the present work were:

- 1.- To evaluate Pten overexpression and the implications of PTEN-PDZ interactions in brain growth, both in the hippocampus and amygdala.
- 2.- To assess the effect of Pten overexpression on principal neuron morphology.
- 3.- To investigate the role of PTEN and PTEN-PDZ interactions in synaptic structure and formation in the hippocampus and the amygdala.
- 4.- To determine the role of PTEN and its PDZ interactions in synaptic plasticity in the hippocampus (CA3-CA1) and the amygdala (thalamic and cortical input to the LA).
- 5.- To study whether PTEN controls the activity of different brain areas, under basal conditions and during associative learning (fear conditioning).
- 6.- To evaluate whether synaptic functions controlled by PTEN could be related to cognitive function, particularly those defined as ASD core symptoms: communication, sociability and stereotyped behavior, as well as related comorbidities, including locomotor activity, nociception and anxiety.

Materials & Methods



Subjects

The animals used for this study were adult mice (6-12 months), with the exception of USV experiments (P3-P12). All mice used were housed in cages type 2L of 500 cm³ (maximum of 5 animals per cage) in standard conditions of temperature (22±1 °C), humidity (40-60%) and on a 12 h light/dark cycle (lights on at 8:00, with 30 min of dawn/sunset). Animal house air filtration is done by HEPA (high-efficiency particulate air) absolute filters, with a rate of 20 air renovations per hour. Animal cages are in auto-ventilated racks IVC (individual ventilated cages) with absolute filters. Irradiated standard safe diet and autoclaved water were available ad libitum. All biosafety procedures and animal care protocols were approved by the bioethics committee from the Consejo Superior de Investigaciones Científicas (CSIC), and were carried out according to the guidelines set out in the European Community Council Directives (86/609/EEC).

***Pten*^{tg} mice** are a transgenic mouse line with moderate *Pten* overexpression driven by its own transcriptional regulatory elements. These mice were generously donated to us by *Dr. Manuel Serrano* (Centro Nacional de Investigaciones Oncológicas, Madrid). Transgenesis procedures to generate these mice were recently described (Ortega-Molina et al., 2012). The genetic background is C57BL6/CBA (75%:25%). Genotyping was carried out by Polymerase Chain Reaction (PCR) using the following primers: Forward-T7: 5'-CCGCTAATACGACTCACTATAGGG-3' and Reverse-T7: 5'-TCATCTCGGCTCCATCGTTT-3'.

PTEN-ΔPDZ mice. This is a new mouse strain in which PTEN lacks the C-terminal PDZ binding motif. It was created using a knock-in strategy by *Dr. Andrew Chan* (The Chinese University of Hong Kong). The *Pten*^{tm(Q399stop)amc} (abbreviated as PTEN-ΔPDZ) knock-in mouse generation has been previously described (Knafo et al., 2016). The PDZ-binding motif was deleted by substituting codon 399 (CAA) with a stop codon (TAA). Genotyping was carried by PCR using the following primers: 5'-GCTGAAGTGGCTGAAGAGCTCTGA-3' and 5'-TTGAGTGAACTGATGAGGTATGG-3'.

Unbiased Stereology

A group of animals were intraperitoneally anesthetized with 16% chloral hydrate and transcardially perfused with saline solution (0.9% NaCl) followed by 4% paraformaldehyde prepared in phosphate buffer (PBS; 0.1 M, pH 7.4). The extracted brains were postfixed using 4% paraformaldehyde overnight. Subsequently, brains were saturated in sucrose gradient solutions: initially brains are placed in a 7% sucrose solution until they sink, and they are then transferred to a 32% sucrose solution with shaking, at 4°C. Serial sections (40μm, every 6th section) of coronal sections were cut in a vibratome Leica VT1200S and cryoprotected by submerging them in an antifreezing solution composed of 3% glycerol (C₃H₈O₃, Panreac ref.141339) and 3% ethylene glycol (CH₂OHCH₂OH, Panreac 141316) in PBS and frozen at -20°C. Subsequently, sections 1, 3 and

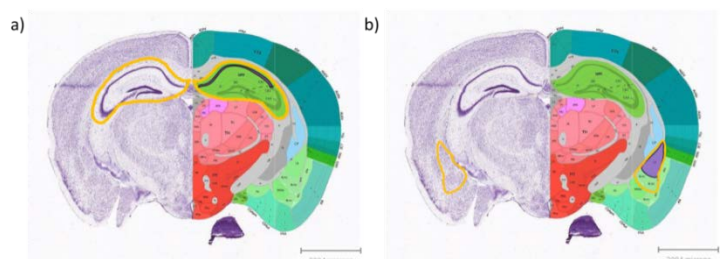


[Figure 6] Coronal slices from mouse brain. Delimitation of hippocampus (a) and basolateral amygdala (b) by a yellow line. Purple shade showing CA1 pyramidal layer (a) and Lateral amygdala nucleus (b). Both panels show Nissl staining on the left and atlas scheme on the right. Modified from Allen mouse brain atlas.

Subsequently, sections 1, 3 and

6 were stained with 0.1% cresyl violet (FLUKA Ref. 61123; Niessl staining), and mounted on histological glass slides with DPX mount (Sigma).

The slices were taken for stereological quantification to measure the volumes of whole forebrain, hippocampus, CA1 hippocampus subsection, basolateral amygdala and lateral nucleus of the amygdala. The above sub-regions were distinguished according to the Allen mouse brain atlas (Fig. 6) (Copyright©2016, Allen Institute for Brain Science, available from mouse.brain-map.org) using a light microscope (Leica DRIV microscope) equipped with a MicroFire digital camera (Optronics) and a motorized stage using a 5x objective lens. Cell number in the hippocampus and amygdala was measured using unbiased stereology, in which samples are taken in such a way that all sampling units in the population had the same probability of being within the given sample (C. V. Howard, 1998).

The volume was calculated with StereoInvestigator software v10 (Micro-BrightField Biosciences, Williston, VT), according to Cavalieri's estimator. Any incomplete stained or torn section was considered a random event, designated missing and then accounted for in the stereological estimate using the fractionator principle. The counting frame was 25x25 μm , the sampling grid was 70x70 μm , the dissector height was 30 μm and the interval was 6 for hippocampus and 2 for amygdala. The precision of our stereological counts was determined by the Gundersen coefficient of error (CE) equation.

Cell counting was performed in CA1 from hippocampus (counting frame 15x15 μm , sampling grid was 65x65 μm , dissector height 30 μm , interval 6) and lateral amygdala (counting frame 14x14 μm , sampling grid was 45x45 μm , dissector height 30 μm , interval 2) using the optical fractionator method in StereoInvestigator software. Cells were marked only if their edges were within the dissector area and they did not intersect forbidden lines. Cells were also marked if they came into focus as the optical plane moved through the height of the dissector. The precision of our stereological counts was determined by the Gundersen coefficient of error (CE) equation (Gundersen et al., 1999; Knafo et al., 2009; Pêgo et al., 2008). This method of sampling and the section intervals were tested in a pilot experiment to ensure that the estimation of the number of cells was representative of their total number.

Neuronal Morphology

To analyze neuron morphology we have filled pyramidal neurons in lateral amygdala in acute slices from adult mice (6-12 months). Principal neurons in the LA were filled during 15 minutes with biocytin during patch clamp recording. Slices were fixed overnight with 4% paraformaldehyde, 4% sucrose in PBS and treated with streptavidin Alexa 488 (1:500, S-32254 ThermoFischer) during 48 hours. Slices were mounted using Prolong Diamond Antifade reagent (P-36970 ThermoFischer).

Neuron images were acquired with a confocal LSM710 microscope using the 40x/1.30 EC "Plan-Neofluar" Oil DIC M27 objective and the Argon 488 nm laser line. I used a tile-scan application to obtain images of the whole neuron, including the dendritic tree. To analyze whole neuron morphology, image stacks were imported to the Neurolucida software (MicroBrightField Inc., Williston, VT) and the neuronal dendritic trees were three-dimensionally traced by marking the dendrites and the bifurcation points while focusing up and down in the stack. A Sholl analysis was performed for each neuron by automatically calculating the number of dendritic intersections and the dendritic length at 10 μm intervals starting from the soma. Total dendritic length and total number of intersections for each neuron were also calculated as an index of dendritic complexity. Tortuosity is calculated as the actual length of a segment divided by the distance between the endpoints of the segment (a straight segment will have a tortuosity of 1).

In order to analyze spine density, dendrite images were acquired with the confocal LSM510 META microscope, through 63 X/1.4 oil Plan-Apochromat M27 objective with a calculated optimal zoom factor of 3.2 and a z-step of 0.14 μm (voxel size, 75.1 X 75.1 X 136.4 nm). To analyze spine density, after image acquisition, the stacks were processed with a three-dimensional blind deconvolution algorithm to reduce the out-of-focus light through Huygens software (Huygens 4.3.1p2 64b S.V.I.). Image stacks were then analyzed with Neurolucida software. Dendrites were traced from the image in three dimensions, and spines were marked during tracing. All protrusions were considered spines. The reconstructed data were exported to Neurolucida Explorer (MicroBrightField Inc., Williston, VT) for quantitative analysis. Total spine density was calculated for each dendrite by dividing the number of spines by the dendritic length. Spine density was

also analyzed as a function of its distance from soma through Sholl analysis, by carrying out this calculation for consecutive segments every 10 μm distance from the soma (Knafo et al., 2009).

Electron Microscopy

Mice were anesthetized with an intraperitoneal injection of TioBarbital (346836, Braun) and perfused with a mixture of paraformaldehyde (4%) and glutaraldehyde (2%) in PB. Brains were postfixed in the same solution overnight. The brains were cut into coronal sections that were postfixed in 1% osmium tetroxide (in 0.1 M cacodylate buffer), dehydrated in ethanol and embedded in Epon-Araldite. Serial ultrathin sections of the CA1 region or the lateral amygdala were collected on pioloform-coated, single-hole grids, and stained with uranyl acetate and lead citrate. The sections were analyzed with a JEM-1010 transmission electron microscope (Jeol, Japan) equipped with a side-mounted CCD camera Mega View III from Olympus Soft Imaging System GmbH (Muenster, Germany). Synapses were sampled randomly in the proximal part of stratum radiatum or in the lateral amygdala and imaged at a magnification of $\times 75,000$ (~150 synapses per mouse, $n = 3$ mice per group). The area of dendritic spines and the length of the PSD were measured with the AnalySIS software (Soft Imaging System GmbH).

Electrophysiology

Slice preparation.

Field recordings: Experimental animals were decapitated, and whole brains were dissected and placed in ice-cold Ca^{2+} -free dissection solution (10 mM D-glucose, 4 mM KCl, 26 mM NaHCO_3 , 233.7 mM sucrose, 5 mM MgCl_2 , 1:1000 Phenol Red) saturated with 5% $\text{CO}_2/95\% \text{O}_2$, to let the brain chill for 1 minute. Slice cutting (300 μm) was done in the same solution using the vibratome Leica VT1200S and kept for 1 h in artificial CSF (aCSF: 119 mM NaCl, 2.5 mM KCl, 1 mM NaH_2PO_4 , 26 mM NaHCO_3 , 11 mM glucose, 1.2 mM MgCl_2 , 2.5 mM CaCl_2 ; osmolarity adjusted to 290 mOsm), gassed with 5% $\text{CO}_2/95\% \text{O}_2$ at 25 °C for recovery. Subsequently, slices were transferred into a submersion-type recording chamber perfused with aCSF at 25°C in the electrophysiology set-up (Knafo et al., 2016; Mathis et al., 2011).

Whole-cell recordings: Mice were anesthetized with an intraperitoneal injection of TioBarbital (346836, Braun) and then transcardially perfused with cold choline-aCSF (92 mM choline chloride, 2.5 mM KCl, 1.25 mM NaH_2PO_4 , 30 mM NaHCO_3 , 20 mM HEPES, 20 mM glucose, 2 mM thiourea, 5 mM sodium ascorbate, 3 mM sodium pyruvate, 0.5 mM CaCl_2 , 3 mM MgSO_4 , pH 7.35) and decapitated. 300 μm thick coronal slices containing the amygdala and the hippocampus were prepared in the same solution using a vibratome. Slices are then embedded for 10 minutes in the same solution at 32 °C and transferred to a recovery chamber with HEPES holding aCSF (92 mM NaCl, 2.5 mM KCl, 1.25 mM NaH_2PO_4 , 30 mM NaHCO_3 , 20 mM HEPES, 25 mM glucose, 2 mM thiourea, 5 mM sodium ascorbate, 3 mM sodium pyruvate, 2 mM CaCl_2 , 2 mM MgSO_4 , pH 7.35). Slices are kept for 1h at 25 °C for recovery before transferring them into a submersion-type recording chamber perfused with aCSF saturated with 5% $\text{CO}_2/95\% \text{O}_2$ at 25°C in the electrophysiology set-up (Ting et al., 2014)

Field recordings in the lateral amygdala. Field potentials (fEPSPs) were recorded using aCSF-filled glass electrodes (1-3 M Ω) placed within the lateral nucleus of the amygdala; aCSF was used also as external solution. Field EPSPs were evoked by stimuli (100 μs) delivered through a bipolar electrode placed near the external capsule (for thalamic stimulation), just medial to the LA, and directly above the central nucleus of the amygdala, in the external capsule (for cortical stimulation). Field EPSPs slope was used to assess synaptic strength. An input/output (I/O) response curve was obtained by varying the intensity of single-pulse stimulation from 10 to 200 μA and averaging responses per intensity. The stimulus intensity that evoked a mean field potential equal to 50% of the maximum response was then used for all subsequent stimulations. The same intensity was used to deliver high-frequency stimulation (HFS), consisting of five trains at 100 Hz for 1 s, with 90 s intermission between trains) for induction of LTP. Before HFS was applied, the response to single stimuli had to remain stable for at least 20 min. LTP was estimated as the increase of the fEPSPs slope 1 h after HFS, expressed as the percentage of the baseline fEPSPs slope. Low-frequency stimulation (LFS) (900 pulses at 1 Hz) was applied to induce LTD at the same stimulus intensity. Before LFS

was applied, the responses to single stimuli had to remain stable for at least 20 min (Paul et al., 2008; Zschenderlein et al., 2011).

Field recordings in the hippocampus Field potentials (fEPSPs) were recorded from the stratum radiatum of CA1 with glass microelectrodes (tip diameter \sim 700 k Ω -1 M Ω) filled with aCSF, used also as external solution. Field EPSPs were evoked by stimuli (50 μ s) delivered through a bipolar electrode located in stratum radiatum, between CA3 and CA1. I/O curves and LTD were done as in amygdala. At least 20 minutes of stable baseline responses, 50% (for LTD) or 30% (for LTP) of the maximum response, were recorded prior to plasticity induction. Following the baseline period, a weak Theta-Burst stimulation is delivered (10 bursts of five stimuli, 100 Hz within burst, 200 ms interburst interval) to induce LTP. Induction of LTD is done as in the amygdala (Knafo et al., 2016).

Whole-cell patch-clamp in lateral amygdala (voltage clamp). We carried out whole-cell patch-clamp that will allow us to fill LA principal neurons for morphology analysis. This patch-clamp was done in acute slices (coronal sections of 300 μ m thick) in aCSF as external solution gassed with 95% O₂ and 5% CO₂. Patch recording pipettes (3-6 M Ω) were filled with internal solution containing 115 mM CsMeSO₃, 20 mM CsCl, 10 mM HEPES, 2.5 mM MgCl₂, 4 mM Na₂-ATP, 0.4 mM Na-GTP, 10 mM sodium phosphocreatine and 0.6 mM EGTA, 10 mM biocytin (SIGMA B4261), pH 7.25.

All electrophysiological data were collected with pCLAMP software (Molecular Devices).

Behavioral Assays

All mice used in this study were adult with the exception of the ultrasonic vocalization experiments, in which we used mice of 3- 12 days old. Behavioral tests were performed during the light period, from 09:00 to 15:00 h to avoid the influence of circadian hormonal fluctuations. Experiments were recorded using a tracking camera fixed above the behavior apparatus and connected to a computer. Any Maze Video Tracking System version 4.82 (Stoelting Co.) software was used for tracking the mice and scoring behavior. The animals were handled for 3 days before the beginning of the experiment, during 5 min each day in the experimental room. Experimental mice were transferred to the behavior testing room 30 min prior to beginning the first trial for habituation.

Novel object location is a cognitive test that takes advantage of rodent's innate preference for novelty to evaluate spatial memory in a hippocampal CA1-dependent manner (Assini et al., 2009). This assay was chosen because conventional reinforcement is not needed and it is not intrinsically stressful (Vogel-Ciernia et al., 2014). Stress is an important factor in mice, as it may affect cognitive performance in other spatial learning procedures, such as for example Morris water maze (Morris, 1984). The memory tests consisted of three phases: habituation period, acquisition and test trials. Mice were first habituated individually to an empty open-field box (35 cm wide \times 35 cm deep \times 15 cm high) for 30 min during three days before acquisition trial. An acquisition trial consisted of placing a mouse into the test box, which contained two identical objects placed in the corners of the experimental apparatus. After 5 minutes the mouse is removed from the test box and returned to its home cage. After a delay (retention period) of 30 min, the mouse was placed back into the test box for a test trial, consisted of switching the location of one of the objects. Location of the displaced object was counterbalanced for each animal. In the test trial, the mouse was reintroduced into the experimental apparatus for 5 min, and its behavior was recorded. A recognition index was calculated by dividing the total time spent exploring the displaced object by the total time spent exploring both objects during the test session. Therefore, a recognition index of 0.5 would correspond to equal exploration of both objects. Due to spontaneous tendency of rodents to explore the novel situation, it is expected that the subject will spend more time exploring the displaced object (recognition index > 0.5) (Murai et al., 2007).

Barnes Maze. The Barnes circular maze (Barnes, 1979) was employed to assess spatial reference memory by training an animal to locate a hidden escape tunnel located directly beneath one of 40 holes at the perimeter of a large circular platform, which was brightly lit to provide a low-level aversive stimulus. Mice learn the location of the escape hole with the help of spatial reference points. This maze is an

alternative to the Morris water maze (Morris, 1984) because is considered to be less anxiogenic, as it does not involve swimming. The Barnes maze consists of a flat, circular disk with twenty holes around its perimeter that permit the animal to exit the maze into an escape box. Only one hole is open (the scape hole), which has underneath a cage with clean bedding (the escape box). The maze was divided into four quadrants of equal size placing the scape hole in the middle of one of the quadrants equidistant from the sidewalls. The testing room contained numerous maze cues. The behavior of the animal was monitored with a video camera mounted on the ceiling above the center of the maze and computerized by a tracking system (Ethovision Noldus IT, Wageningen, Netherlands). The Barnes maze task was performed in two successive phases. The acquisition phase was divided into 4 training sessions (day 1–4) and one probe session (day 5). Each training session includes four trials of 5 minutes each with 30 s inter-trial intervals between trials 1-2 and 3-4, and a 30 minutes inter-trial interval between trials 2-3. The starting point was the middle of the maze, where the animals are place inside a wire cage during 30 s before each trial. A training session ended when the mouse entered the scape hole or when 5 min had elapsed, whichever came first. If the mouse did not find the scape hole within the 5 minutes of the trial, the experimenter gently guided the animal to the escape hole. In this case, 300 s was recorded as the escape latency. The mouse was then allowed to remain in the cage for 30 s. A 60 s probe session (day 5), during which the scape hole is closed, was performed 24 h after the last trial of the learning period. Different parameters of mice performance were analyzed: the latency to find the escape hole, total distance traveled until the scape hole is reached, the number of holes searched by each mouse before finding the escape hole (number of errors), mean speed, and time spent by the mouse exploring in each quadrant (to calculate the percentage of time spent in the quadrant in which the scape hole was placed at training) (FOX et al., 1998).

Reversal Barnes Maze. This reversal task evaluates the ability to change a routine behavior or something previously learned, and it depends on the orbitofrontal cortex. A day after the memory test, the location of the escape hole is changed to a different quadrant of the maze. The ability of the subjects to find the new location is evaluated as described previously, and quantified by the number of re-training sessions required to consistently choose the new hole (Crawley, 2004a).

Fear conditioning test is a classical “Pavlovian” conditioning used to investigate memory and emotional behaviors. Fear conditioning is an associative form of learning depending on hippocampus and amygdala, where animals learn to associate a previously neutral sensory stimulus (CS) with a coinciding aversive stimulus (US) (Pape and Pare, 2010). This test consists of three days trials: training, contextual test and cued test. Training and testing took place in a rodent observation cage (30 × 37 × 25 cm) that was placed in a sound-attenuating chamber. In the training (conditioning), the mouse was exposed to the conditioning context (CS) during 180 sec followed by a tone (CS, 20 seconds, 2 kHz, 85 dB). After termination of the tone, a footshock (US, 0.75 mA, 2 sec) was delivered through a stainless steel grid floor. Mice received three footshocks with an intershock interval of 60 s. Mice were removed from the fear conditioning box 30 seconds after shock termination and returned to their home cages. For memory testing in the contextual fear conditioning version, mice were placed back into the original training context for 5 min, during which no footshock was delivered. In the auditory-cued fear-conditioning version, animals were placed into a novel context (same cages, but with different walls, floor, and background odor), and after a 3 min baseline period, they were continuously re-exposed to the tone (same characteristics as at conditioning) for 5 min, but in the absence of shocks. The animal behavior was scored by an observer. Using a time-sampling procedure every 2 s, each mouse was scored blindly as either freezing or active at the instant the sample was taken. Freezing was defined as behavioral immobility except for movement needed for respiration (Fanselow MS, 2003). The cage is cleaned between animals with 0.1% acetic acid, in the training or contextual test, or with solutions containing oil essences with water in the cued test.

Pain threshold. One day after cued fear conditioning test, each mouse was placed individually in the conditioning chamber. After 120 s, the electric current was gradually increased at a rate of 0.05 mA/20 s until the animal showed the first signs of discomfort (moving backwards and flicking their hindlegs) or pain (jumping and vocalization). At this moment, the current was immediately switched off, and the corresponding current was recorded as a measure of the animal's discomfort/pain threshold.

SHIRPA is a three-stage protocol designed as a series of individual tests that provide quantitative data about an individual performance. This primary screen provides a behavioral observation profile. Such

test-specific performance is directly comparable between animals, over time, and between groups. In addition, the tests also provide an opportunity to identify abnormalities or changes in the mouse. The protocol is divided in three stages: (1) First stage is performed to detect the occurrence of defects in the viewing jar, attending to body position, tremor, palpebral closure, coat appearance, whisker appearance, presence of lacrimation and number of defecations. (2) The second stage evaluates behavior in a closed arena, such as spontaneous locomotor activity, gait, the immediate reaction to a new environment, the position of the tail, response to an external stimulus and pelvic elevation. (3) The third stage evaluates the reaction of the mouse when placed above the arena, gripped by the tail. Evaluation of skin color, forward curling, limb grasping, pinna reflex, corneal reflex, contact reflex, biting and vocalization is done in this stage. We follow the procedure indicated in the protocol (Rogers et al., 1997) filling the SHIRPA score sheet.

Isolation-induced pup ultrasonic vocalization are emitted by pups when separated from mother and littermates. Such calls play an important role in pup survival, since they can elicit maternal behavior, like retrieval (Sewell, 1970). Ultrasonic vocalization is measured in days 3, 6, 9 and 12 after birth. Pups were isolated from mother for 15 min, controlling the temperature with infrared light and an electric blanket. Pups were individually removed from the nest at random and gently placed into an isolation container, a plastic dish (100 x 20 mm). USV emission was monitored by an UltraSoundGate Condenser Microphone CM 16 / CMPA (Avisoft Bioacoustics). The microphone was connected via an UltraSoundGate 16Hb audio device (Avisoft Bioacoustics) to a personal computer, where acoustic data were recorded with a sampling rate up to 300 kHz in 16-bit format by Avisoft RECORDER (version 4.2.21; Avisoft Bioacoustics). The microphone that was used for recording was sensitive to frequencies of 20 to 135 kHz with a flat frequency response (3 dB). The accuracy of call detection by the software was verified manually by an experienced user. Prior to each test and between animals, the behavioral equipment was cleaned using a 70% ethanol solution and dried with paper towels (Mosienko et al., 2015; Wöhr et al., 2008a).

Self-grooming is considered as a stereotyped or repetitive behavior when the sequence persists for unusual periods of time. Mice were scored for spontaneous grooming behaviors as described earlier (Silverman et al., 2010). Each mouse was placed individually into a standard mouse cage with a thin (1 cm) layer of bedding to reduced neophobia, while preventing digging, a potentially competing behavior. Each mouse was scored for 10 min for cumulative time spent grooming all body regions. Cage and wood-chip bedding is changed between animals.

Nesting. To assess nest construction, we used adult male mice, because of the influence of hormones or reproductive status in female subjects (Deacon, 2006a). One hour previous to dark phase, mice were placed into individual testing cages with clean wood-chip bedding. In each testing cage, we placed 3 g pressed cotton squares (Nestlets Ref: CS3A01, Sodispan Research). Nest building was observed after 30 minutes, 12 hours, 24 hours and 36 hours, when we could confirm that the nest is completed in most of the cases, as previously described for wild type mice (Moretti et al., 2005). Nest weight and depth was measured. A score is also given to the nest according to the following criteria. A score of 1 is given if the Nestlet is more than 90% intact; 2 if 50 to 90% intact; 3 corresponds to less than 50% of the Nestlet intact; 4 to an identifiable but flat nest; and 5 to a near perfect nest with walls higher than mouse body height (Deacon, 2006a).

Elevated plus-maze is used to measure anxiety-like behaviors in laboratory animals, as it has been described to be a useful test to investigate both anxiolytic and anxiogenic agents (Lister, 1987). The test is based on the natural aversion of mice for open and elevated areas, as well as on their natural spontaneous exploratory behavior in novel environments. Animals were placed in a maze made of methacrylate, and consisted of a central square (5 x 5 cm), with four arms (5 x 25 cm). Two of the arms had opaque walls (16 cm high) around the edge (closed arms), whereas the other two arms did not have walls (open arms). The maze was elevated 45 cm above the floor on a plus-shape plywood stand. The animals were placed at the center of the maze, facing one of the enclosed arms. During a 5-minutes test period the following parameters were measured: the time spent in each arm, and the total number of arm entries, both open and closed (Pellow & File, 1986) (Komada et al., 2008).

Three-chamber social recognition test. This task is typically used for quantitating social behaviors in mice. It measures the tendency of the subject mouse to approach another mouse and engage in social investigation (Crawley, 2004b). The mice are exposed to an interaction for social versus inanimate target allowing olfactory and minimal tactile interaction. The social testing arena was a rectangular, three-chambered box. Dividing walls were made from clear methacrylate, with openings allowing access into each chamber. In one of the chambers, an unfamiliar mouse that had no prior contact with the subject mouse is placed in the middle (social target). This animal is always the same background, age and gender as the experimental subject. The social target mouse was enclosed in a wire cage, which allowed visual, olfactory, auditory, and some tactile contact through the bars, but preventing fighting. The animals serving as targets had previously been habituated to placement in the small cage during 3 days, 10 minutes each. An identical wire cage was placed in the opposite chamber, with a small black object inside (nonsocial target), serving as a control for exploring a novel object in a novel environment. The center chamber is empty. The chambers of the arena and the wire cages were cleaned with 0.1% acetic acid between trials. The test mouse was first placed in the middle chamber and allowed to explore for five minutes; this habituation period makes the animals recognize it as a familiar “home base”. Both openings to the side chambers were then unblocked and the subject mouse was allowed to explore the entire social test arena for a 10 min session. The amount of time spent in each chamber and the number of entries into each chamber, as well as the time and number of visits to each target, were recorded by video-tracking system and analyzed by Any-Maze software. To determine that these data really reflect actual exploration of the social target, a human observer recorded the time that the subject spent directly sniffing the wire cage containing the stranger mouse or the non-social target (Jamain et al., 2008)

Social novelty. This is investigated using the same three chambered apparatus. Thirty minutes after the social recognition task, the object (non-social target) is taken out and replaced with another unfamiliar mouse (stranger 2) that had no prior contact with the subject mice. The time that the test subject spends investigating the new mice (stranger 2) and the familiar one (stranger 1) was measured as previously described (Crawley, 2004a; Hitti and Siegelbaum, 2014b).

PET

PET-CT acquisition before and during cued fear conditioning. PET-CT scans were acquired 30 min after intravenous injection of 14 MBq of ^{18}F -FDG, with an eXplore Vista PET-CT system and reconstruction was made with 3D OSEM. Images were analyzed with Amide (NIH) software. Twenty four hours before the training, In order to obtain a baseline signal from the brain, ^{18}F -FDG was injected to the mice and a basal PET image was acquired 30 minutes afterwards. In the training (conditioning) day, the mouse is injected with ^{18}F -FDG 20 minutes before the beginning of conditioning. The mouse is then exposed to the conditioning context (180 sec) followed by a tone (CS, 20 sec, 2 kHz, 85 dB). After termination of the tone, a footshock (US, 0.75 mA, 2 sec) was delivered through a stainless steel grid floor. Mice received four footshocks with an intertrial interval of 60 s. The mouse was removed from the fear conditioning box 30 sec after shock termination and was anesthetized with isoflurane for PET scan. On the next day, mice are injected with ^{18}F -FDG 20 minutes before the memory retrieval test. Mice were placed into a novel context (same cages, but with different walls, floor, and background odor), and after a 3 min baseline period, they were continuously re-exposed to the tone (with same characteristics as at conditioning) for 5 min, but in the absence of shocks. Using a time-sampling procedure every 2 s, each mouse was scored blindly as either freezing or active at the instant the sample was taken. Freezing was defined as behavioral immobility except for movement needed for respiration. The mouse was removed from the fear conditioning box 30 sec after tone termination and was anesthetize with isoflurane for PET scan. The study was carried out in a blind manner, without any information about the genotype of the mice before the analysis of the behavior and images.

PET-CT data analysis. The analysis of PET images was performed in collaboration with Dr. Jesús Cortés (BioCruces Health Research Institute). We first segmented manually the mouse skull from the CT image to calculate the brain volume. We used this brain segmentation as a mask for individual PET normalization, consisting in dividing each value of voxel intensity by the average intensity within the mask.

Finally, all voxel intensities were spatially smoothed using a 0.6 mm full width at half maximum (FWHM) isotropic Gaussian kernel. To perform group comparison in the PET activation maps (WT vs Pten^{tg}), we first co-registered each PET image to its corresponding CT using the Slicer software (<https://www.slicer.org/>), applying the linear transform (BRAINS) from the PET to the CT. Next, all PET images were transformed to a common space using the FMRIB's Linear Image Registration Tool (FLIRT) transformation (Jenkinson and Smith, 2001), incorporated as part of the open-source software FSL. The common space (to which all PET images were transformed to) was defined by the *In vivo Mouse Brain Atlas* (Bai et al., 2012) (available at http://www.bioeng.nus.edu.sg/cfa/mouse_atlas.html) and by the AtlasGuide (Li et al., 2013). Using these atlases, 6 different regions of interest (ROI) were defined: the amygdala, the thalamus, the auditory cortex and the frontal cortex, the dorsal hippocampus and the ventral hippocampus. Group comparison was performed using Randomize, a FSL tool for non-parametric testing that uses threshold-free cluster enhancement (TFCE) and family-wise error (FWE), with a corrected value of $p < 0.05$. After applying Randomize, six different brain activity maps were obtained, two maps for the recording of basal brain activity ($\text{activity}_{\text{WT}} > \text{activity}_{\text{Pten}^{\text{tg}}}$ and $\text{activity}_{\text{WT}} < \text{activity}_{\text{Pten}^{\text{tg}}}$), two maps for the activity during conditioning with respect to the basal activity and two maps for the activity during retrieval with respect to basal activity. Next, we obtained the intersection between each of the 6 maps resulting from Randomize with the 6 ROIs identified from the atlases to extract all voxels within each ROI belonging to each of the 6 maps, and we did the same for each of the mice. Next, we calculated the mean activity in each of these regions and performed a two-sample t-test to search for significant differences in the two genotypes; the test was performed with the function *t-test2* incorporated in Matlab (The MathWorks, Inc).

Western Blot

Antibodies. PTEN 138G6 (9559, Cell Signaling), P-T308Akt (4056, Cell Signaling), P-S473 AKT (4060, Cell Signaling), AKT (9272, Cell Signaling), PSD-95 (75-028, Neuromab), actin clone 4 (MAB1501R, MILLIPORE), tubulin (T6199, SIGMA).

Hippocampal and amygdala total extracts. Animals were decapitated and brains were immediately removed and transferred into cold PBS. Coronal brain slices (1 mm) were obtained on a Zivic Brain matrix (Zivic Instruments Pittsburgh, PA, USA). Amygdala and hippocampus areas were dissected following Allen brain atlas distribution. Samples were homogenized on ice in homogenization buffer (10 mM HEPES pH 7.4, 150 mM NaCl, 10 mM EDTA, 1% Triton X-100, Roche protease inhibitor cocktail tablets "Complete mini EDTA-free" and Roche phosphatase inhibitor cocktail tablets "PhosStop") by pipetting or by a glass potter-dounce homogenizer. Samples were centrifuged at 13,000 RPM during 5 minutes, and supernatants were used for protein determination. Protein concentration was determined following Bio-Rad protein assay (Ref. 500-0006, Bio-Rad).

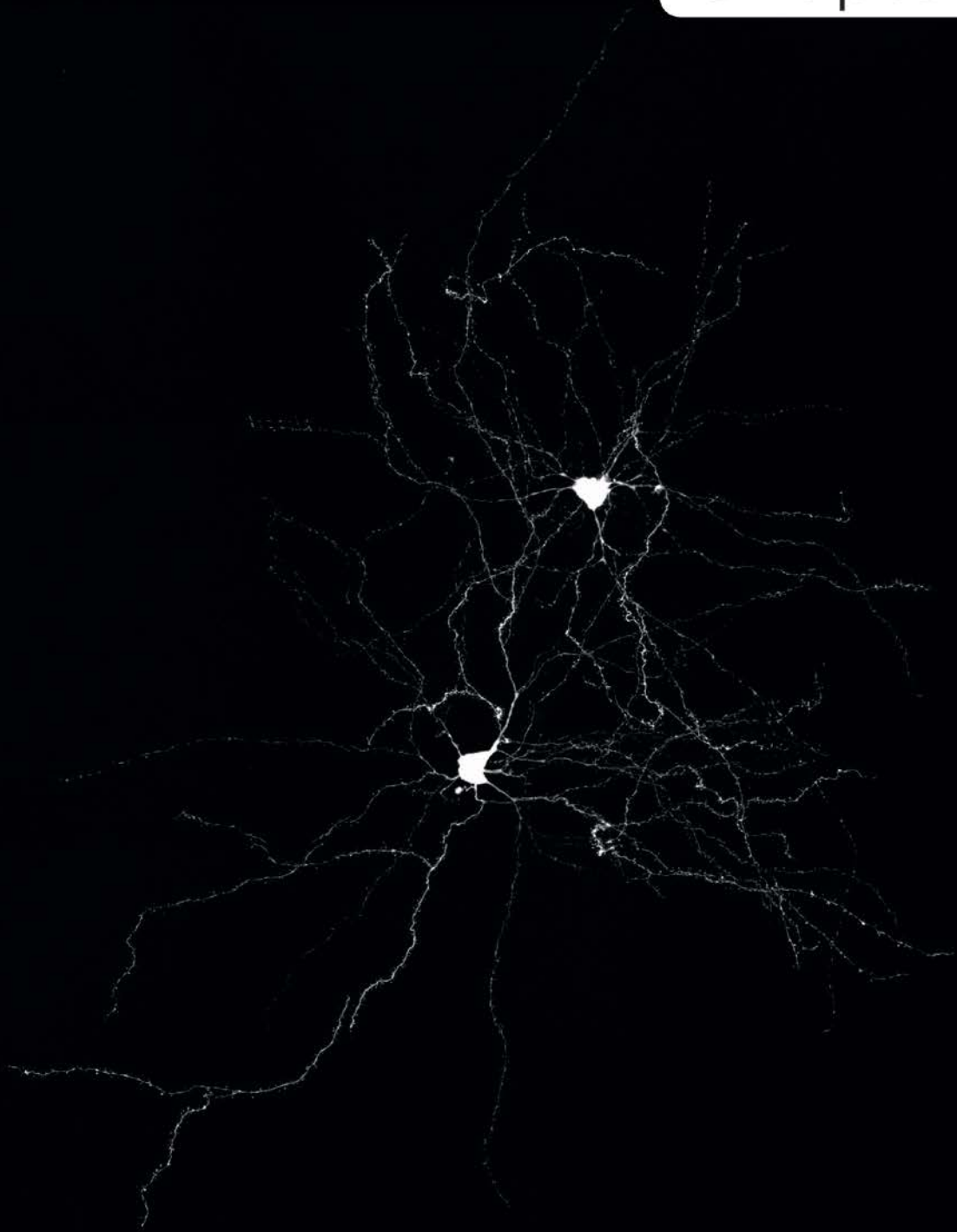
Synaptosomal preparations. For synaptosomal preparations, mouse hippocampi were homogenized in buffer A (0.32 mM sucrose, 1 mM MgCl₂, 0.5 mM CaCl₂, 10 mM HEPES, 1 mM EGTA, 1 mM dithiothreitol with Roche protease and phosphatase inhibitors) and centrifuged at 1,400 *g* for 10 min at 4°C to obtain supernatant S1 and pellet P1. P1 was homogenized in buffer A and centrifuged at 700*g* for 10 min at 4°C. The resulting supernatant was combined with the previous S1 and centrifuged at 13,800*g* for 10 min at 4°C. The obtained pellet (P2) was resuspended in homogenization buffer and used as crude synaptosomal fraction for analysis.

Western Blot procedure. Same protein quantity is prepared in 6x sample loading buffer (300 mM Tris-HCl pH 6.8, 12% (w/v) SDS, 0.6% (w/v) Bromophenol blue, 60% (w/v) glycerol, 600 mM β-mercaptoethanol). Samples were boiled to 95 °C for 5 min and subjected to 8% SDS-PAGE. The SDS-PAGE was transferred to PVDF membrane (Cat. IPVH00010 pore size: 0.45 μm, Immobilon) and blocked for 1 h in 0.1 % Tween-20 in Tris-NaCl buffer and (TBS-T) 5% milk. The membrane was incubated over night at 4°C in primary antibody in the same blocking buffer. Then after washing with blocking buffer, membranes were incubated with secondary antibody coupled to horseradish peroxidase for 1 hour at room temperature. After three washes with TBS-T protein was visualized with enhanced chemiluminescence (Immobilon™ Western Chemiluminescent HRP Substrate, Millipore) (Sambrook and Russel, 2001).

Statistical analysis

Statistical differences were calculated according to non-parametric two-sided tests unless indicated otherwise. Comparisons between multiple groups were carried out with the Kruskal-Wallis ANOVA. When significant differences were observed, *P* values for pairwise comparisons were calculated according to Dunn's Multiple Comparison *post hoc* Test two-tailed Mann-Whitney tests (for unpaired data) or Wilcoxon tests (for paired data). For input-output curves, *P* values were determined with two-way ANOVA with Bonferroni post-tests.

Chapter 1



PTEN overexpression

1. PTEN overexpression results in microcephaly with neuronal atrophy and hypoconnectivity.

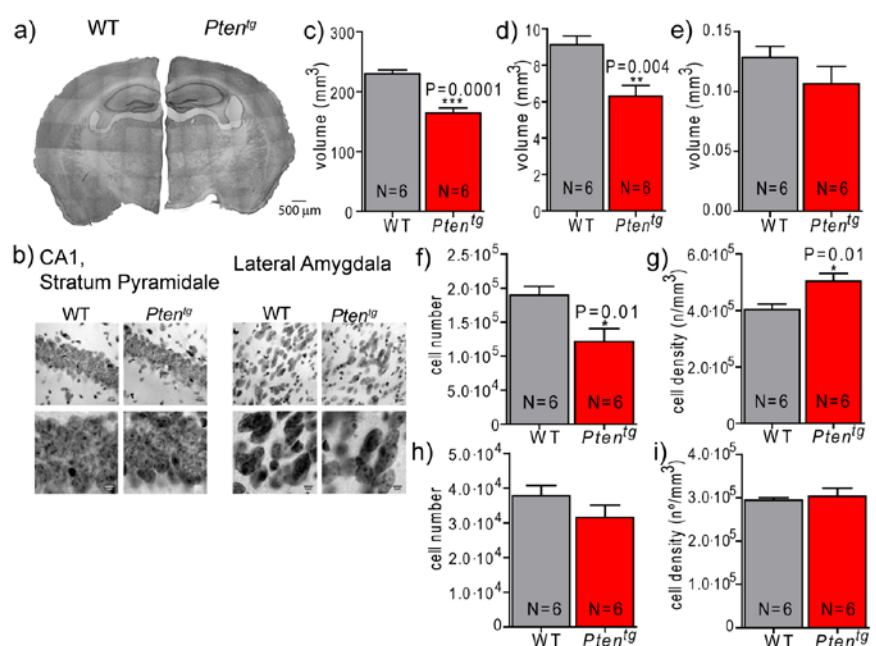
1.1 PTEN overexpression results in microcephaly.

Germ-line heterozygous mutations in PTEN lead to macrocephaly/autism syndrome (OMIM #605309) in an autosomal dominant manner (Tilot et al., 2015). This macrocephaly has also been documented in mouse models with PTEN deletions, such as Nse-Cre PTEN mouse (Kwon et al., 2006). To begin to evaluate the impact of PTEN overexpression on the brain I used unbiased stereology on Nissl-stained slices (representative examples shown in fig.7a). I detected a decrease in forebrain brain volume in *Pten^{tg}* mice (Fig. 7c), which is also reflected in a decreased hippocampal volume (Fig. 7d), as compared to WT littermates. There was also a trend for a reduction in the volume of the Lateral Amygdala (LA) of *Pten^{tg}* mice, but this was not significant (Fig. 7e).

To further understand the basis for these volume alterations, I carried out cell counting in CA1-stratum radiatum of the hippocampus and in the lateral amygdala (representative images fig. 7b, left and right respectively). Using unbiased stereology, I observed a decreased in cell number in CA1 (Fig. 7f). Paradoxically, cell density was increased in this area (Fig. 7g), possibly because of the strong reduction in hippocampal volume (Fig. 7d). In the LA, no significant differences were detected in the number of cells (Fig. 7h) or in cell density (Fig. 7i), when compared to WT littermates.

To summarize, PTEN overexpression results in a decreased brain volume, with a concomitant decrease in hippocampal total cell number. The increased cell density in the hippocampus would suggest that the reduction of hippocampal volume is stronger than the reduced cell number, leading to a more compact packing of hippocampal neurons in the mutant mice.

[Figure 7] Brain anatomy analyzed by Unbiased Stereology. (a, b) Bright field representative images of brains stained with Niessl. (a) Forebrain images were obtained using a 40x objective and tile scan, noted the difference in brain volume between WT (left) and *Pten^{tg}* (right) mice. (b) Images from CA1 (left) and LA (right) acquired through a 63x objective (top) and with an additional 3x zoom (bottom). (c) Forebrain volume from WT and *Pten^{tg}* mice. (d) Hippocampus volume means obtained from WT and *Pten^{tg}* mice. (e) LA volume from WT and *Pten^{tg}* mice. (f) Number of cells contained in CA1 (stratum pyramidale) from WT and *Pten^{tg}* mice. (g) Cell density in CA1 shown for WT and *Pten^{tg}* mice. (h) Number of cells contained in LA from WT and *Pten^{tg}* mice. (i) Cell density in CA1 shown for WT and *Pten^{tg}* mice. Means and SEM are shown for all the measurements. N indicates the number of animals.



1.2 Dendritic atrophy and decreased spine density in principal neurons from the LA of *Pten^{tg}* mice.

Several studies had revealed the important role of PTEN in neuron growth and development, as altering PTEN levels or function leads to alterations in neuronal morphology (Fraser et al., 2008; Haws et al., 2014; Luikart et al., 2011; Stephens et al., 1998). Brain macrocephaly in *Pten* mutated mouse models is generally accompanied by neuronal hypertrophy with a dendritic overgrowth (Kwon et al., 2006). Therefore, I determined the morphology of biocytin-filled pyramidal-like neurons in the LA injected during whole-cell patch-clamp (Fig. 8a). As an indirect method to estimate cell size, I also calculated total membrane cell capacitance from these cells during the electrophysiological recordings (Luikart et al., 2011). Cell capacitance was lower in *Pten^{tg}* mice compared to WT cells (Fig. 8d), indicating that total membrane surface is lower in *Pten^{tg}* neurons, and therefore suggesting that these cells are smaller than WT ones.

To analyze dendritic complexity, the measurements of all the dendrites were summed, as there is no apparent polarization into basal and apical dendrites in LA projection neuron (Humeau et al., 2005). By tracing with Neurolucida, I found that PTEN overexpression induces a substantial dendritic atrophy with a decrease in total dendritic length (Fig. 8b) and in total number of intersections (Fig. 8f) that becomes apparent at 50 μm from cell body (Fig. 8c and g, respectively). Total neuron branching remains normal (Fig. 8e), while there is a slight increase in tortuosity in *Pten^{tg}* mice (Fig. 8h). Using higher magnification, spine density was measured in WT and *Pten^{tg}* dendrites (representative images, fig. 8i). Total spine density is decreased in *Pten^{tg}* mice (Fig. 8j). This effect was detectable over the entire dendritic length (Fig. 8k).

These results reinforce the interpretation of a critical role for PTEN on neuron morphology, as a decrease in its function results in neuron hypertrophy (Fraser et al., 2008; Kwon et al., 2006; Takeuchi et al., 2013) and the opposite phenotype is obtained when PTEN is overexpressed.

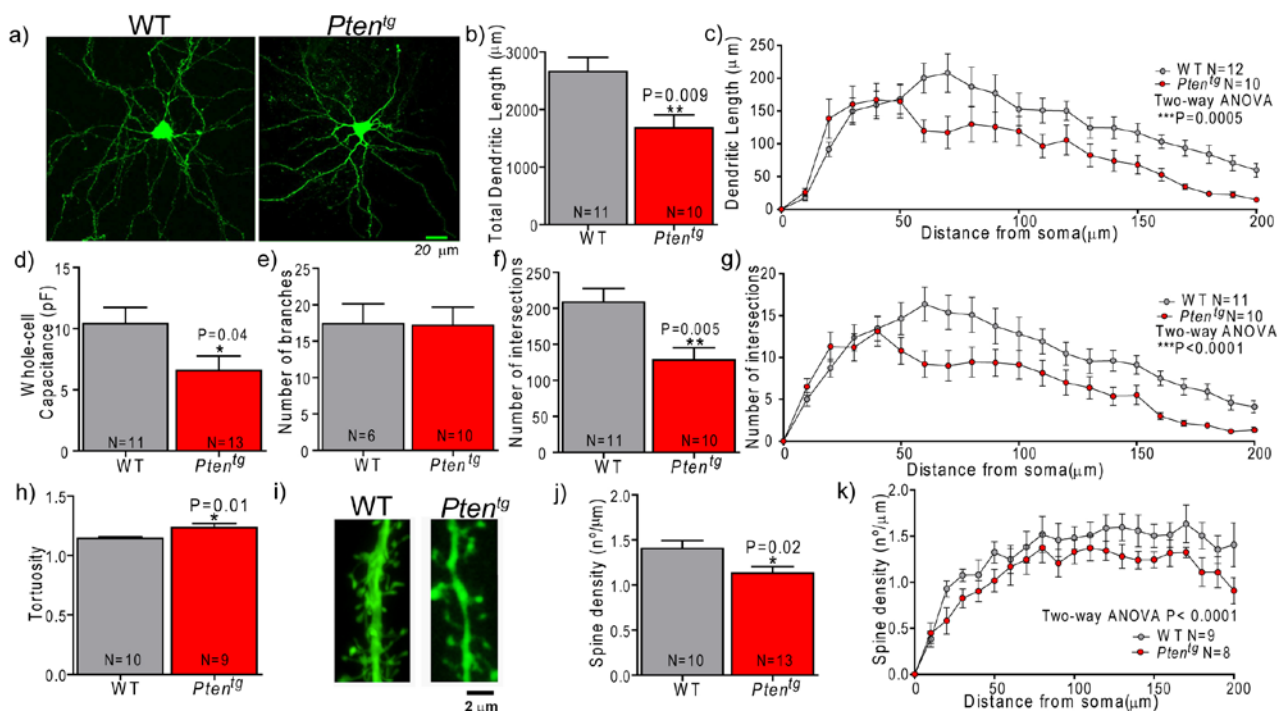


[Figure 8] Lateral amygdala principal neurons morphology. (a) Representative confocal images (20x, tile scan) from LA principal neurons injected with biocytin and labeled with Streptavidin-488 in WT (left) and *Pten^{tg}* mice (right). (b) Total dendritic length of principal neurons from WT and *Pten^{tg}* animals. (c) Sholl analysis showing the dendritic length as a function of the distance from the soma. (d) Whole-cell capacitance from WT and *Pten^{tg}* principal neurons. (e) Total number of dendritic branches for WT and *Pten^{tg}* principal neurons. (f) Total tortuosity of LA principal neurons of both genotypes. (g) Total number of intersections. (g) Sholl analysis showing the number of intersections as a function of the distance from the soma. (h) Dendritic tortuosity from WT and *Pten^{tg}* principal neurons. (i) Representative projection of images of dendrites from WT and *Pten^{tg}* mice (63x, deconvoluted). (j) Total spine density. (k) Spine density as a function of the distance from the soma (Scholl analysis) from WT and *Pten^{tg}* mice. Means and SEM are shown for all the measurements. N indicates the number of cells.

1.3 Neuronal hypoconnectivity in hippocampus and LA of *Pten^{tg}* mice.

Based on changes in volume as well as in dendritic spines observed in *Pten^{tg}* mice, I used electron microscopy in collaboration with Dr. Rafael Luján (Univ. Castilla-La Mancha) to evaluate synaptic structure in more detail in the CA1 hippocampus (stratum radiatum) and in the LA of adult mice (representative images in figure 9a, e, respectively). As shown in Fig. 9b, I observed that the density of excitatory synapses, determined as asymmetrical synapses (from the presence of a PSD dense staining), was significantly reduced in *Pten^{tg}* mice CA1, without any effect on PSD length (Fig. 9c, d). In the case of LA principal neurons, synaptic density was significantly lower in *Pten^{tg}* mice (Fig. 9f). There was also a trend for a reduction in PSD length at *Pten^{tg}* synapses (Fig. 9g), which was particularly prominent on large synapses (PSD length > 0.45 μm) (Fig. 4h). Thus, PTEN overexpression leads to a decreased synaptic density in the hippocampus and LA, which is also accompanied by a reduction in synapse size in the LA.

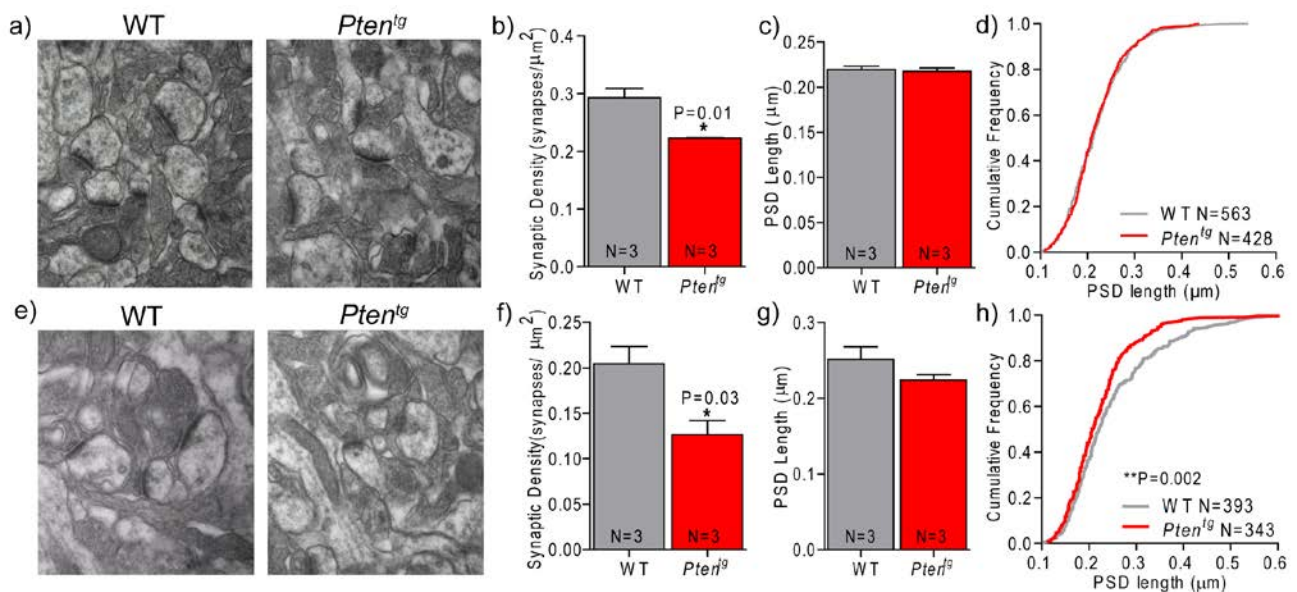


[Figure 9] Electron microscopy analysis of synapses. (a) Electron micrographs of synapses in the hippocampal CA1 stratum radiatum for WT (left) and *Pten^{tg}* mice (right). Means and standard error deviation representation of synapse density (b) and PSD length (c) in WT and *Pten^{tg}* mice hippocampus (CA1). (d) Cumulative frequency of PSD length from WT and *Pten^{tg}* mice hippocampal synapses from CA1. (e-h) Similar to (a-d) for WT and *Pten^{tg}* mouse synapses from LA.

2. PTEN overexpression leads to a shift towards synaptic depression.

After having detected differential effects of PTEN overexpression on CA1 hippocampus and LA at the anatomical level, I decided to evaluate the physiological consequences of these changes for synaptic transmission. These results will be extremely valuable to attribute specific synaptic dysfunctions to particular behavioural impairments.

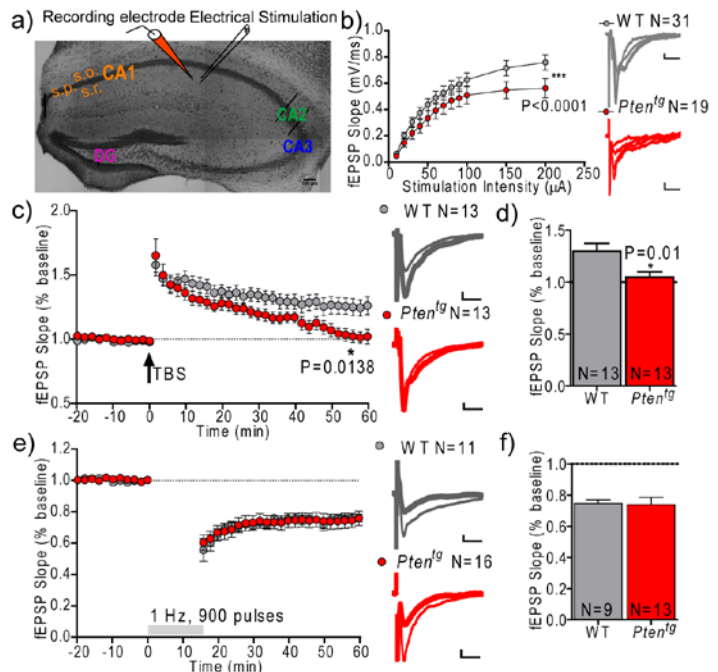
The general aim of these experiments is to try and understand how PTEN modulates neuronal circuitry and synaptic function with behavioural consequences related to autism (Takeuchi et al., 2013). To start addressing this question, I measured basal synaptic transmission and plasticity at excitatory CA3-CA1 synapses in the hippocampus and in the cortical and thalamic inputs to LA.

2.1 Depressed transmission in the CA1 of *Pten^{tg}* mice.

To assess basal synaptic transmission in CA3-CA1 synapses of *Pten^{tg}* mice, I stimulated Schaffer collateral afferents from CA3 and monitored the responses (fEPSP) to increasing stimulation intensities at synapses on CA1 pyramidal neurons (fig. 10a, hippocampal field recordings configuration). Field recordings were performed in acute slices from adult WT and *Pten^{tg}* mice. Basal transmission was decreased in *Pten^{tg}* mice, as indicated from the lower input/output curve (Fig. 10b). This reduction in basal synaptic transmission is in good agreement with the anatomical alteration observed in *Pten^{tg}* CA1, with a decrease in synaptic density. Long lasting forms of synaptic plasticity, such as LTP and LTD, are the main substrates to memory and learning (Malenka and Bear, 2004). LTP was induced with a Theta-burst stimulation protocol (TBS-LTP: 10 bursts of five stimuli, 100 Hz within burst, 200-ms interburst interval). This type of induction mimics firing patterns seen in vivo and induces a PI3K-dependent form of LTP (Opazo et al., 2003). TBS-LTP was impaired in *Pten^{tg}* mice (Fig. 10c), as responses were dramatically reduced to baseline at 50-60 minutes after a transient potentiation (Fig.10c, d). Low frequency stimulation was used to induce NMDA receptor-dependent LTD (900 pulses/1 Hz), a form of plasticity which requires PTEN function (Jurado et al., 2010). LTD was normal in *Pten^{tg}* mice when compared to WT littermate (Fig. 10e, f). In conclusion, PTEN overexpression results in decreased excitatory basal transmission and impaired LTP.

[Figure 10] Electrophysiological recordings from the CA1 subfield of the hippocampus.

(a) Schematic representation of recording configuration. (b) Left, input-output curves of field excitatory postsynaptic potentials (fEPSPs) evoked by stimulation of CA3 Schaffer collateral afferents using slices from WT and *Pten^{tg}* mice. Right, superimposed representative fEPSPs at 50, 100, 150 and 200 μ A of stimulation intensity. N represents number of slices. (c) Left, LTP was induced by TBS and recorded for 60 min post-induction, following at least 20 min of stable baseline. Right, representative field recordings at baseline (thin line) and after LTP induction (thick line) from slices from WT and *Pten^{tg}* mice. Scale bars represent 0.1 mV, 50 ms. (d) Quantification of average fEPSP maximal slopes at 50–60 min after induction. P value was calculated using t-test. N represents number of slices. Data are represented as mean \pm s.e.m. (e) Left, LTD was induced by LFS and recorded for 60 min post-induction, following at least 20 min of stable baseline. Right, representative field recording traces at baseline (thin line) and after LTD induction (thick line) from slices taken from WT and *Pten^{tg}* mice. Scale bars represent 0.1 mV, 50 ms. (f) Quantification of average fEPSP maximal slopes at 50–60 min after induction. N represents number of slices. Data are represented as mean \pm s.e.m.



2.2 Depressed transmission in the LA of *Pten^{tg}* mice.

I then asked whether the morphological alterations of the amygdala in *Pten^{tg}* mice could be reflected in impairments in excitatory synaptic function. Thus, I first examined the basal excitatory neurotransmission by electrophysiological recordings of field excitatory postsynaptic potential (fEPSPs) in acute coronal slices containing the LA. Thalamic afferents were stimulated near the external capsule medial to the LA, and fEPSC were recorded from the lateral nucleus of the amygdala (Fig. 11a). In slices from *Pten^{tg}* mice synapses receiving thalamic input exhibited a small but significant decrease in the slope of synaptic response (input-output curve, Fig. 11b). Nevertheless, these synapses exhibited normal levels of LTP and LTD (Fig. 11c-f). In contrast, in slices from *Pten^{tg}* mice, synapses receiving input from the auditory cortex, stimulating in the external capsule above the central nucleus of the amygdala (Fig. 11g), exhibited normal basal transmission (input-output curve; Fig. 6h). Strikingly, these synapses failed to express normal levels of LTP (fig. 11i). Thus,

synaptic potentiation was reduced to 24% at 50-60 minutes after induction, as compared to 50% potentiation in the WT (Fig. 11j). In addition, cortical LA synapses showed exaggerated levels of NMDAR-dependent LTD (Fig. 11k), with a 34% depression with respect to baseline in *Pten^{tg}*, as compared to 20% in WT (fig. 11g). These findings imply that PTEN overexpression induces pathway-specific functional changes in LA synapses, with an overall depression and a significant effect in synaptic plasticity of cortical synapses. This result is in good agreement with the hyperactivity obtained from Pten heterozygous deletion in cortical-BLA circuit (Huang et al., 2016) and the alterations observed in VPA-rat ASD model with dysregulation of PIP₃ pathway (Wu et al., 2016).

3. *Pten^{tg}* mice present behavioral alterations in cognitive assays, with impaired hippocampal and amygdala-dependent memory.

3.1 Normal short-term hippocampal-dependent memory in *Pten^{tg}* mice.

To investigate short-term hippocampal-dependent memory, the novel object location task was performed. In this test mice explore two identical objects during 5 minutes. After 30 minutes one of the objects was displaced and mice are expected to explore the displaced object for longer periods of time if their short-term spatial memory is intact. Both, *Pten^{tg}* and WT mice showed no preference between objects before displacement (Fig. 12a, c), and they both showed a clear preference for the displaced object afterwards (Fig. 12 b, d). Therefore, PTEN overexpression does not affect the performance in the novel object location task, suggesting normal short-term hippocampal-dependent memory in *Pten^{tg}* mice.

3.2 Impaired hippocampal-dependent learning and normal reversal-learning in *Pten^{tg}* mice.

Previous studies show a possible implication of PTEN in learning and memory, as Pten mouse models present deficiencies in hippocampal-dependent tasks, such as Morris-Water Maze (Kwon et al., 2006). My electrophysiological recordings in CA1-hippocampus determined alterations in *Pten^{tg}* mice in basal excitatory transmission and LTP, as well as decreased synaptic density as determined by electron microscopy. These results suggested that *Pten^{tg}* mice might present alterations in learning and memory. To further characterize the role of PTEN in memory, *Pten^{tg}* mice were evaluated in the Barnes maze (fig. 12e), a less anxiogenic task than Morris-water maze (Fox et al., 1998). Indeed, *Pten^{tg}* mice made more errors until they find the escaping hole during the four days of the learning phase and during the test on the fifth day (Fig. 12f). Moreover, the latency until the hole was found was increased in *Pten^{tg}* mice (Fig. 12g).

Afterwards, reversal learning was examined by changing the escape hole to the opposite quadrant (fig. 12h), so the animals have to learn the new location. Reversal spatial learning depends on the medial prefrontal cortex (mPFC) (de Bruin et al., 1994). This task represents a form of cognitive flexibility, which is altered in some forms of ASD, as patients present problems in their ability to get used to changes in their routine (Ey et al., 2011). The procedure to evaluate this type of learning is the same as the previous learning task, so number of errors and latency to the escape hole were measured. After two days of training the mice had learned the new location of the scape hole, with similar results in both genotypes (fig. 12i, j).

Therefore, *Pten^{tg}* mice display deficits in hippocampal-dependent learning and memory, which may correlate with the morphological and electrophysiological alterations observed for these animals in the hippocampus.

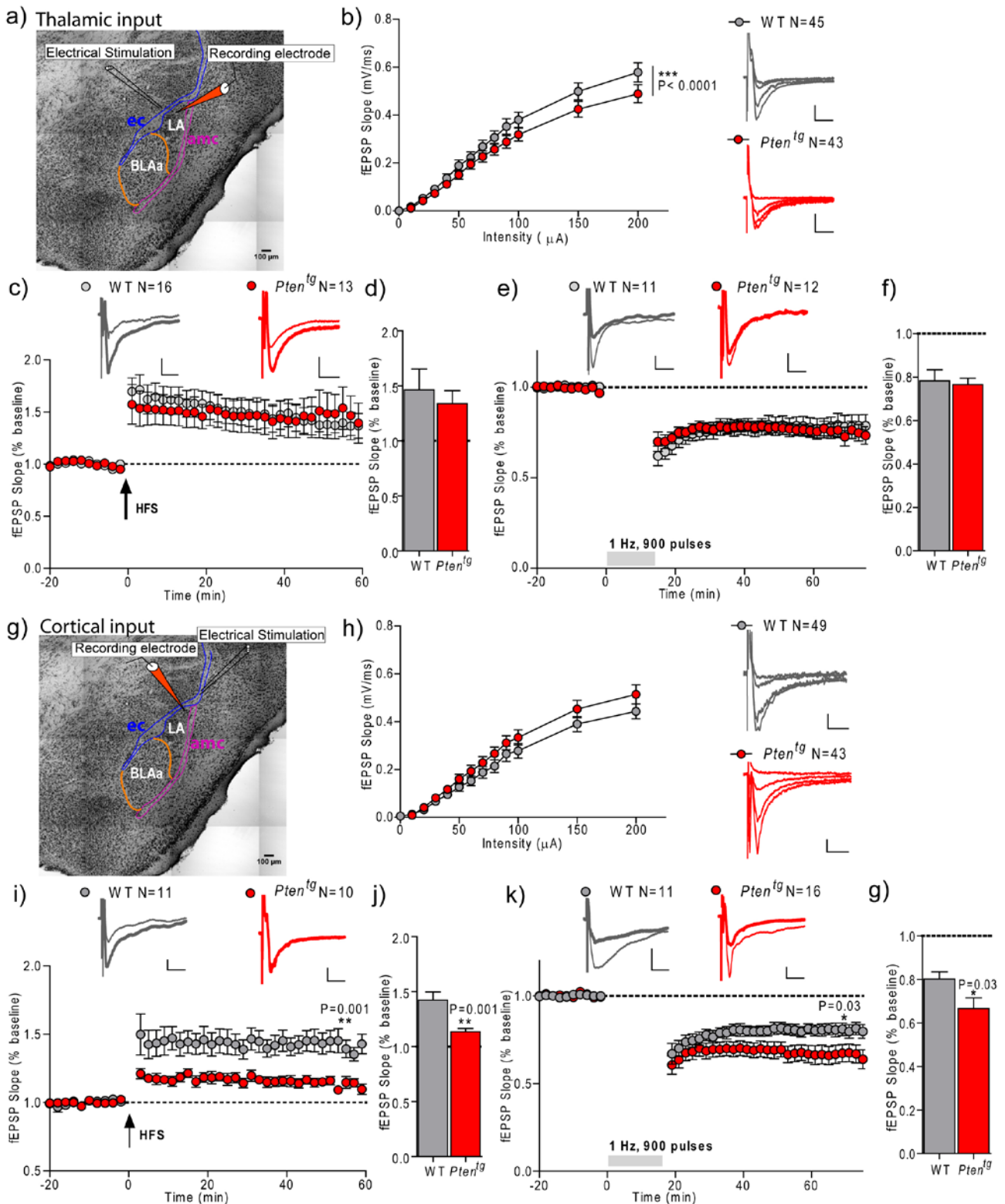


[Figure 11] **Electrophysiological recordings from LA.** Schematic representation of recording configuration from the thalamic input (a) and cortical input (g). ec: external capsule; amc: amygdalar capsule; LA: lateral amygdalar nucleus; BLA: basolateral amygdalar nucleus anterior part. (b, h) Basal synaptic transmission. Left, input-output curves of fEPSPs evoked by stimulation of thalamic afferents (b) and cortical afferents (h). Right, superimposed representative fEPSPs at 50, 100, 150 and 200 μ A of stimulation intensity from thalamic (b) and cortical (h) recordings. LTP was induced by high frequency stimulation of thalamic (c) and cortical (i) afferents and recorded for 60 min post-induction, following at least 20 min of stable baseline. Representative fEPSPs at baseline (thin line) and after LTP induction (thick line) from slices from WT and *Pten*^{tg} mice are represented on top of LTP graphs. Scale bars represent 0.1 mV, 50 ms. Quantification of average fEPSP maximal slopes at 50–60 min after induction from thalamic (d) and cortical (j) recordings. LTD was induced by LFS of thalamic (e) and cortical (k) afferents and recorded for 60 min post-induction, following at least 20 min of stable baseline. Representative field recordings traces at baseline (thin line) and after LTD induction (thick line) from slices taken from WT and *Pten*^{tg} mice are represented on top of LTD graphs. Scale bars represent 0.1 mV, 50 ms. Quantification of average fEPSP maximal slopes at 50–60 min after induction from thalamic (f) and cortical (g) recordings. Data are represented as mean \pm s.e.m. N represents number of slices.

3.3 Deficits in cued fear conditioning and a failure to activate key areas during retrieval

To evaluate whether PTEN overexpression has consequences on amygdala function, I carried out fear conditioning assays. In this form of Pavlovian learning, an aversive stimulus (e.g., an electrical shock) is associated with a neutral stimulus (e.g., a tone), resulting in the expression of fear responses (freezing) to the originally neutral stimulus (Kim and Jung, 2006). I trained mice repeatedly with mild electrical foot shocks that occurred immediately after an auditory cue and I observed similar learning curve for both genotypes (Fig. 12k). After 24 hours, I scored WT and *Pten*^{tg} mice for fear response in the same context (hippocampal and amygdala-dependent test), but without the tone, and no significant difference was observed when comparing both genotypes (fig. 12l). Twenty four hours later, mice were exposed to a novel environment in the presence of the training auditory cue, the tone, in an amygdala-dependent task. Freezing to the tone was increased compared to pre-tone freezing in both genotypes, indicating some cued conditioning, although with considerably lower absolute rates of freezing in the *Pten*^{tg} mice (fig. 12m). To conclude, I analyzed pain sensibility, to assure that the observed differences are not due to changes in the sensitivity to pain, and I observed that sensitivity is similar in both genotypes (fig. 12n). These alterations in amygdala-dependent memory are consistent with the deficits in LTP and with the synaptic loss I observed in this structure in *Pten*^{tg} mice.

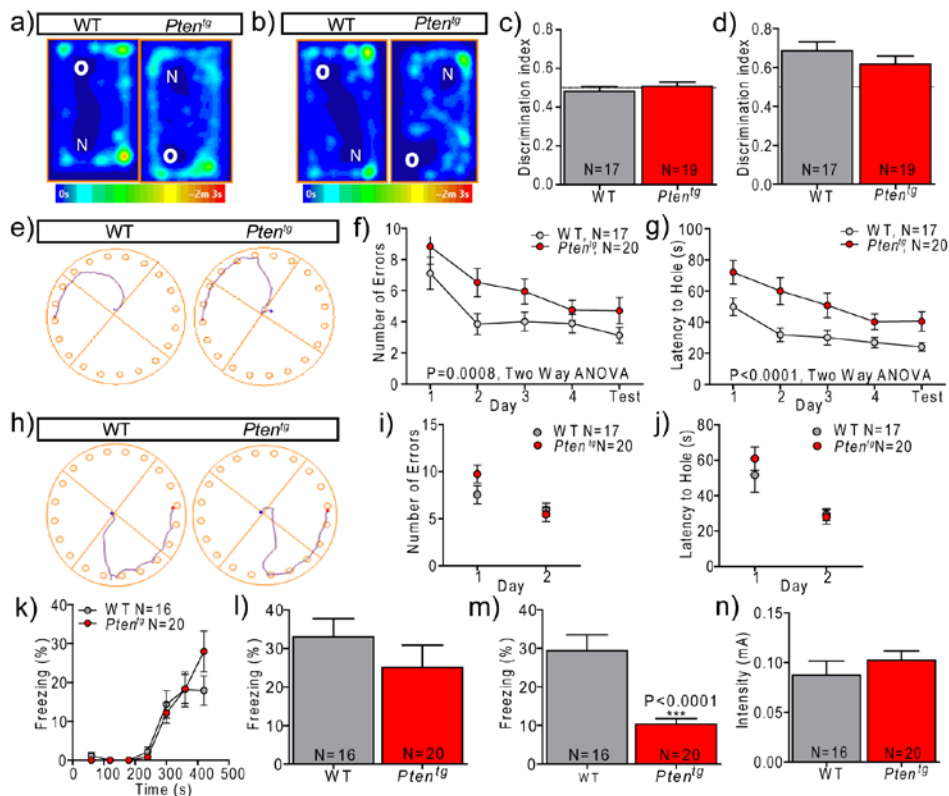


[Figure 12] **Memory measurements.** (a-d) Novel object location task. Occupancy plots of representative examples of WT and *Pten*^{tg} exploration during habituation to the cage (a) and during the test (b), where N represents novel or displaced object and O the old or not displaced object. Discrimination index from the habituation task (c) and the test (d) was calculated as the time exploring the novel object over the time exploring both objects. (e-g) Barnes maze memory analysis. (e) Representative images of WT and *Pten*^{tg} mice exploratory behavior tracking. (f) Total primary errors for each day of the experiment before the scape hole was found by the animal. (g) Time until the scape hole was found. (h-j) Barnes maze reversal memory analysis. (h) Representative images of WT and *Pten*^{tg} mice behavior tracking. (i) Total primary errors for each day of the experiment before the scape hole was found. (j) Time until the scape hole was found. (k-n) Fear Conditioning. (k) Percentage of freezing represented per minute during the habituation task. (l) Percentage freezing to the context during 5 minutes test. (m) Percentage freezing to the tone during 5 minutes test. (n) Sensitivity to pain was evaluated as the shock intensity in which the mouse reacts to it. Mean and SEM are shown for WT mice and for *Pten*^{tg} mice in all the graphs. N represents number of animals.

To explore the mechanisms underlying this impairment and to define the brain areas activated during training and retrieval of this form of memory, we carried out microPET scan of the brains of some of the mice before fear conditioning and immediately after conditioning and memory retrieval. First of all, basal activation was measured. Consistent with my results with unbiased stereology, CT scanning indicated that *Pten^{tg}* mice have a significant decrease in the dimensions of their heads (Fig. 13 a, b). To determine if this microcephaly is accompanied by changes in basal brain activity I scanned mice in a micro positron emission tomography (microPET) employing a radiolabeled glucose analogue (2-deoxy-2-[18F]fluoro-D-glucose, ¹⁸F-FDG) as the tracer. Positron emission tomography (PET) signals detect blood flow, oxygen consumption and glucose use associated with neuronal activity (Magistretti and Pellerin, 1999). The selective uptake of ¹⁸F-FDG depends on glycolytic metabolism and it is directly related with cell activity. I identified a lower glucose uptake, implying lower activity, in most cortical areas including the frontal and auditory cortices and the ventral hippocampus (fig. 13c-e). Interestingly, the decrease in glucose uptake was region-specific as it was not detected in subcortical areas such as the amygdala and the thalamus and it was even enhanced in the dorsal hippocampus. Thus, *Pten^{tg}* mice present lower cortical activity reflected by glucose hypometabolism.

I then performed similar microPET immediately after fear conditioning (Fig. 14a) and after memory retrieval (Fig. 14e). As observed before (Fig. 12k), WT and *Pten^{tg}* mice displayed similar freezing levels during training (fig. 14b). PET evaluation immediately after training showed little change in overall brain activation in WT mice, and a general trend for a decreased activation in different areas of the brain in *Pten^{tg}* mice (fig. 14c, d), as compared to basal activity. Cued memory retrieval was reduced in *Pten^{tg}* mice (fig. 14 f), as we had observed before (Fig. 12m). Interestingly, WT mice showed a general trend for enhanced glucose uptake (as compared to their basal glucose uptake) in the brain. This enhanced activity in response to the tone was particularly noticeable in areas known to be involved in cued fear conditioning, such as the hippocampus, the amygdala and the thalamus (Fanselow, 2010; Kim and Jung, 2006). In contrast, these changes in activity compared to baseline were virtually opposite in *Pten^{tg}* mice, as the same areas showed a decrease in activity in response to the tone (Fig. 14g, h). In conclusion, PTEN overexpression leads to a decreased activity or cortical and subcortical areas of the brain, with a decreased activation of key areas during retrieval of fear memory.

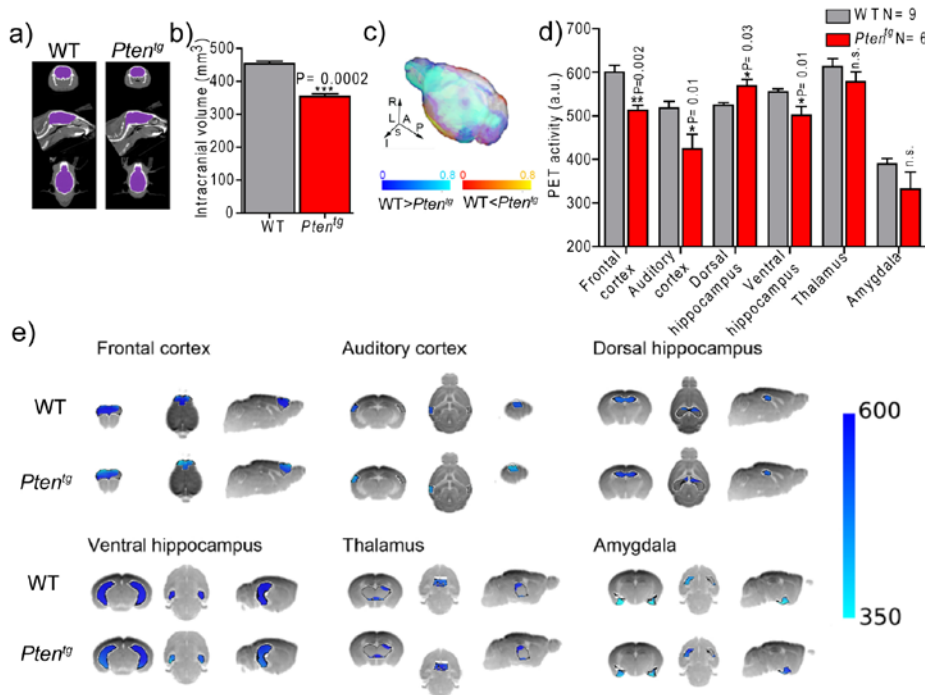


[Figure 13] PET analysis of WT and *Pten^{tg}* mice brain activity in basal conditions. (a) Representative images from PET-CT acquisition, Mouse skull was segmented manually (purple) from the CT image to calculate the brain volume. (b) Means and SEM are shown for intracranial volume. (c) Representative image of brain activity from WT and *Pten^{tg}* mice in basal conditions. (d) PET activity in basal conditions. Means and SEM are shown for frontal cortex, auditory cortex, dorsal and ventral hippocampus, amygdala and thalamus. t-test, * $P < 0.05$, ** $P < 0.01$. N represents number of animals. (e) Representative images from WT and *Pten^{tg}* mice in basal conditions.

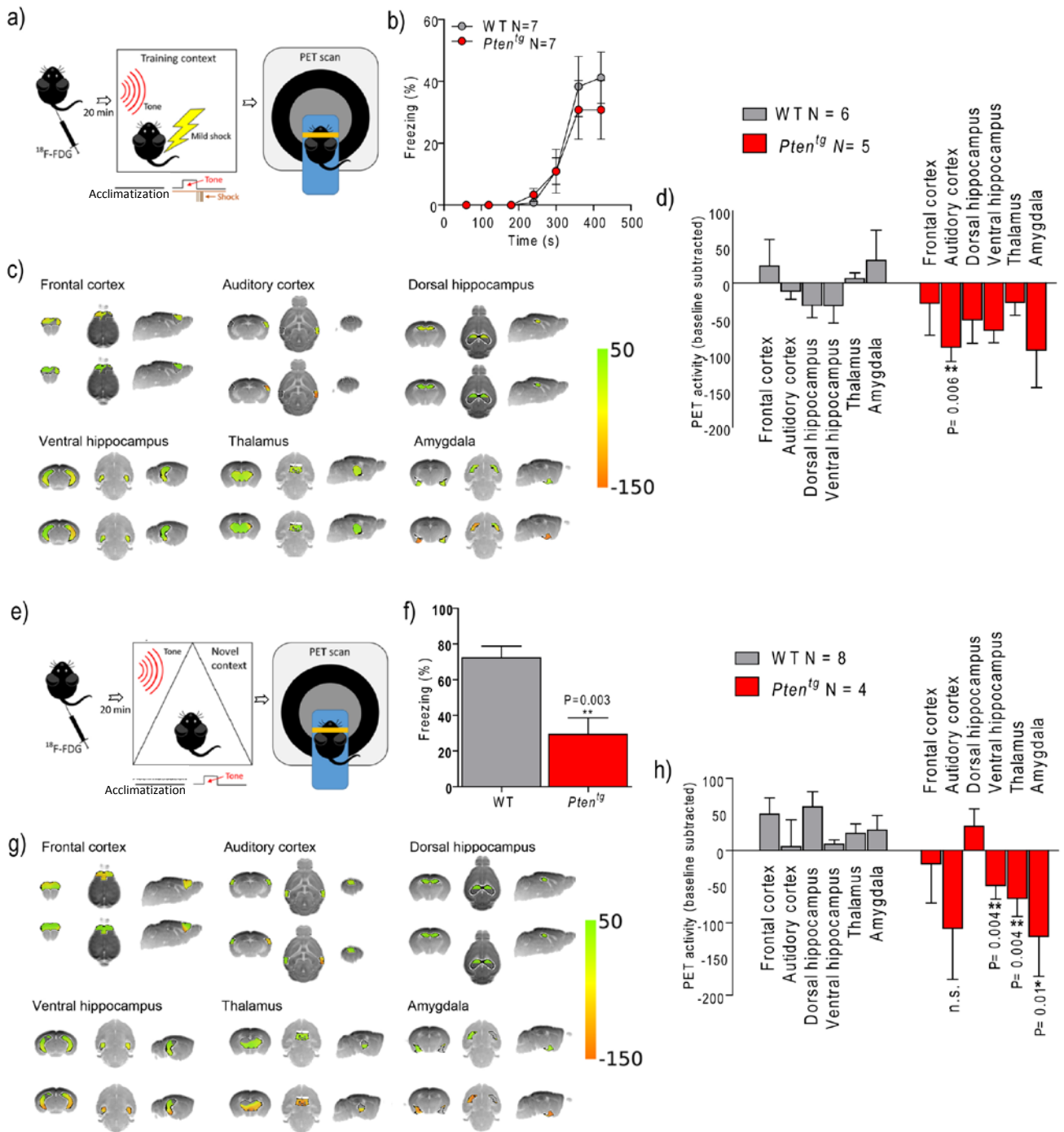


[Figure 14] PET analysis of WT and *Pten^{tg}* mice associated with the fear conditioning task. (a) Experimental procedure during the training day. (b) Percentage of freezing represented per minute during the 7 minutes of the habituation task. Mean and SEM are shown for WT and *Pten^{tg}* mice at 60 s, 120 s, 180 s, 240 s, 300 s, 360 s and 420 s. (c) Representative images from WT and *Pten^{tg}* mice brain areas after fear conditioning training. (d) PET activity after fear conditioning training was detected and represented as the activity after the training minus the basal activity; means±SEM for different brain areas activity are shown. (e) Experimental procedure during cued-test day. (f) Percentage freezing to the tone during 5 minutes is represented for WT mice and for *Pten^{tg}* mice. t-test **P<0.01. (g) Representative images of WT and *Pten^{tg}* brain areas after cued test (h) PET activity after cued test is detected and represented subtracting baseline activity, means±SEM are shown. t-test, * P<0.05, **P<0.01. N represents number of animals.

4. *Pten*^{tg} mice present early communication alterations, reduced anxiety and pro-social behavior.

Patients with ASD usually exhibit impairment in social interaction, communication, and increased anxiety accompanied by stereotypic behaviors. In some cases, this behavioral defects appear in combination with intellectual disability, abnormal sensory perception or motor coordination alterations (Lázaro and Golshani, 2015). As the diagnostic criteria for ASD is behavioral, phenotyping autism mouse models require behavioral assays with high relevance to each category of the diagnostic symptoms. Robust phenotypes in mouse models hold great promise as translational tools for discovering effective treatments for ASD (Silverman et al., 2010). Indeed, most of these behavioral alterations have been described for knock-out mouse models (Huang et al., 2016; Kwon et al., 2006; Lugo et al., 2014). To determine if any of these behaviors could be controlled by PTEN in a bi-directional manner, I studied ASD-related behaviors upon PTEN overexpression.

4.1 PTEN overexpression does not altered mice basal features except vocalization.

We tested basic behavioral features in adult WT and *Pten*^{tg} mice through a systematical observational method described by Dr. Irwin (Irwin, 1968). The procedure that follows was developed to comprehensively assess the state of the mice through direct observation. I first documented the behavior in the viewing jar. Thus, I measured the body position, tremor, palpebral closure, coat appearance, whiskers state, lacrimation and defecation. I did not detect significant differences between genotypes (shown for defecation in Fig. 15a). Second, behavior in an open arena was recorded, where I observed no changes in the immediate reaction of the mice when they were placed in a new environment (Fig.15b), either in the number of squares the mice entered with all four feet (Fig. 15c), or in tail elevation (Fig. 15d) or in touch scape reaction (Fig. 15e). Third, the behavior of the animals was recorded when held above the arena. The response to different ways of handling of the mouse was measured, measuring the mouse struggling while being held. No differences between genotypes were found when the animals were held by the tail, the neck, or when lying supine (Fig.15f). No differences in limb grasping were found either between genotypes (Fig. 15g). Some other features were similar in WT and *Pten*^{tg} animals, and are not represented in graphs, including skin color, forward curling (head to abdomen) when held by the tail, pinna and corneal reflex, and biting. Finally, number of vocalization events during the screen was scored, with a significant decrease in *Pten*^{tg} mice (Fig. 15h). As expected by the work of Dr. Manuel Serrano's lab (Ortega-Molina et al., 2012), *Pten*^{tg} animals had a lower body weight compared to their WT littermates (Fig. 15i). Locomotor activity was measured by open-field test during 10 minutes. I observed that mean speed and total distance traveled were similar in *Pten*^{tg} mice compared to WT mice (fig. 15 j, k).

4.2 ASD-related behavior in *Pten*^{tg} mice.

4.2.1 PTEN overexpression modulates ultrasonic vocalizations (USV) induced by isolation of pups.

In rodent models for autism, behavioral phenotypes are typically assessed in adulthood, since few behavioral test paradigms are available that allow the reliable assessment of such complex behavioral alterations in juvenile animals. Yet, a remarkable exception appears to be the induction of ultrasonic vocalizations (USV) in pups during isolation from the mother and littermates for a short period of time (Mosienko et al., 2015). It has been described that mothers preferentially attend to calls with higher duration (Ehret and Haack, 1981), with a frequency between 65-45 kHz more than 75-55 kHz (Smith and C., 1976) and with higher peak amplitude (Wöhr et al., 2008b). Such isolation-induced USV are commonly studied to assess developmental delays and communication deficits in rodent models for ASD, with model organisms typically displaying overall reduced USV levels, such as Shank 1 knock-out mice (Sungur et al., 2016). To assess if PTEN is important for early communication, I measured the ultrasonic vocalization in isolated pups of 3, 6, 9 and 12 days of age. To induce USV, pups were isolated from their mother for 15 minutes previous to the recordings. Pups were individually removed from the nest at random and gently

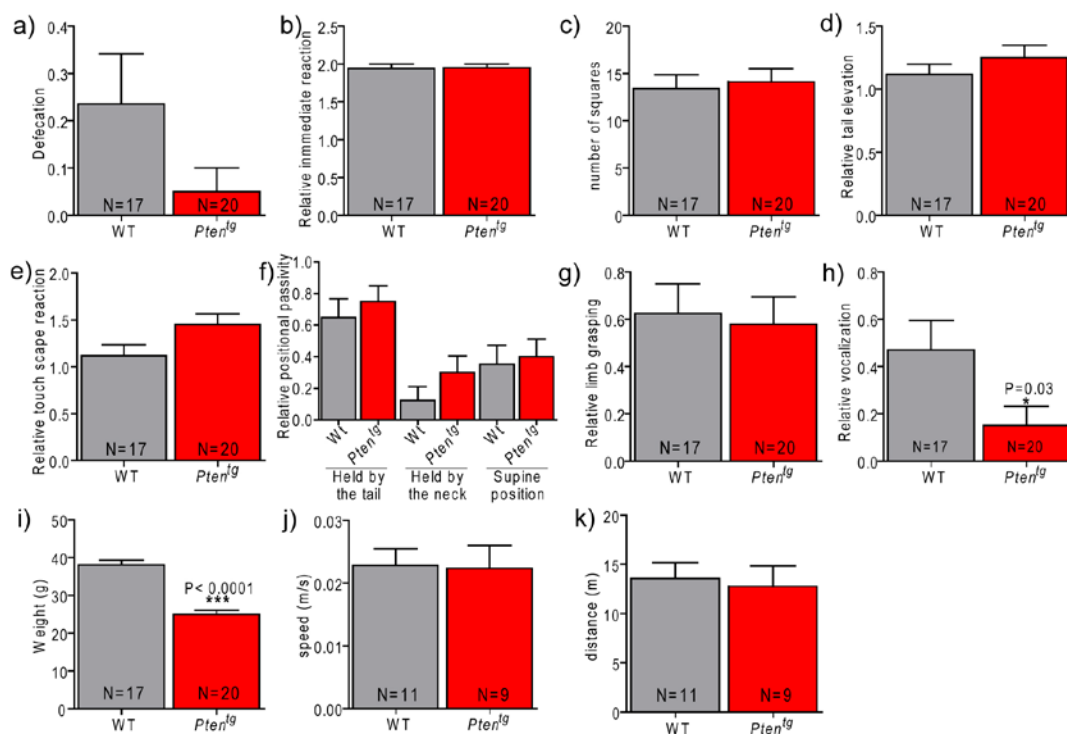


[Figure 15] **General phenotypic characterization.** (a-i) SHIRPA protocol: (a) Representation of presence (1) or absence (0) of defecations during SHIRPA characterization. (b) Immediate reaction to a new environment, noted as 0 when the mouse appears to freeze for a period longer than 5 seconds, 1 as a brief freeze followed by movement or 2 to an immediate movement. (c) Locomotor activity measured as total number of squares a mouse entered with all four feet in 30s. (d) Relative tail elevation evaluated as 0 when dragging, 1 as horizontal extension or 2 as elevated tail. (e) Relative touch scape reaction annotated with a 0 when there were no response, 1 when the mouse made a response to touch or 2 when it fled prior to touch. (f) Relative positional passivity represented as 0 when the mouse did not struggle and 1 when it did, this is measured with the mouse held by the tail, by the neck and in supine position. (g) Limb grasping representation as present (1) or absent (0). (h) Vocalization during SHIRPA observations, 1 when present or 0 when absent. Mann-Whitney t-test * $P < 0.05$. (i) Weight of the animals used for this study. unpaired t-test *** $P < 0.0001$ (j, k) Open-field test for locomotor activity: mean speed (j) and total distance (k) during 10 minutes test session. In all graphs, mean and SEM are shown for WT and *Pten^{tg}* mice.

placed into a petri dish. To further evaluate the effect of the genotype on early communication, I also assessed the effect of mother care by measuring USV from pups in response to WT versus *Pten^{tg}* mothers.

When comparing WT and *Pten^{tg}* pups in response to WT mothers, the clearest differences were found in call duration and intensity (measured as amplitude, in decibels), which were both decreased in *Pten^{tg}* pups (Fig. 16d and f, respectively). Some differences were also observed in call frequency (Fig. 16e) and number of calls (Fig. 16c), but these were not consistent at different ages. When comparing the response of WT and *Pten^{tg}* pups from *Pten^{tg}* mothers, I found that the number of calls (Fig.16i), their duration (Fig.16j) and their intensity (Fig. 16l) were decreased for *Pten^{tg}* pups at the beginning of the experiment, although they reached WT values by PND12. Call peak frequency was similar in *Pten^{tg}* pups compared to WT pups (Fig. 16k). As expected, *Pten^{tg}* pups body weight is reduced compared to WT mice irrespective of the genotype of the mother (Fig. 16b, h). Interestingly, body temperature was decreased in *Pten^{tg}* pups, but only in those from *Pten^{tg}* mothers (compare Fig. 16a and g). In conclusion, and considering all these acoustic parameters, the calls from *Pten^{tg}* pups present an overall reduced communicative value, as compared to WT pups.

4.2.2 Normal nesting-behavior and self-grooming.

Typically, homecage behavior is altered in PTEN-ASD mouse models, with decreased nest-building activity (Kwon et al., 2006) and altered grooming (Clipperton-Allen and Page, 2014, 2015; Lugo et al., 2014), which is reminiscent of repetitive behavior alterations in ASD patients. The analysis of these behaviors is used as a screening for the ability to perform “activities of daily living” (ADL), as preclinical assessment for several diseases (Deacon, 2012), such as obsessive compulsive disorder (OCD) and ASD (Angoa-Pérez et al., 2013).

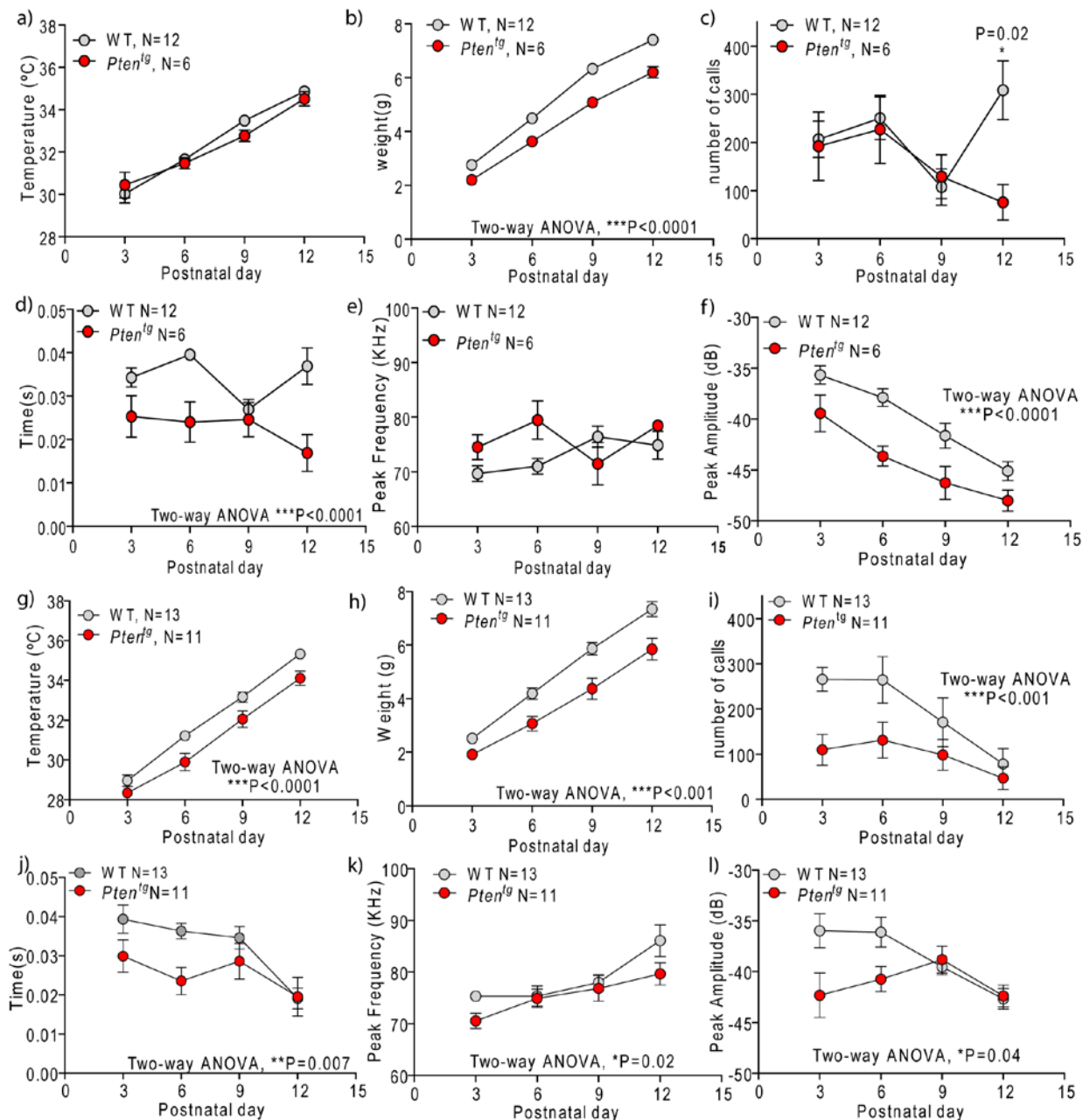


[Figure 16] Isolation-induced ultrasonic vocalization (USV) from Wt and *Pten^{tg}* mice. USV emitted by pups from WT mother (a-f) and from *Pten^{tg}* mother (g-l). (a, g) Representation of the temperature right after the vocalization assessment was done. Means±SEM of temperature is represented for pups from WT mother (a) and from *Pten^{tg}* mother (g). (b, h) Weight of the pups is observed each experimental day. Means±SEM are shown for pups from WT mother (b) and from *Pten^{tg}* mother (h). (c, i) Total number of USV emitted during the 5 minutes test session. Means±SEM are shown for pups from WT (c) mother from *Pten^{tg}* mother (i). (d, j) Mean duration of USV calls. Means±SEM are shown for pups from WT mother (d) and from *Pten^{tg}* mother (j). (e, k) Mean peak frequency of USV. Means±SEM are shown for pups from WT mother and from *Pten^{tg}* mother (k). (f, l) Mean peak amplitude of USV. Means±SEM are shown for pups from WT mother (f) and from *Pten^{tg}* mother (l). N represents number of animals.

For rodents, nests are important for heat conservation, reproduction and shelter from predators, as well as for avoiding harsh environmental conditions and for protecting the pups (Deacon, 2006b; Gaskill et al., 2013). Therefore, this type of behavior is associated with the survival of wild mice, and alterations on nesting activity are useful to identify the animal's overall welfare. Nest construction is controlled by several hormones and brain areas, such as the hippocampus (Deacon, 2006b). For these experiments, I scored nesting behavior of adult WT and *Pten^{tg}* mice during 36 hours. Thirty minutes after the Neslet was placed in the cage, most of the material remained intact, but after 12 hours, during the dark phase, more than 50% of the material was used. After 24 hours both genotypes had an identifiable nest, but still flat, and at 36 hours,

a near perfect nest was present in the cages for both *Pten^{tg}* and WT mice (Fig. 17a). Nest weight was measured at the same time points and no differences were observed when comparing *Pten^{tg}* and WT littermates (Fig. 17b).

One experimental approach to measure repetitive behavior is self-grooming, a complex stereotyped behavior involving rapid movement of forepaws over facial area and along the body (Moretti et al., 2005). The role of PTEN in this behavior is not clear. Thus, heterozygous animals lacking one copy of the *PTEN* gene (*Pten^{+/-}*) exhibited enhanced grooming (Clipperton-Allen and Page, 2014, 2015). In contrast, PTEN conditional KO animals with the *Gfap* promoter (*Gfap-Cre; Pten^{loxP/loxP}*) exhibited a decreased grooming (Lugo et al., 2014). To explore whether *Pten^{tg}* mice present alterations in stereotyped behavior, I analyzed self-grooming events during 10 minutes in these animals. *Pten^{tg}* mice performed the same number of grooming events (Fig. 17c) with the same total duration (Fig. 17d) and mean duration per event (Fig. 17e).

In conclusion, *Pten^{tg}* mice did not show differences in nesting construction or in self-grooming, suggesting that PTEN does not contribute to these types of behaviors.

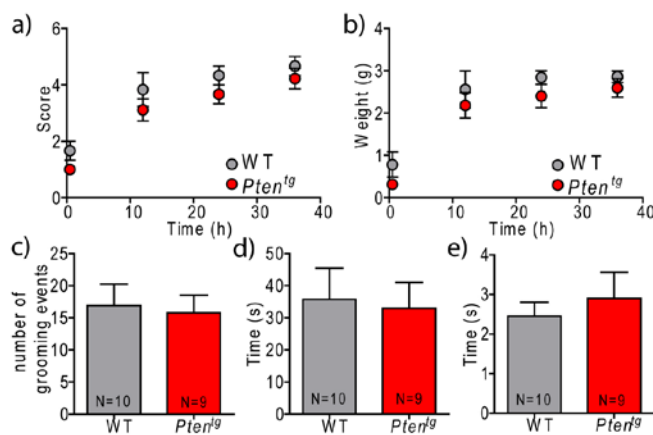


[Figure 17] Homecage behaviors. (a, b) Nesting behavior evaluated as quality score (a) and weight (b) of the nest, measured 30 minutes, 12, 24 and 36 hours after introduction of nesting material into the cage. (c-e) Self-grooming, represented as total number of grooming events (c), total time grooming (d) and mean time of grooming events (e). Means±SEM are shown. N represents number of animals.

4.2.3 *Pten^{tg}* mice display reduced anxiety.

ASD patients exhibit enhanced anxiety (Silverman et al., 2010). In *Pten* models for ASD, the anxiety phenotype is not completely clear, probably due to the differential expression of *Pten* deletion in different areas of the brain (Kwon et al., 2006; Lugo et al., 2014). To characterize *Pten^{tg}* anxiety-like behavior, I used the elevated plus-maze assay. This is based on a cross-shaped platform with two open arms and two closed arms (fig. 18a). In general, a reduction in the time spent in the open arms is interpreted as a sign of anxiety. We calculated an exploration index as the time spent in the open arms divided by the total time spent in closed and open arms. As shown in Fig. 18b, the exploration index in *Pten^{tg}* mice was significantly higher than in their WT littermates (fig. 18b). This indicates a decreased in anxiety in *Pten^{tg}* mice, as they spend more time in the open arms. This phenotype may also be consistent with the reduced communicative value of the USV in *Pten^{tg}* pups, since isolation-induced USVs may reflect an anxious-like behavior (Benton and Nastiti, 1988).

4.2.4 *Pten^{tg}* mice display pro-social behavior

Mice are social species and display behavioral social interactions (Murcia et al., 2005). Thus, social interaction and nesting have been proposed as core paradigms to test autistic behavior in mice (Moy et al., 2004). Mice with a conditional *Pten* deletion exhibit a reduced social interaction (Kwon et al., 2006). Therefore, it was interesting to test whether this behavior was altered in *Pten^{tg}* mice. To this end, social recognition was measured using a three-chamber cage, where I measure the time that the experimental mouse spends directly exploring an inanimate object versus the time spent exploring a novel conspecific mouse (representative occupancy plot in fig. 18c). The three-chamber social interaction test allows for assessment of both social motivation (preference trial) and social novelty preference (memory trial) (Tilot et al., 2014). Indeed, I found that while both genotypes spent significantly more time in the chamber with the stranger mouse than in the other chamber containing an identical cage with an inanimate object, *Pten^{tg}* mice exhibited higher levels of social interaction compared to their WT littermates (Fig. 18d). After the stranger

vs. inanimate presentation, I substituted the inanimate target by a second social target to study social novelty behavior, a task to evaluate social memory (Fig. 18e). A similar increase in the exploration of the familiar vs. the unfamiliar mouse was observed for both genotypes (fig. 18f). This finding implies that *Pten^{tg}* mice exhibit enhanced social recognition with normal social novelty preference. Therefore, PTEN overexpression leads to an increase in social interest or discrimination when the animal is first exposed to choose between a social target or an inanimate target.

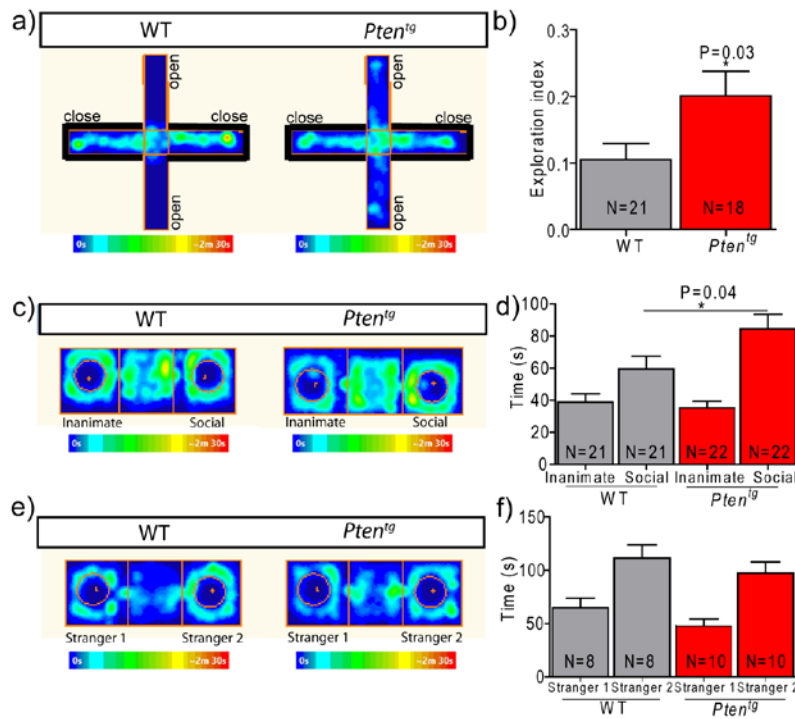
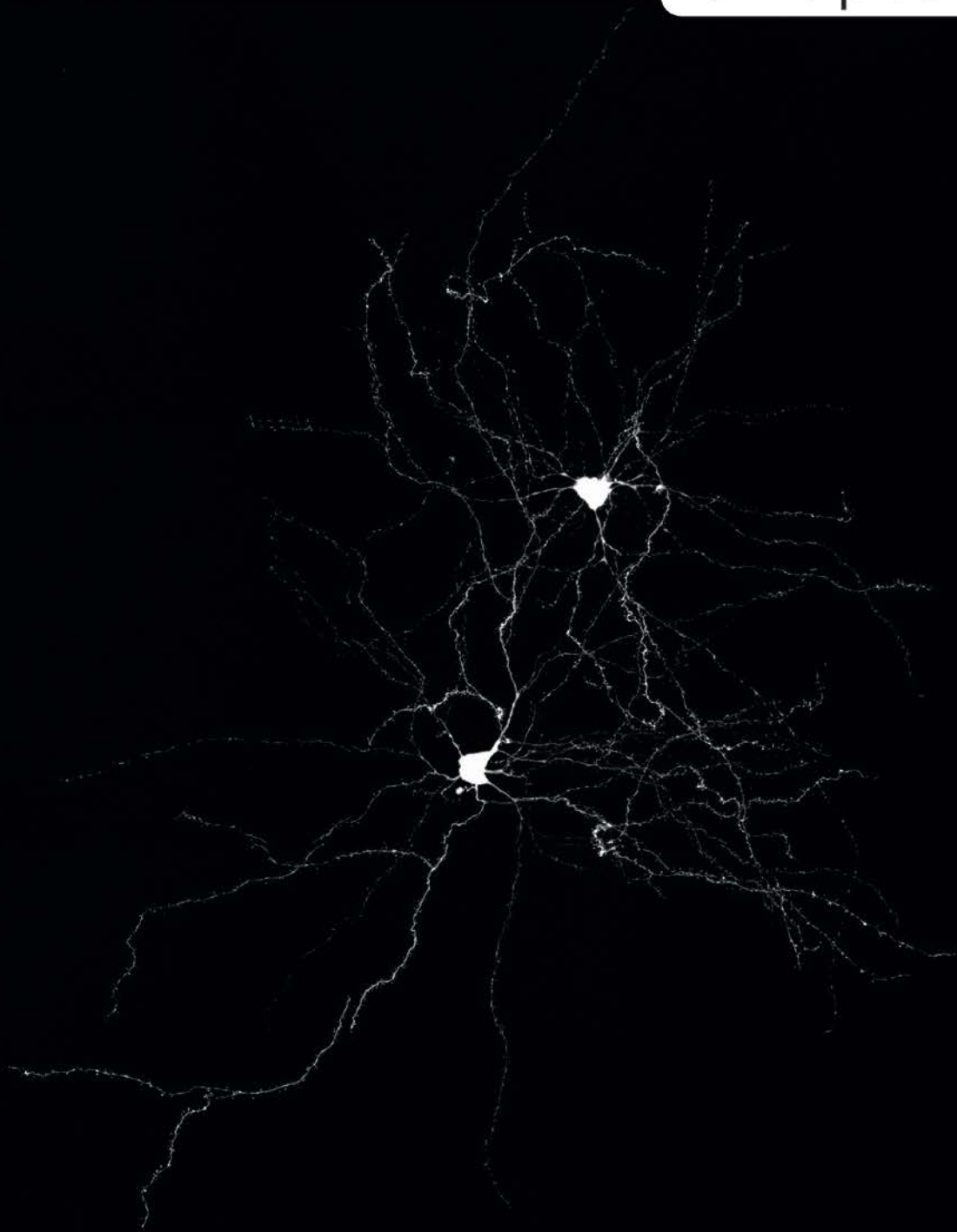


[Figure 18] Anxiety-like and social behavior. (a) Representative occupancy plot of anxiety-like behavior, measured in the elevated-plus maze, of WT and *Pten^{tg}* mice. (b) Exploration index was calculated as total time in open arms/total time in open and closed arms. Mean and SEM are shown for WT mice and *Pten^{tg}*, t-test * $P < 0.05$. (c) Representative occupancy plot of social recognition, measured in three-chamber apparatus, from WT and *Pten^{tg}* mice. (d) Total time exploring inanimate and social target is represented. Mean and SEM are shown for WT and *Pten^{tg}*; t-test * $P < 0.05$. (e) Representative occupancy plot of social novelty, measured in three-chamber apparatus, from WT and *Pten^{tg}* mice. Total time exploring stranger 1 and stranger 2 is represented. Mean and SEM are shown for WT mice and *Pten^{tg}*.

Chapter 2



Consequences of the removal of PTEN PDZ interaction

1. PI3K pathway modulation in PTEN- Δ PDZ mice:

To test the modulation of the PI3K pathway upon PDZ motif truncation, I analyzed the phosphorylation state of AKT, direct effector of PI3K pathway activation. This was analyzed by western blot in hippocampus and amygdala, two important structures in ASD. Also, levels of PTEN were tested, to evaluate if the elimination of the PDZ motif from the protein could affect protein expression or stability (Ecker et al., 2015).

1.1 Normal levels of PTEN protein in amygdala and hippocampus from PTEN- Δ PDZ mice.

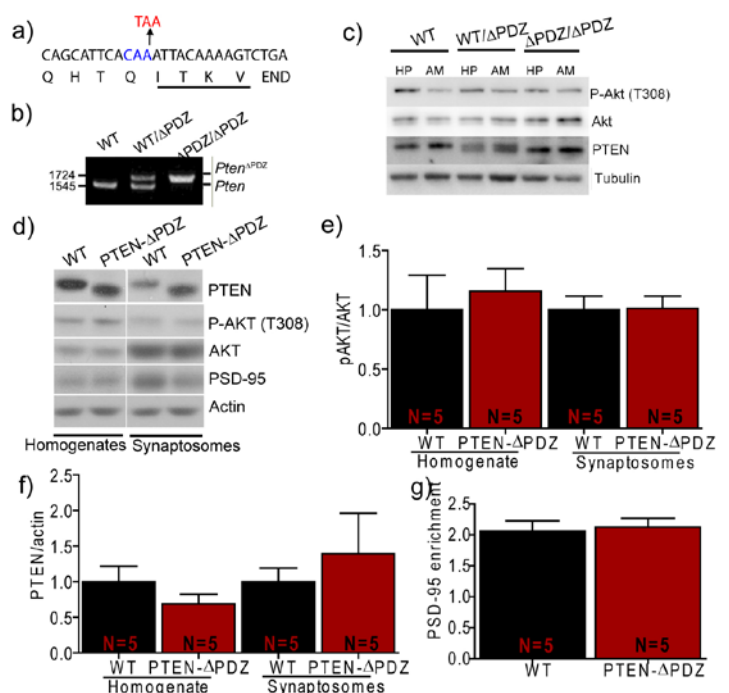
Amygdala and hippocampus from WT and PTEN- Δ PDZ heterozygous and homozygous mice were dissected (described in Materials and Methods) and PTEN protein levels and AKT phosphorylation were evaluated. PI3K pathway activation appears to be equivalent in WT and PTEN- Δ PDZ mice brains structures, as shown by AKT phosphorylation levels in the Threonine 308 (Fig. 19c). In addition, PTEN total levels are not changed in PTEN- Δ PDZ mice, as compared to WT mice. To note, we could also confirm the genotype of the animal from its PTEN migration pattern, since PTEN- Δ PDZ protein migrates slightly faster than the WT protein (Fig. 19c). In conclusion, these results indicate that eliminating the PDZ motif from PTEN protein does not affect to the protein expression or PI3K pathway activation.

1.1 Normal levels of PTEN and phosphorylation of AKT in hippocampal synaptosomes from PTEN- Δ PDZ mice.

The PDZ motif at the C-terminus of PTEN is important for protein-protein interaction and stabilization of the protein (Bonifant et al., 2007; Valiente et al., 2005). Specifically, it has been described that interaction of PTEN with PSD-95 at the postsynaptic density in the spine is important for synaptic plasticity (Jurado et al., 2010). Therefore, it was important to evaluate total PTEN levels and activation of the PI3K pathway in synaptosomes from PTEN- Δ PDZ mice. Total extracts and synaptosomal extracts were prepared

[Figure 19] PTEN- Δ PDZ molecular characterization.

(a) The amino acid and nucleotide sequences of the knock-in region with the substitution of codon 399 (CAA, glutamine) with TAA (Stop codon). The PDZ-binding motif is underlined. (b) PCR-genotyping of the PTEN- Δ PDZ mouse model and control. DNA from WT and PTEN- Δ PDZ was analyzed by PCR with the primers described. Representative PCR reaction result from transgenic animal and wild-type littermate is shown. (c) Western blot showing PTEN, pAKT(Thr308), total AKT and tubulin in total extract from hippocampus (HP) and amygdala (AM) from homozygous PTEN- Δ PDZ, heterozygous and wild type littermates. Note the lower position of PTEN lacking the PDZ-binding motif. (d) Western blot analysis of hippocampal homogenates (left) and synaptosomes (right) of homozygous PTEN- Δ PDZ mice and their WT littermates. Quantification of pAKT/tAKT ratio (e) and PTEN levels normalized by actin (f) in homogenates and synaptosomes from PTEN- Δ PDZ mice and their WT littermates. (g) PSD-95 enrichment in synaptosomes, calculated by dividing PSD-95 levels in synaptosomes over total homogenate levels.



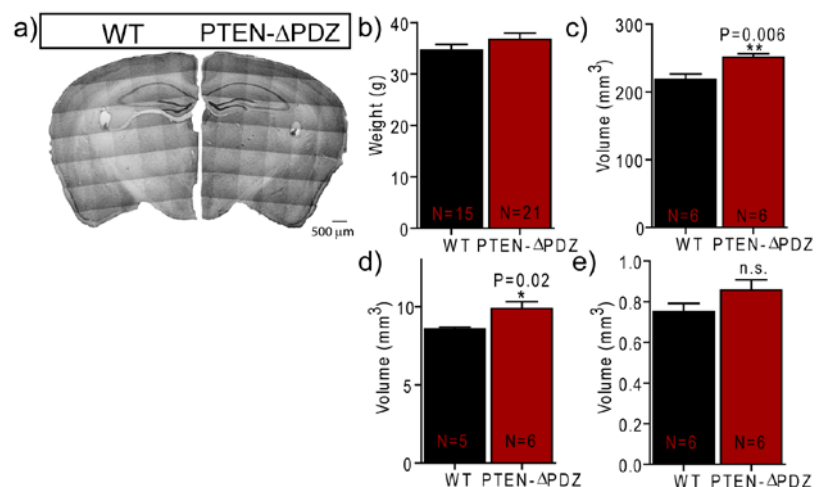
from whole hippocampus using WT and PTEN- Δ PDZ mice (detailed in Materials and Methods). Total PTEN protein levels and activation of the PI3K pathway (as monitored by phosphorylation of Threonine 308 in AKT) (Alessi et al., 1996; Stephens et al., 1998) were evaluated by western blot (see representative example in Fig. 19d). Total PTEN and phospho-AKT were similar in both total extracts and synaptosomes from PTEN- Δ PDZ mice and WT mice (Fig. 19 e, f). To conclude this molecular analysis, the efficiency of the synaptosomal preparation was estimated from the enrichment of PSD-95, a scaffolding protein present in the PSD (Sampedro et al., 1981). In both WT and PTEN- Δ PDZ mice, I detected a two fold enrichment of PSD-95 in synaptosomes with respect to total hippocampal extracts (Fig. 19 g). Thus, PDZ motif truncation does not alter PTEN levels in synaptosomes from hippocampus, or the activation status of the PI3K pathway.

2. Brain and synapse anatomy in PTEN- Δ PDZ mice.

2.1 Increased brain and hippocampal volume due to PDZ truncation.

PTEN loss of function drives brain overgrowth and neuron morphological alterations, including dendritic hypertrophy and increase in spine density (Kwon et al., 2006; Orrico et al., 2009). Conversely, I have determined that PTEN overexpression leads to the opposite phenotype, with a decrease in spine density, confirmed by a decrease in synapse density in hippocampus and amygdala and a decrease in PSD length in the lateral amygdala, using electron microscopy techniques. To analyze if just lacking the PDZ motif could have consequences in synaptic morphology we used electron microscopy (see representative examples in Fig. 21a, e). In both, CA1-hippocampus and lateral amygdala, synapse density (Fig. 21 b, f; respectively) and PSD length (Fig. 21 c, g; respectively) are normal compared to WT mice. Only when comparing the whole distribution of synapses, using cumulative frequencies, I observed a slight but significant decrease in PSD length in the hippocampus (Fig. 20d), and the opposite effect in the amygdala (fig. 20h). Therefore, these results suggest that synapse density and morphology are mostly determined by the amount of PTEN and not (to a major extent) by PTEN PDZ interactions.

[Figure 20] Brain anatomy analyzed by Unbiased Stereology. (a) Representative images of WT (right) and PTEN- Δ PDZ (left) forebrain stained with Niessl acquired in bright field with 10x objective and tile scan. (b) Body weight. (c) Forebrain volume. (d) Hippocampus volume. (e) Basolateral amygdala volume. In all graphs, mean and SEM are shown for WT and PTEN- Δ PDZ mice. N represents number of animals.



2.2 PTEN- Δ PDZ mice present normal synapse density and PSD length in hippocampus and amygdala.

PTEN loss of function drives brain anatomical alterations, brain overgrowth, and neuron morphological alterations, including dendritic hypertrophy and increase in spine density (Kwon et al., 2006; Takeuchi et al., 2013). PTEN overexpression leads to the opposite phenotype, with a decrease in spine density, confirmed by a decrease in synapse density in hippocampus and amygdala and a decrease in PSD length in the lateral amygdala, using electron microscopy technique. To analyze if just lacking the PDZ motif could have consequences in synaptic morphology we used electron microscopy. In both, CA1-hippocampus and lateral amygdala, synapse density (Fig. 21 b, f; respectively) and PSD length (Fig. 21 c, g; respectively) are normal compared to WT mice. But when population of synapses are studied, using cumulative frequency, we observed that in hippocampus PSD length is decreased (Fig. 20d), but a slightly increase was found in

amygdala (fig. 20h). These results pointed to a PTEN PDZ-independent effect on synapse density, with a slight alteration on PSD length. Moreover, just in lateral amygdala PSD length results in an opposite phenotype when comparing genotypes, with a decrease in *Pten*^{tg} mice and an increase in PTEN-ΔPDZ lateral amygdala synapses.

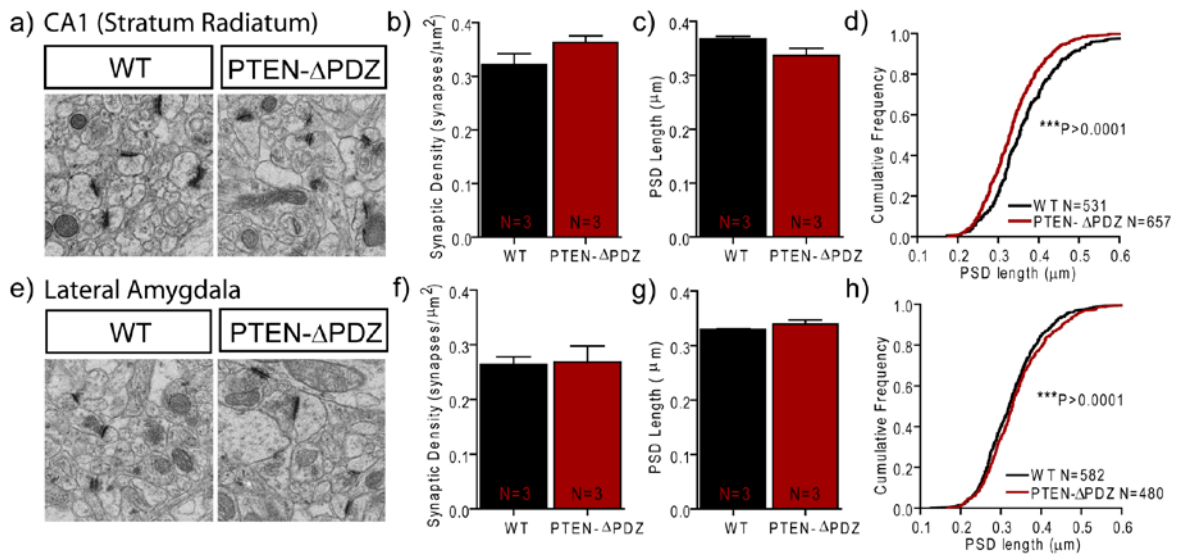


[Figure 21] Electron microscopy analysis of synapses. (a) Electron micrographs of synapses in the hippocampal CA1 stratum radiatum for WT (left) and PTEN-ΔPDZ mice (right). Quantification of synapse density (b) and PSD length (c) in WT and PTEN-ΔPDZ mice from micrographs as those shown in (a). Mean and standard deviation are plotted. N represents number of animals. (d) Cumulative frequency of PSD length from WT and PTEN-ΔPDZ mice from the same data as in (c). N represents number of synapses. (e-h) Similar to (a-d), from lateral amygdala.

3. LTD impairment in the cortical pathway of the amygdala due to PDZ motif truncation.

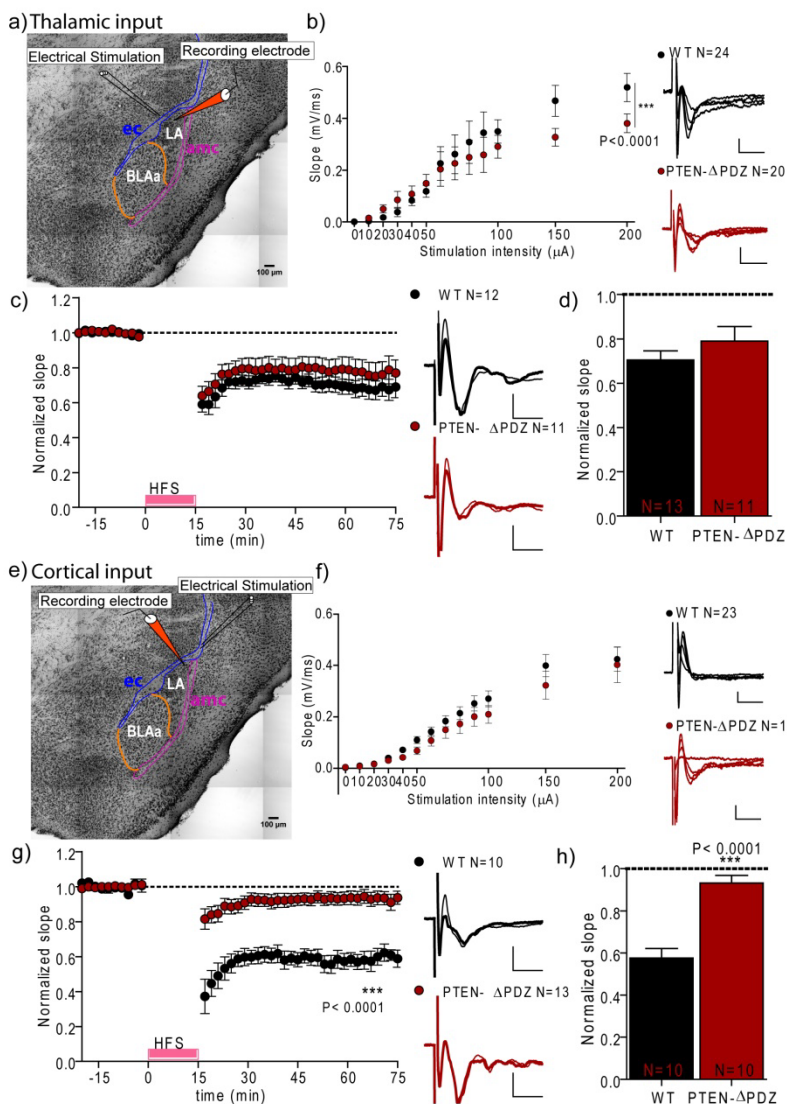
ASD mouse models based on PTEN deficiency present pleiotropic effects on synaptic transmission, depending on the area or the age studied (Sperow et al. 2012; Takeuchi et al. 2013). This is probably due to a mixed effect of direct synaptic functions of PTEN and its well established neurodevelopmental roles. Using acute modulations of PTEN function in the hippocampus, our laboratory has established that PTEN is an essential protein for NMDA receptor-dependent LTD in a PDZ-dependent manner, through its interaction with PSD-95 (Jurado et al., 2010). Therefore, I decided to evaluate whether PDZ-dependent interactions of PTEN are important for synaptic plasticity in the amygdala.

As shown in the first chapter, PTEN overexpression leads to pathway-specific alterations in synaptic transmission in the amygdala. Thus, basal synaptic transmission is decreased only in the thalamic input to the amygdala, whereas LTP is decreased and LTD is increased exclusively in the cortical input of lateral amygdala (fig. 11). These results are in good agreement with recently found relationships between social behavior, PTEN and synaptic plasticity in cortical-amygdala, after alterations in the PI3K pathway in VPA-rat models of autism (Wu et al., 2016; Yang et al., 2016). This is also consistent with the connection between the basolateral amygdala (BLA) and the prefrontal cortex (mPFC) pathway controlling social interaction and anxiety-like behavior (Felix-Ortiz et al., 2015). Taking into account that *Pten*^{tg} mice present an increased social interaction and reduced anxiety, together with pathway-specific alterations in synaptic plasticity in the amygdala, I decided to further evaluate whether there is a causal relationship between these forms of synaptic plasticity and the modulation of social behaviors by PTEN. To this end, I carried out field recordings in acute slices from PTEN-ΔPDZ and WT adult animals. As shown in Fig. 22b, PTEN-ΔPDZ animals have slightly decreased basal synaptic transmission in the thalamic pathway, as compared to WT animals, while cortical basal transmission remains normal (Fig. 22 f). Interestingly, LTD is normal when stimulating the thalamic pathway (Fig. 22c, d), but it is strongly impaired in the cortical pathway (Fig. 22 g, h). Therefore, PTEN appears to be particularly important for cortico-amygdala LTD, where its PDZ motif seems to be essential.

Importantly, this form of synaptic plasticity can be modulated bi-directionally, with PTEN overexpression leading to an increase in NMDA-LTD, and removing PTEN PDZ interactions producing the opposite effect.

[Figure 22] Electrophysiological recordings from the LA.

(a) Schematic representation of thalamic recordings configuration; the stimulation electrode is placed near the external capsule (blue) and the recording electrode (red) within the lateral nucleus of the amygdala. (b) Input-output curves of fEPSPs evoked by stimulation of thalamic afferents. Right, superimposed representative fEPSPs at 50, 100, 150 and 200 μA of stimulation intensity. *N* represents number of slices. (c) LTD was induced by LFS and recorded for 60 min post-induction, following at least 20 min of stable baseline, by thalamic stimulation. Right, representative fEPSPs traces at baseline (thin line) and after LTD induction (thick line) from slices taken from WT and PTEN- ΔPDZ mice. Scale bars represent 0.2 mV, 20 ms. (d) Quantification of average fEPSP maximal slopes at 50–60 min after induction, normalized to the average baseline response. *N* represents number of slices. Data are represented as mean \pm s.e.m. (e) Schematic representation of cortical recordings configuration: the stimulation electrode is directly above the central nucleus of the amygdala, in the external capsule (blue), and the recording electrode (red) within the lateral nucleus of the amygdala. (f-h) Similar to (b-d) upon stimulation of cortical afferents from WT and PTEN- ΔPDZ mice.



4. Behavioral characterization in PTEN- ΔPDZ .

ASD is a neurodevelopmental disease characterized by persistent social and communication deficits with stereotyped and repetitive patterns of behavior. Several mouse models with conditional deletions of PTEN have been characterized, observing different cognitive behaviors related with memory and learning deficits, but with a coincident aberrant social phenotype (Kwon et al., 2006; Sperow et al., 2012; Takeuchi et al., 2013). In addition, we have seen that PTEN overexpression leads to a prosocial behavior. In this part of the study I evaluated the effect of the PDZ motif of PTEN on sociability, as well as other behavior measured previously in *Pten^{tg}* mice, in order to extract the implication of the protein in these behaviors and, specifically, of its PDZ-dependent interactions.

4.1 Hippocampal-dependent memory evaluation: PTEN- ΔPDZ mice do not have alterations in hippocampal dependent memory.

To analyze hippocampal-dependent short term memory I have test the novel object location task in WT and PTEN- ΔPDZ homozygous animals. In this test direct exploration time of the displaced (novel) or not displaced (old) object was measured (Fig. 23a). Discrimination index, calculated as the time exploring the object at the novel location divided by exploration time of both objects, was similar for PTEN- ΔPDZ mice and WT littermates (fig. 23b). Therefore, neither PTEN levels nor PTEN PDZ-dependent interactions seems to be

important for short-term hippocampal-dependent memory. Importantly, the total distance traveled in this assay was similar for the two genotypes (Fig. 23c), suggesting the absence of motor phenotypes.

4.2 PTEN- Δ PDZ mice exhibit a normal anxiety-like behavior.

In order to define the implication of PTEN PDZ interactions in anxiety-like behavior I evaluated the performance of PTEN- Δ PDZ mice in the elevated-plus maze. Thus, I scored total time in open arms (more anxiogenic), and in closed arms (less anxiogenic) (Fig. 23d). Exploration index was similar in homozygous PTEN- Δ PDZ mice (Fig. 23e) and in heterozygous PTEN- Δ PDZ mice (Fig. 23g, h), as compared with WT littermates. Therefore, the PDZ motif of PTEN does not appear to be important for anxiety-like behavior.

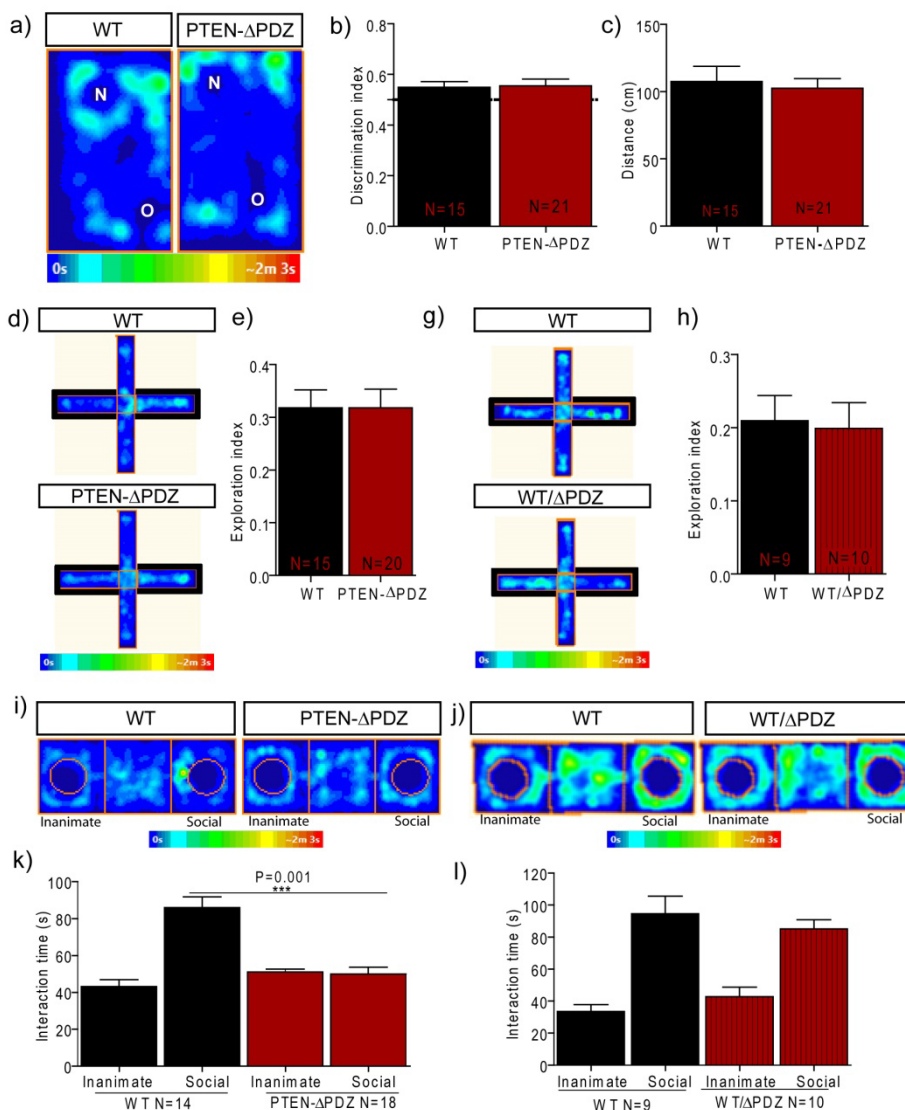


[Figure 23] **Novel object location, anxiety-like and social behavior.** (a-c) Novel object location task. (a) Occupancy plots of representative examples of WT and PTEN- Δ PDZ exploration, where N represents the displaced object (novel location) and O the not-displaced object (old location). (b) Discrimination index was calculated as the time exploring the novel object over the time exploring both objects. (c) Total distance traveled during the 5 minutes test. (d-h) Anxiety-like behavior in the elevated-plus maze task. Occupancy plot of representative behavior of PTEN- Δ PDZ (d) and heterozygous (g) mice, compared to WT. Exploration index was calculated as total time in open arms over total time in open and closed arms for homozygous (e) and heterozygous (h) PTEN- Δ PDZ compared with their WT littermates. (i-l) Social recognition measured in three-chamber apparatus. Occupancy plot of representative behavior of WT mice compared to homozygous (i) and heterozygous (j) mice. Total time exploring inanimate and social target is represented for homozygous (k) and heterozygous (l) PTEN- Δ PDZ mice compared to WT mice.

4.3 Impaired sociability in homozygous PTEN- Δ PDZ mice.

To test whether the PDZ motif is important for social behavior I analyzed homozygous and heterozygous PTEN- Δ PDZ animals in the three chambers social recognition assay (Fig. 23i, j). In contrast to WT mice, homozygous PTEN- Δ PDZ mice spend the same time exploring the inanimate target as the social target, therefore displaying no preference for the social target (Fig. 23k). To evaluate the haplosufficiency of this effect, I evaluated sociability also in heterozygous PTEN- Δ PDZ mice. As shown in Fig. 23l, these animals display a preference in exploration time for the social target similar to their WT littermates. These results imply that the PDZ-dependent interactions of PTEN are essential for social recognition, but just one copy of the *WT-Pten* gene is enough for this behavior.

4.2 Normal ultrasonic vocalization in isolated PTEN- Δ PDZ pups, but modified depending on maternal genotype.

To assess if PTEN PDZ motif is important for early communication, I have measured ultrasonic vocalizations in isolated pups of 3, 6, 9 and 12 days of age. Number of calls (Fig. 24c), as well as acoustic features, such as call duration (Fig. 24d), peak frequency (Fig. 24e) and peak amplitude (Fig. 24f), were similar when comparing WT mice with heterozygous and homozygous PTEN- Δ PDZ littermates from heterozygous PTEN- Δ PDZ mothers. Body weight and temperature were monitored after recording ultrasonic vocalizations to detect possible differences due to genotype and also health stage of the animals each day of the experiment. Littermate pups from heterozygous mothers did not present variances in body weight or temperature (Fig. 24a, b). To complete this characterization I evaluated the influence of the genotype of the mother for this behavior. I observed that homozygous PTEN- Δ PDZ pups presented different ultrasonic vocalizations in response to isolation from homozygous or heterozygous PTEN- Δ PDZ mothers. Specifically, I found an increase in the number of calls (Fig. 24i) and peak frequency (Fig. 24k) from homozygous PTEN- Δ PDZ pups responding to homozygous PTEN- Δ PDZ mothers. This effect was evident at the beginning of the experiment (PND 3-6) and was lost by PND 12. Call duration (Fig. 24j) and peak amplitude (Fig. 24l) were similar throughout the experiment. Intriguingly, body weight had a trend to increase more quickly in homozygous raised by homozygous mothers, as compared to those from heterozygous mothers (Fig. 24h). Body temperature was normal, with a slight little increased observed at PND12 (Fig. 24g). This influence of the genotype of the mother was not observed when comparing the response of WT pups to WT versus heterozygous mothers, or responses of heterozygous pups to homozygous versus heterozygous mothers (Supplementary figure 1).

This result showed that PTEN- Δ PDZ animals do not present problems in early communication due to PDZ truncation, but that this behavior is influenced by the genotype of the mother, suggesting possible changes in maternal care depending on the PDZ motif.

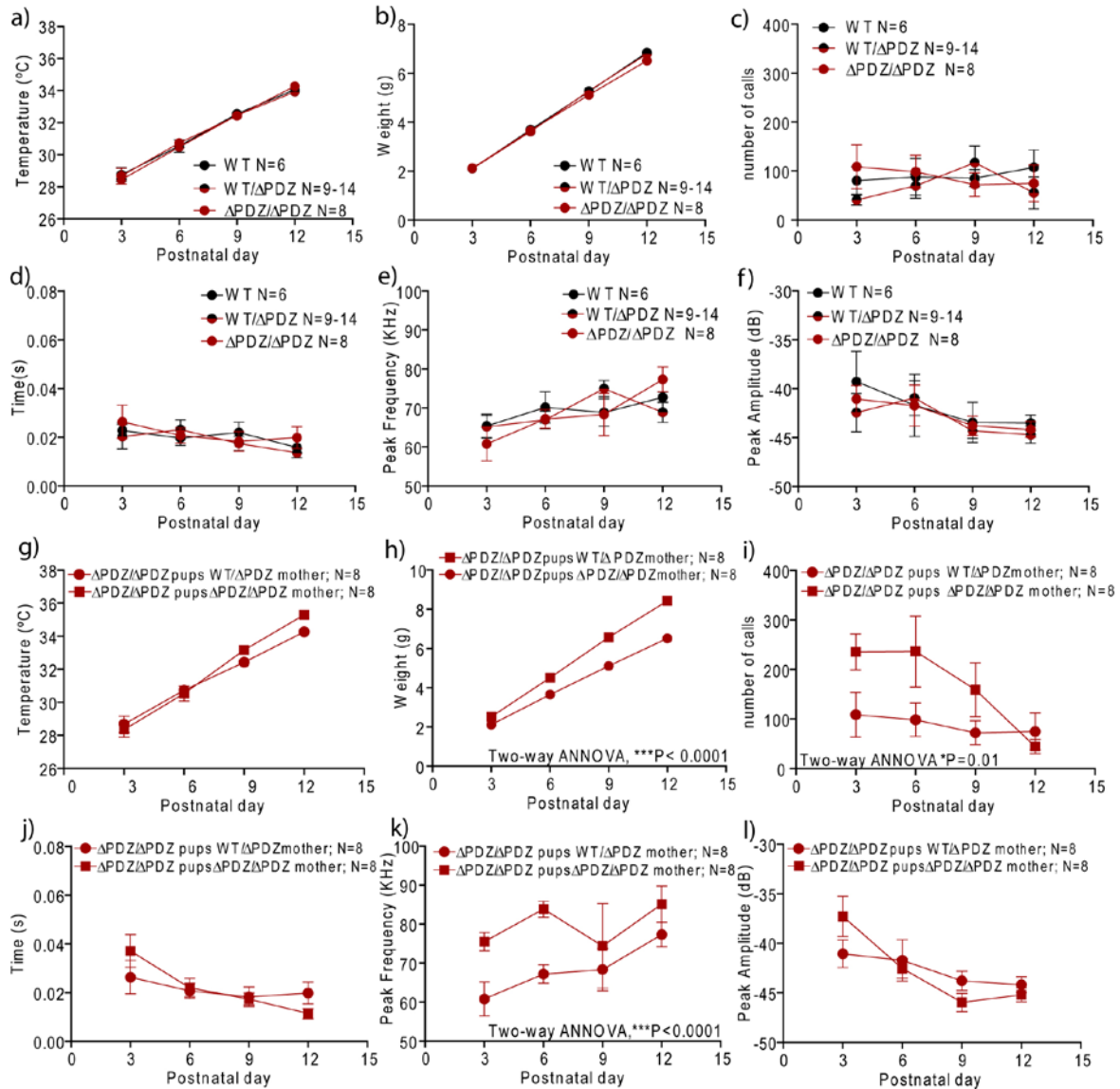
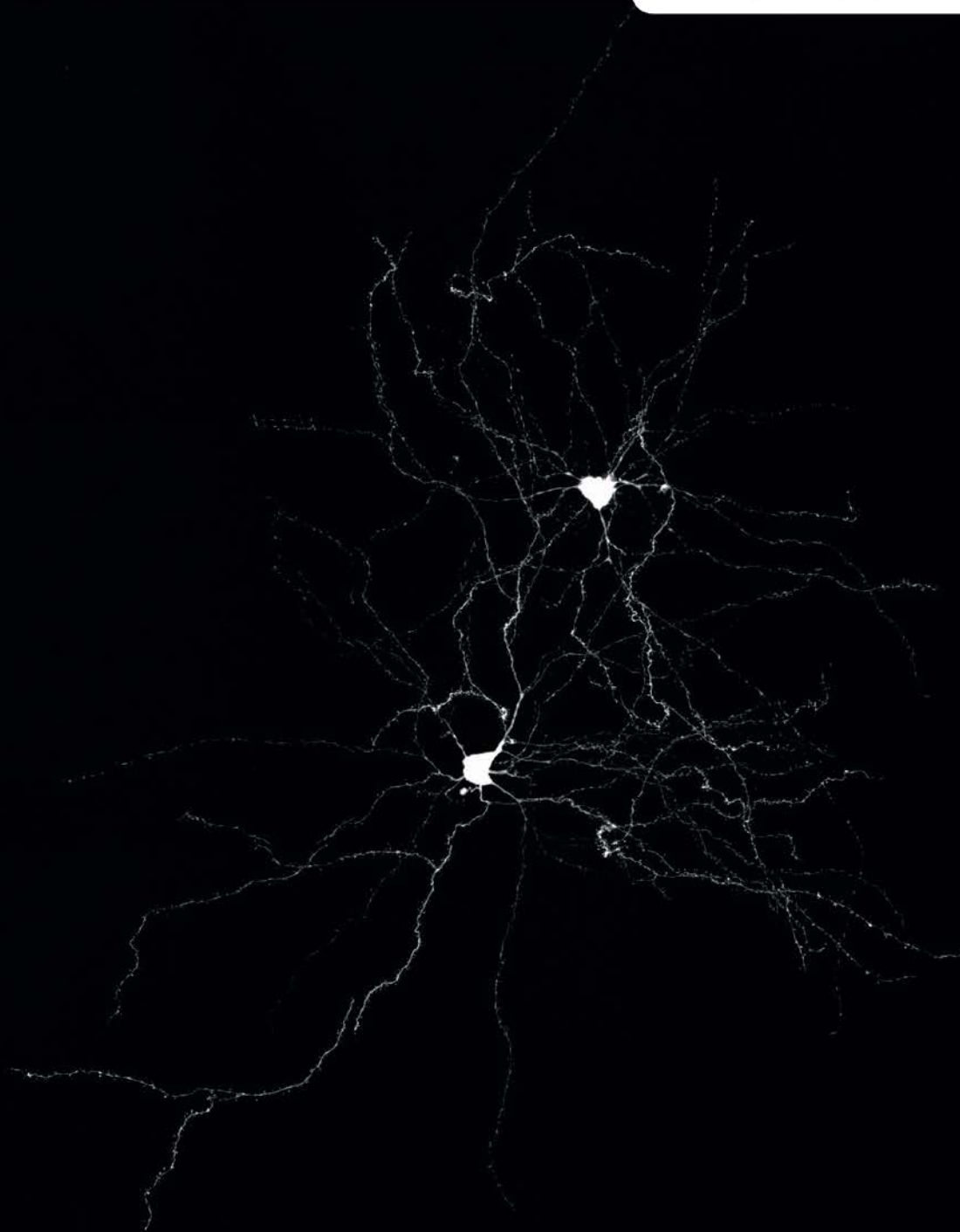


[Figure 24] Isolated induced ultrasonic vocalization (USV) in pups. Representation of the temperature of the pups from heterozygous (a) and homozygous mother (g) right after the vocalization assessment was done. Weight of the pups from heterozygous (b) and homozygous mother (h) observed each experimental day. Total number of USV emitted by pups from heterozygous (c) and homozygous mother (i). Mean duration of USV emitted by pups from heterozygous (d) and homozygous mother (j). Mean peak frequency of USV emitted by pups from heterozygous (e) and homozygous mother (k). Mean peak amplitude of USV emitted by pups from heterozygous (f) and homozygous mother (l). N represents number of animals.

Discussion





Modulation of brain volume by PTEN

The findings of this PhD dissertation suggest that PTEN could modulate brain growth in a bidirectional manner. Pten overexpression results in microcephaly, opposite to the preceding reports of macrocephaly in PTEN-ASD patients (Frazier et al., 2015) or in Pten-deleted mouse models (Clipperton-Allen and Page, 2014; Fraser et al., 2004; Kwon et al., 2006). Besides manipulating global PTEN activity, we also have evaluated the role of PTEN PDZ interactions for the regulation of brain growth. To this end I have used PTEN- Δ PDZ mice, in which PTEN lacks the PDZ binding motif. Interestingly, these animals also display macrocephaly, despite having wild-type levels of global PTEN activity.

Pten^{tg} mice exhibit smaller hippocampus whereas PTEN- Δ PDZ exhibit larger hippocampus. Hippocampus volume alteration has been found in patients with ASD (Amaral et al., 2008). It is an important region of the brain in processing memory and learning (Andersen et al., 2007), but also anxiety (Felix-Ortiz et al., 2013) and sociability (Felix-Ortiz and Tye, 2014; Hitti and Siegelbaum, 2014a; Okuyama et al., 2016). Thus, behavioral and anatomical alterations could be related to hippocampal abnormal growth, and PTEN levels would be a key regulatory point. On the other hand, BLA volume is not significantly different in these transgenic mice when compared to their WT littermates. Nevertheless, the amygdala as is a key element in socio-emotional processes and results abnormal in most of ASD cases (Baron-Cohen et al., 2000), although previous studies on amygdala volume or cell number are quite controversial, as have been reported alterations in the amygdala of ASD patients in both directions (Munson et al., 2006; Schumann and Amaral, 2006). Additionally, it is important to point out that hippocampus is altered as expected, with a reduction in volume and cell number, probably due to the activity of PTEN down-regulating cell proliferation; but this is not happening to the same extent in the amygdala. Therefore, the lack of significant effect of PTEN abnormalities on the amygdala volume suggests a region-specific cell growth modulation by PTEN.

The variation in brain volume seen in PTEN- Δ PDZ mice (13% increase) is smaller than the one observed in Pten KO mice (30% increase)(Kwon et al., 2006) or in *Pten^{tg}* mice (30% decrease). Hence, appropriate total levels of PTEN protein appear to be more important to regulate global brain growth and development, resulting in changes in brain volume. The fact that deletion of the PDZ motif has a smaller effect (13%) may indicate that this motif (and the protein interactions mediated by it) is not related to AKT-mTOR activation(Leslie et al., 2001), which is more strongly linked to cell growth and proliferation (Fayard et al., 2010). Nevertheless, PTEN- Δ PDZ mice do have slight macrocephaly, suggesting that targeting PTEN to specific subcellular localizations by its PDZ motif or its maintenance in specific molecular complexes (Valiente et al., 2005) is important, to some extent, for the correct development of the brain.

I measured the number of cells in both hippocampus and amygdala. This study reports that the total number of cells in the hippocampus is reduced in *Pten^{tg}* animals compared to WT mice, in accordance with PTEN canonical role in cell proliferation. This finding is in accordance with previous reports describing an increase in neuronal proliferation and differentiation rate upon Pten KO in hippocampal progenitor cells (Amiri et al., 2012).

To summarize, I propose here that PTEN modulates brain growth in a bidirectional manner. In addition, the PDZ binding motif is necessary for proper brain development. Moreover, I propose that PTEN interaction with PDZ proteins may contribute to neurodevelopmental alterations found in PTEN-ASD. Furthermore, these anatomical alterations occur differentially in different brain areas, as it has been found in several ASD patients (Ecker et al., 2015).

Regulation of neuron morphology by PTEN

I have analyzed principal neurons morphology in the LA. The LA represents a part of the social brain and it modulates emotional memories and anxiety, as well as being an area affected in ASD (Baron-Cohen et al., 2000).

Pten overexpression results in neuron atrophy accompanied by a reduction in dendritic complexity and reduced spine density. It is widely accepted that PTEN modulates neuron morphology, since Pten KO mice exhibit neuron hypertrophy and increased spine density (Fraser et al., 2008; Haws et al., 2014; Luikart et al., 2011). Therefore, and similar to our observations on brain size, the effects on neuronal structure also appear to occur in a bidirectional manner. The increase of Pten levels during development might lead to a decrease in cellular growth in a cell-autonomous manner (as a result of downregulation of the PIP₃ pathway), resulting in neuronal hypoconnectivity.

The present findings are somewhat different from the effect of shRNA knockdown of PTEN in the BLA and DG of adult animals. In these mice Pten deletion only alters spine density at the distal parts of the dendrites, and induces a shift in the morphology from thin protrusions to mushroom spines (Haws et al., 2014). This difference may be related to development functions of PTEN. Thus, PTEN shRNA knockdown was carried out on mature neurons, whereas overexpression in *Pten^{tg}* mice is present from embryonic development.

Hence, I proposed that the increased PTEN activity *Pten^{tg}* mice promotes an overall reduction in neuronal growth and spine formation, and possibly also in spine maturation. These effects are likely linked to PTEN's ability to downregulate the PIP₃ pathway and then decrease cell growth and proliferation.

PTEN regulation of the synaptic morphology and density

I analyzed the ultrastructure of excitatory synapses (asymmetric synapses) from hippocampal CA1 and LA in both *Pten^{tg}* and PTEN-ΔPDZ animals. It is known that PTEN influences neuronal cytoarchitecture, and, as long it is present in the synapses (Jurado et al., 2010), it might regulate synapse formation, number and size.

In the present study I had observed a reduction in synaptic density in both CA1 and LA of *Pten^{tg}* animals. The result in the LA is in agreement with the spine density reduction observed; and opposite to the increase of synaptic boutons observed in the BLA of heterozygous Pten mice (*Pten^{-/-}*) (Huang et al., 2016), highlighting again the bidirectional modulation by PTEN of neuron morphology. The analysis of synapse structure revealed that *Pten^{tg}* mice present normal PSD length in CA1 synapses, but it is reduced in the LA. The opposite results has been previously reported, after Pten deletion, which results in altered synaptic structure in cerebral cortex, with enlarged presynaptic terminals and PSDs (Fraser et al., 2008). Thus, PTEN control synaptic structure, but this modulation is region specific.

Interestingly, PTEN-ΔPDZ mice present normal synaptic density when compared to WT, in both CA1 and LA. Accordingly, lacking the PDZ motif does not have consequences in synapse formation. In addition, I analyzed population synaptic length in both structures and I observed a decrease in the PSD length in the CA1 of PTEN-ΔPDZ, but a slightly increase in the LA suggesting a region specific modulation of the PSD structure by PTEN PDZ interactions. This may be due to the specific functions that PTEN exerts on the synapse, for which it requires protein-protein interactions through the PDZ motif to be directed and maintained in the synaptic complex (Valiente et al., 2005). Hence, PDZ lacking PTEN could not be able to perform its function in the PSD, thus leading to alterations in the PSD structure.

To summarize, PTEN is necessary for synapse formation, as alteration in PTEN protein levels leads to variations in synapse density, and in PSD structure, in a region and PDZ motif- dependent manner.

PTEN regulation of synaptic transmission and plasticity

Human genomic studies have identified several key mechanisms that underlie the pathogenesis of ASD, many of which involve synaptic dysfunction. Thus, ASD is increasingly considered as a synaptopathy (Won et al., 2013). In this sense, the activity of PTEN-PI3K signalling, as an important regulator of synaptic structure and function, is particularly noteworthy. I have demonstrated that PTEN overexpression leads to neuron atrophy in the LA and hypoconnectivity in hippocampus and the amygdala. In addition, PDZ binding motif results important for synapse structure, but not for synapse formation. What is the functional impact of the neuronal atrophy and abnormal synaptic structures resulting from Pten overexpression in the brain? Does the PDZ binding motif have a specific role in synaptic transmission in the LA?

We have separately study the role of PTEN in synaptic transmission in the amygdala and hippocampal pathways, and have observed that PTEN plays distinct roles in different neural circuits. This is particularly relevant, because these results offer us the possibility to correlate specific synaptic dysfunctions to particular behavioural impairments.

With respect to PTEN overexpression, in the present work I found that *Pten*^{tg} mice display decreased basal synaptic transmission in the CA1 compared to their WT littermates. This is accompanied by decreased LTP and normal LTD. These results are consistent with our previous finding that PTEN governs synaptic strength under basal conditions in the hippocampus (Jurado et al., 2010; Knafo et al., 2016), and with the interpretation that LTP expression requires up-regulation of the PIP₃ pathway (Arendt et al., 2014). With respect to PDZ interactions, we have already examined synaptic transmission in PTEN-ΔPDZ mice in the hippocampus (Knafo et al., 2016). We found that the slope of the synaptically evoked field potentials was normal compared to their WT littermates, as well as LTP, but NMDAR-dependent LTD was not present. Therefore, we concluded that PTEN PDZ dependent interactions are not necessary for LTP but specifically for NMDAR-dependent LTD in the hippocampus (Jurado et al., 2010; Knafo et al., 2016).

The situation was significantly more complex in the LA. I found that PTEN overexpression leads to a decreased basal synaptic transmission when stimulating the thalamic input, but it does not affect the cortical input, compared to WT littermates. Similar results were obtained with the PTEN-ΔPDZ mice: decreased basal transmission in the thalamic input, but normal in the cortical input. These results reinforced the importance of PTEN in controlling synaptic strength. Thus, we can propose that normal PTEN function is needed for maintaining appropriate synaptic transmission in the thalamic-LA synapses, and that PTEN PDZ dependent interactions are required for basal synaptic transmission.

Interestingly, synaptic plasticity in the LA was also altered in a pathway-specific manner, but opposite to the one observed for basal transmission: in the cortico-LA synapses PTEN overexpression leads to a shift towards synaptic depression, since LTP is impaired but LTD is enhanced in this pathway. In addition, PTEN-ΔPDZ mice present impaired NMDAR-dependent LTD in the cortical pathway, highlighting the importance of PTEN PDZ interactions in NMDAR-dependent LTD. In contrast, none of these synaptic plasticity alterations was present in thalamo-LA synapses. Therefore, I observed in this work that PTEN PDZ dependent interactions are essential for NMDAR-dependent LTD not only in the hippocampus (Jurado et al., 2010; Knafo et al., 2016), but also in the cortico-LA synapses. Probably, both excitatory synapses share mechanisms of synaptic plasticity. The thalamo-LA synapses may express unknown compensatory mechanisms that mask the effect of PDZ motif deficit, or alternatively, they may be mechanistically different. In fact, previous findings have demonstrated that inputs differ in both afferent activity and postsynaptic mechanisms of synaptic plasticity (Humeau et al., 2005). In the LA, cortical and thalamic inputs contact functionally and morphologically distinct types of dendritic spines and this heterogeneity determines calcium influx, underlying the differentiated influence of specific afferents intermingled on the same dendritic arbor (Humeau et al., 2005).

These findings suggest that PTEN modulates synaptic plasticity in a pathway specific manner. This region specificity will be further discussed regarding the PET study in resting state and in response to fear conditioning.

To summarize, NMDAR-dependent LTD requires appropriate PTEN function and, particularly, PTEN PDZ interactions in both the CA3-CA1 and the cortico-LA synapses. In the hippocampus the activation of NMDAR induces the association between PTEN and PSD-95, targeting PTEN to the PSD to form part of the molecular complex needed for NMDAR-dependent LTD (Jurado et al., 2010). These interaction occur between the PTEN PDZ binding motif and the PDZ domains of PSD-95 (Knafo et al., 2016). Therefore, PTEN- Δ PDZ mice do not exhibit NMDAR-dependent LTD, since PTEN cannot be driven to the PSD; and this seems to be a common mechanism for CA3-CA1 and cortico-LA synapses. The fact that LTD is enhanced by PTEN overexpression (*Pten*^{tg} mice) in cortico-LA synapses but not in CA3-CA1 hippocampal synapses may be due to a saturation effect. For example, in the case of cortico-LA synapses, PTEN overexpression may increase the amount of PTEN recruited to the PSD after LTD induction, leading to a stronger depression. In contrast, this mechanism may already be saturated by endogenous PTEN in the hippocampus, so that PTEN overexpression does not result in increased PTEN recruitment at synapses.

What is the downstream mechanism by which PTEN drives synaptic depression? PTEN seems to participate in the modulation of PIP₃ during NMDAR-dependent LTD induction, not in LTP, counteracting PIP₃ increase in spines (Arendt et al., 2014). It has been described that downregulation of PIP₃ leads to increased mobility of AMPARs, resulting in a redistribution from the postsynaptic to the extrasynaptic membrane, probably facilitating their endocytosis (Rácz et al., 2004), and leading to synaptic depression (Arendt et al., 2010). PTEN overexpression could be driving this balance to PIP₂ formation, thus decreasing synaptic AMPAR. In addition, PIP₂ turnover by the PLC is required for LTD to initiate structural and functional changes in the spine (Horne and Dell'Acqua, 2007). Therefore the dephosphorylation of PIP₃ to PIP₂ by PTEN could be an initial step for further structural changes in the spine that may convert into structural plasticity, which might be enhanced by PTEN overexpression. Furthermore, this dephosphorylation of PIP₃ into PIP₂ in the synapses would need PTEN to be located in the PSD through its PDZ binding motif, thus PDZ lacking PTEN will not be able to control PIP₂-PIP₃ balance upon NMDAR-dependent LTD.

PTEN activity during synaptic plasticity might be important for downstream regulation of PIP₃ pathway, as GSK3 is required for LTD (Peineau et al., 2009a) and PTEN downregulates the pathway, leading to AKT inactivation and the dephosphorylation of GSK3 in the residue Ser9, then activating it (Cohen et al., 1997). GSK3 is needed for NMDAR-dependent LTD in the CA1, but not for LTP or depotentiation (DPT) (Hooper et al., 2007). GSK3 can prevent LTP, since upon LTP induction GSK3 is inactivated (Hooper et al., 2007) and it was observed that a transgenic mice overexpressing GSK3 exhibit LTP deficits in the hippocampus (Hooper et al., 2007), similar to what I observed in *Pten*^{tg} mice. Thus, PTEN may modulate synaptic plasticity through the activation of GSK3. Conversely, during NMDA-dependent LTD, AKT is dephosphorylated, which corresponds to GSK3 activation, as was reported by the reduction of the phosphorylation of the Ser9 (Peineau et al., 2009b), event that can explain a possible molecular mechanism for PTEN control of LTD. Thus PTEN overexpression results with GSK3 activation, thereby preventing LTP, and enhancing LTD.

The type of synaptic plasticity usually altered under conditions of PTEN KO is NMDAR-dependent LTD (Sperow et al., 2012; Wang et al., 2006). Additionally, it has been previously reported upon acute modulation of PTEN its importance in synaptic plasticity, in which PTEN lipid phosphatase activity is needed specifically for NMDAR-dependent LTD, while it is not needed for LTP or mGluR-LTD (Jurado et al., 2010). Further work would be needed to completely understand how the modulation of LTD by PTEN changes neuronal function and cognition. Nevertheless our results suggest that PTEN is essential for modulating NMDAR-dependent LTD in the hippocampus and the amygdala (cortico-LA pathway), and that this modulation is done in a PDZ dependent-manner.

PTEN elevation orchestrates a synaptic switch impacting two of the most pronounced synaptic features of ASD: LTD and LTP. Recent studies defined ASD as synaptopathy (Lugo et al., 2014), since synaptic

malfunction appears in ASD models (Takeuchi et al., 2013), thus synaptic functioning may represent a potential clinical target for ASD pathology.

PTEN may control synaptic pruning and neuron proliferation

One of the most consistent findings in ASD mouse models is a dysregulation of LTD (Piochon et al., 2016). It has been proposed that LTD impairment and the excess of dendritic spines (Hutsler and Zhang, 2010; Kwon et al., 2006) reflect alterations in synaptic pruning mechanisms, and this prevents proper development of neuronal circuits. Therefore synaptic pruning deficits may represent a possible molecular mechanism underlying ASD pathology (Piochon et al., 2016). There are similarities in the molecular mechanisms involved in both LTD and synaptic pruning, as the requirement of NMDA receptor activation, AMPAR phosphorylation and calcium signaling, implying that synaptic pruning is also an activity-dependent event (Piochon et al., 2016). Thus, these similarities revealed that both processes share elements of their underlying molecular pathways. PTEN is needed for LTD (Jurado et al., 2010) and alteration in PTEN levels leads to hyperconnectivity, in *Pten* KO (Fraser et al., 2008; Huang et al., 2016; Kwon et al., 2006; Williams et al., 2015), and hypoconnectivity, in *Pten*^{tg} mice. Thus I hypothesize that PTEN may control synaptic pruning during brain development, and this leads to alterations in synaptic plasticity and brain circuitry in the adult.

PTEN is involved in brain development and it is proposed to take part in several processes, including neuronal proliferation, axonal and dendritic sprouting and synapse formation (Pardo and Eberhart, 2007), thus alterations in PTEN function could change synaptic growth during development, as well as the numbers of cells, either through initial overproduction or reduction of cell death, leading to changes in brain size. These findings underscore the importance of PTEN in brain development. The PTEN PDZ motif may also take part in these processes, but it would not be the critical region of PTEN implicated, since the effect on brain growth by altering PDZ interactions is considerably smaller than the one observed upon changes in protein levels (Kwon et al., 2006). On the other hand, the lack of LTD observed in the PTEN- Δ PDZ mice allows me to propose the hypothesis that the PDZ motif, by participating in LTD mechanisms, would be very important for synaptic pruning during development, which may rely on LTD-like mechanisms.

PTEN role on spatial and emotional learning and memory: hippocampal and amygdala function.

ASD mouse models with mutations in proteins of the PIP₃ pathway, including PTEN or the TSC1/2 complex, present generally more impaired spatial learning and fear memory than those carrying mutations within the synaptic proteins, such as Shank-1 or NRX (Ey et al., 2011). This observation highlights the regulatory role of the PIP₃ pathway controlling several cellular functions, including synaptic plasticity, essential for the consolidation of both types of memories; and the possible implication of this process in ASD pathology.

PTEN modulation of spatial memory.

A frequent comorbidity in PTEN-ASD patients is mental retardation (Garcia-Junco-Clemente and Golshani, 2014). *Pten* overexpression results with alterations in hippocampal volume and neuronal number in the CA1, probably due to the modulation of cell proliferation during brain development. These alterations are accompanied by a lower basal synaptic transmission, reduced synaptic density, and LTP impairment. Do these changes have consequences on hippocampal function?

I have checked spatial learning throughout different tests, revealing that short-term memory is normal, since the performance in the novel object location is intact. In contrast, long-term learning and memory, is impaired in *Pten^{tg}* mice since performance in the Barnes Maze is significantly impaired. Processes of LTP occur during learning, and are considered the cellular correlate of learning and memory (Andersen et al., 2007). Thus the impairments in hippocampal LTP of *Pten^{tg}* mice may contribute to the deficits in hippocampal-dependent learning.

Pten conditional deletion in ASD mouse models results in problems in spatial learning, accompanied by LTP impairment in the hippocampus (Kwon et al., 2006; Lugo et al., 2013; Sperow et al., 2012). This phenotype is similar to the observed in *Pten^{tg}* mice. Therefore it seems that any change in PTEN level results with synaptic and cognitive impairments. This observation suggests that appropriate Pten levels are needed for a correct learning ability.

Additionally, I have checked reversal spatial learning to measure the plasticity of the learning, which depends on the medial prefrontal cortex (mPFC)(de Bruin et al., 1994). Mental flexibility is altered in some forms of ASD, as patients present problems in the ability to adjust to changes in their routine (Ey et al., 2011; Hull et al., 2017). This type of learning is not altered in *Pten^{tg}* mice, suggesting that PTEN is not implicated in mPFC function on reversal spatial learning, further supporting the circuit-specific modulation done by PTEN.

PTEN modulation of fear memory

The morphology of amygdala neurons and their synaptic structure and function are altered in *Pten^{tg}* mice. To analyze amygdala function and the possible consequences of these alterations I have performed Pavlovian conditioning, the classical method to study the amygdala function, particularly, the LA, since this is the center of associative plasticity (Janak and Tye, 2015), in which we have previously detected synaptic alterations.

Previous results in PTEN-ASD mouse models are not consistent. Specifically, normal fear conditioning has been detected in two conditional Pten KO mice. This finding may arise from the fact that the deletion is restricted to the cortex and the hippocampus, and the amygdala is not affected (Kwon et al., 2006; Lugo et al., 2013). On the other hand, reduced freezing has been detected in *Pten^{+/-}*, but only in females (Clipperton-Allen and Page, 2014). These contrasting findings made it difficult to interpret the role of PTEN in fear conditioning.

My work reveals that the associative process of learning, in which the tone (CS) and the shock (US) is presented several times, is normal in *Pten^{tg}* mice, as freezing levels increased in the same manner as in WT mice, suggesting a normal amygdala-dependent learning in these animals. Contextual memory test (hippocampal- and amygdala-dependent) is not significantly altered, while in the cued fear conditioning test (amygdala-dependent) freezing is reduced, indicating deficient amygdala function in memory consolidation upon Pten overexpression. Finally, sensitivity to pain was normal in *Pten^{tg}* mice compared to their WT littermates. Normal pain sensitivity suggests that Pten does not modulate this feature, accordingly with previous results showing that pain sensitivity is not affected in Pten KO (Clipperton-Allen and Page, 2014) or Pten misslocalization (Tilot et al., 2014). Since PTEN abnormalities affect the function of the amygdala and given that the amygdala function is generally abnormal in ASD (Baron-Cohen et al., 2000), my findings may suggest that abnormal function of the amygdala may underlie some cognitive deficits seen in PTEN-ASD patients.

LA function impairment probably arise from alterations in the LA synapses, as sensory inputs converge into the LA neurons in response to CS-US pairings inducing LTP of excitatory synapses and conditioned freezing (Janak and Tye, 2015; Pape and Pare, 2010). This experience-dependent synaptic strengthening occur in both cortical and thalamic pathways of the LA (Janak and Tye, 2015; Lin et al., 2001), but the relative contributions of both inputs to fear conditioning it is not completely known, although cortical inputs may be more involved in the long-term storage of fear memories, as was shown through lesion-

based experiments (Sigurdsson et al., 2007). This data led me to hypothesize that the alteration observed in the cortical input of the LA in *Pten^{tg}* mice triggers cued fear conditioning impairment. My results support previous findings describing the requirement of the PIP₃ pathway for NMDAR-dependent LTP in the cortical input of the LA during fear memory consolidation (Lin et al., 2001). Thus, an overexpression of PTEN leads to a downregulation of the pathway, similarly to PI3K inhibition (Lin et al., 2001), impairing synaptic plasticity and memory consolidation in the LA.

PTEN modulation of region-specific brain activity during fear conditioning.

It has been shown previously that ASD patients present functional alterations in different areas of the brain, and that these functional alterations usually are related with region structural brain abnormalities (Ecker et al., 2015). Through PET scan, which detects neuronal activity associated with glucose uptake (Magistretti and Pellerin, 1999), we evaluated the basal activity in different areas of *Pten^{tg}* mice brains compared to their WT littermates. *Pten* overexpression results in lower activity in most cortical areas, including the frontal and auditory cortices, as well as the ventral hippocampus. Remarkably, the lower activity was region-specific as it was not detected in other areas, such as the amygdala and the thalamus, and it was even enhanced in the dorsal hippocampus. In support of this result, previous data correlate alterations in cortical areas (Bailey et al., 1998; Ecker et al., 2015) and in the hippocampus (Amaral et al., 2008) to ASD pathologies.

PET evaluation after fear conditioning training showed a general decreased activation of different areas of the brain. This reduced activation was more prominent in the frontal cortex and the amygdala of *Pten^{tg}* mice compared to WT, suggesting some failure in essential areas during fear memory acquisition. Interestingly, during retrieval, WT mice showed activation of specific areas compared to baseline values, particularly in those known to be involved in cued fear conditioning, including the amygdala (Fanselow, 2010), and may be regarded as a form of neuronal plasticity. In contrast, this plasticity associated to memory retrieval was reversed in *Pten^{tg}* mice, as key areas for fear conditioning showed diminished activity during the tone, including ventral hippocampus (vHPC), the amygdala and the thalamus (Fanselow, 2010; Kim and Jung, 2006). These experiments suggest that PTEN overexpression attenuates the learning-induced plasticity of key areas. This hypoactivation of the hippocampus and the amygdala may correlate with the impairment of LTP in these areas.

To summarize, *Pten^{tg}* mice exhibit severe deficits in cued fear conditioning, accompanied by impaired LTP in the lateral nucleus of the amygdala. In addition, critical brain areas fail to activate during the retrieval of this memory.

PTEN regulation of ASD behavior and related comorbidities.

Finally, I aim to determine whether the morphological and physiological alterations derived from PTEN modifications translate into broader effects on behavior in these mice, and whether these effects are restricted to specific domains or vulnerable neural systems. In this manner, I am trying to link specific neural alterations with the behavioral profile controlled by PTEN, and more specifically, with its PDZ-dependent function.

Autism diagnosis is based purely on behavioral criteria, as biological markers have not been identified yet (Silverman et al., 2010). Mice and humans present similarities in genetics, neuroanatomical, biochemical and electrophysiological features (Silverman et al., 2010), making the use of ASD mouse models a good approximation for understanding the mechanisms underlying behavioral alterations in humans. Nevertheless, for this approximation to be valid, a good design of mouse behavioral tasks related to human

ASD is essential. To address this point, I tested behaviors relevant to ASD core symptoms, including communication, repetitive/stereotyped behavior (grooming-like behavior) and social behavior (social recognition and novelty). In addition, I also assayed behaviors relevant to disorders commonly comorbid with ASD, including anxiety disorders (London, 2014) or motor difficulties (London, 2014; Tilot et al., 2015).

As a general health assessment approach I used the SHIRPA protocol (Irwin, 1968), which allowed me to determine that PTEN is not affecting general features of mice health, including hair state or body position. Locomotor activity was normal in these mice when checked through SHIRPA. This finding was confirmed with the open field test, in which *Pten^{tg}* mice showed normal locomotion. Thus, PTEN levels do not influence locomotion, in accordance with previous results obtained from PTEN-ASD mouse models (Amiri et al., 2012; Clipperton-Allen and Page, 2014; Kwon et al., 2006; Tilot et al., 2014).

Communication

During SHIRPA analysis I noticed a decreased vocalization in *Pten^{tg}* mice. To further evaluate the communication abilities in animals with PTEN alterations, I evaluated pup-isolated ultrasonic vocalizations (USV). This experimental approach may represent a conceptual analogue to the poor communication skills and delayed language that appears in ASD patients (Wöhr et al., 2011). In mice, USV serves as an important communicative function in coordinating mother-pup interactions, as USV calls elicit maternal search and retrieval behavior (Wöhr et al., 2011). Alterations in this behavior has been previously described in ASD-mouse models, typically displaying overall reduced USV levels (Wöhr et al., 2011; Young et al., 2010)(Mosienko et al., 2015).

In addition, it has been shown that dams can distinguish between different types of USV, with higher preference for calls of higher duration (>30ms)(Ehret and Haack, 1981), lower frequency (Smith and C., 1976) and louder intensity (Wöhr et al., 2008b), indicating that acoustic parameters affect the communicative value of isolation-induced USV (Wöhr et al., 2011). Present results indicate that *Pten* overexpression leads to an overall reduced communicative value, including lower duration calls (20-30 ms) and lower mean peak amplitude, compared to their WT littermates. Conversely, PTEN-ΔPDZ homozygous and heterozygous mice present similar values of acoustic parameters when compared to their WT littermates. I only observed an effect when comparing the response of homozygous PTEN-ΔPDZ pups from dams with different genotype. Specifically, pups from homozygous mothers presented higher number of calls and with increased frequency than those from heterozygous mothers. This result could indicate a difference in maternal care, as it seems that pup's genotype did not influence USV emission. Therefore, it seems that PTEN PDZ-binding motif is not necessary for early communication function, but it could be influencing maternal care behavior. It has been shown that call frequency solely depends on pup genotype, whereas early environmental factors lead to changes in call number and call amplitude (Wöhr et al., 2008b).

Additionally, USV is influenced by anxiety, and can be modulated by anxiogenic and anxiolytic drugs (Wöhr et al., 2008b). Specifically, anxiolytic compounds reduce the number of calls (Benton and Nastiti, 1988; Nastiti et al., 1991); and pup-isolated USV is a good predictor of adult anxiety-related behavior (Wöhr and Schwarting, 2008). Therefore, the reduction of anxiety-like behavior detected in *Pten^{tg}* mice could be reflected in their USV. In agreement with this hypothesis, PTEN-ΔPDZ mice have normal anxiety levels and displayed normal USV. Nevertheless, it is important to keep in mind that the anxiety state of the pup does not depend only in the pup genotype, but it is also affected by maternal care (Wöhr and Schwarting, 2008).

USV alterations could also reflect an impairment in development, as pup vocalization represents a sensitive marker of alterations in neurobehavioral development (Wöhr et al., 2008b) resulting in ASD (Kanner, 1943). This is consistent with the observation that characteristics of acoustic calls are controlled by a number of genes, particularly those involved in brain development, as it is the case of PTEN (Wöhr et al., 2008b).

In conclusion, my results show a general decrease in the call parameters in *Pten^{tg}* mice, suggesting that early communication ability is reduced by PTEN overexpression, probably due to the decreased anxiety or due to developmental alterations. On the other hand, I propose that the PTEN PDZ interactions are not implicated in USV or in anxiety behavior, but they may be controlling maternal care behavior.

Sociability

Finally, sociability, a core behavior altered in most of ASD mouse models (Ey et al., 2011; Hulbert and Jiang, 2015), was examined in both transgenic PTEN mouse lines. I detected a prosocial behavior in *Pten^{tg}* mice and an impaired social behavior in PTEN-ΔPDZ mice. Heterozygous PTEN-ΔPDZ mice show normal sociability, suggesting that one copy of WT-PTEN is sufficient for normal social behavior. Sociability is a critical component on a PTEN-ASD mouse models, which has been shown to be impaired in *Pten* deleted mutants (Amiri et al., 2012; Kwon et al., 2006; Lugo et al., 2014) and *Pten^{+/-}* mice (Clipperton-Allen and Page, 2014; Huang et al., 2016; Page et al., 2009). Previous studies and my results with *Pten^{tg}* mice suggest that sociability is modulated bidirectionally by PTEN. In addition to social interaction, social memory has also been described to be altered in *Pten* KO mice (Nse-Cre; *Pten^{loxP/loxP}*) (Kwon et al., 2006) and *Pten^{+/-}* mice (Clipperton-Allen and Page, 2014). In contrast, I did not detect changes in social memory for *Pten^{tg}* or PTEN-ΔPDZ mice, suggesting that this behavior is not altered upon PTEN overexpression nor controlled by the PDZ binding motif.

Clinical data suggest a significant link between anxiety and social interaction, with a high rate of comorbidity between high anxiety and ASD (London, 2014) and common pathological mechanisms (Allsop et al., 2014). Therefore, it is worth discussing both behaviors together. Anxiety is defined as a heightened state of arousal and vigilance that occurs in the absence of immediate threat (Allsop et al., 2014). Two brain circuits have been proposed to control both behaviors: the BLA projections to the vHPC (BLA-vHPC)(Allsop et al., 2014) and to the mPFC(Felix-Ortiz et al., 2015) (BLA-mPFC), with robust and reciprocal connections between the circuits. In the present work an increased in sociability is presented with a decrease in anxiety in *Pten^{tg}* mice. This is in accordance with the finding that the inhibition of the activity of the BLA projections to the vHPC or to the mPFC reduces anxiety and increases sociability. Thus, the decreased activation of these areas in *Pten^{tg}* mice, as seen by PET scan, could explain the alterations in both anxiety and sociability.

Nevertheless, there is not always a coincidence between social deficits and alterations in anxiety, suggesting these two forms of behavior also engage differential mechanisms. Thus, while *Pten* KO mouse model (Nse-Cre; *Pten^{loxP/loxP}*) show both social deficits and increased anxiety-like behavior (Kwon et al., 2006), other models show social deficits with no changes in anxiety-like behaviors (Amiri et al., 2012) or even decreased anxiety-like behavior (Clipperton-Allen and Page, 2014; Lugo et al., 2014). Indeed, I have observed that PTEN-ΔPDZ mice present impaired social behavior, but normal anxiety. These results support the notion of independent mechanisms that govern sociability and anxiety; in addition, these data reveal the specific implication of PTEN PDZ interactions for modulating social (but not anxiety-like) behavior.

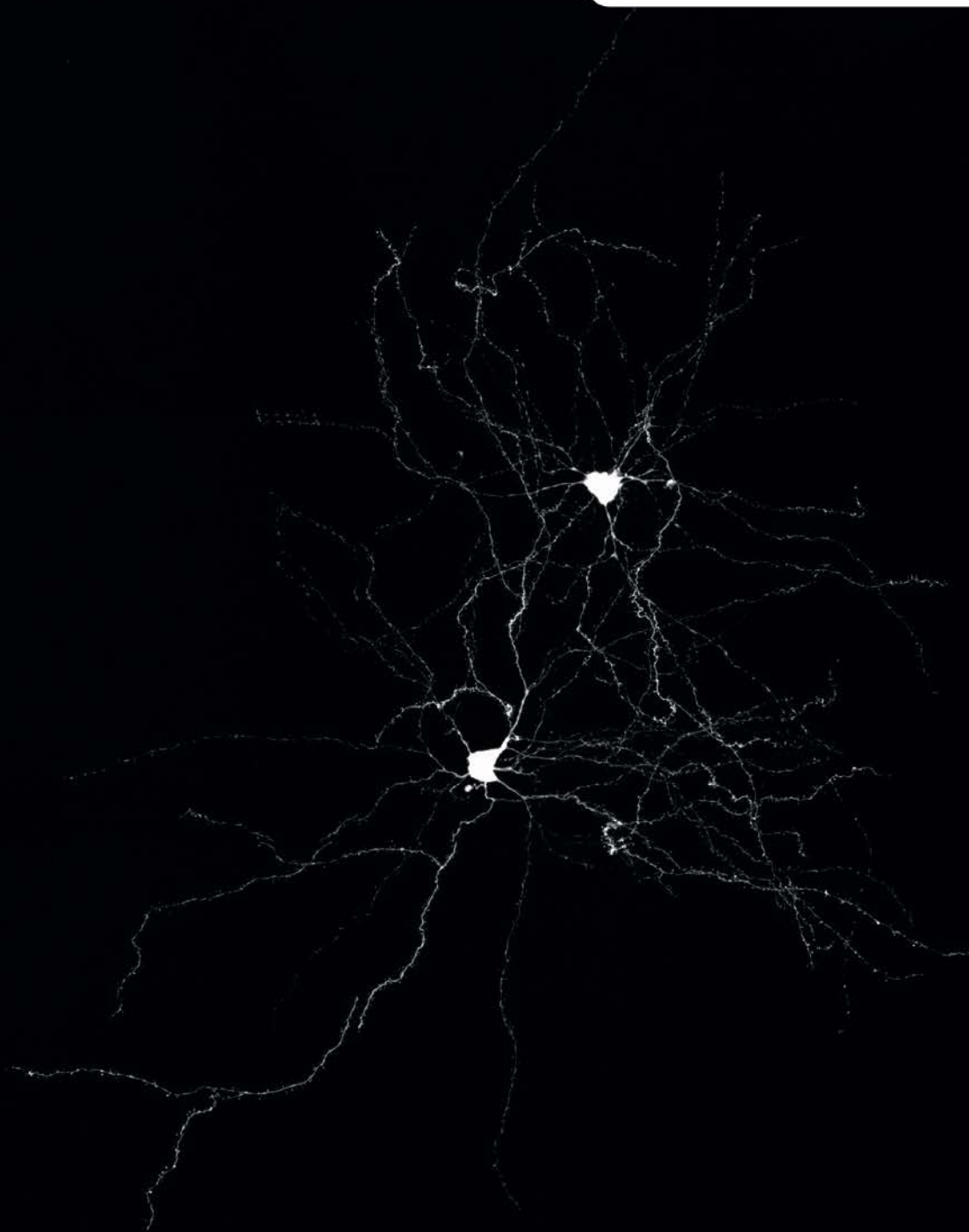
In addition to the amygdala-cortical projections, the reciprocal circuit that involves projections from the mPFC to the BLA has been proposed to be essential for the processing of social information and autism pathophysiology (Huang et al., 2016). Thus, dysregulated mTORC1 signaling in *Pten^{+/-}* mice during development leads to mPFC-BLA hyperconnectivity, accompanied by impaired social behavior (Huang et al., 2016), suggesting a relationship between sociability and the cortical input to the amygdala. This interpretation is in good agreement with my data on *Pten^{tg}* amygdala activity, which not only present a reduction in glucose uptake induced by activity, but also a shift into synaptic depression in the cortical input, as assessed by electrophysiological recordings. This is also supported by my results with the PTEN-ΔPDZ mice, which develop alterations in these synapses as well as impaired social behavior.

Thus, summarizing previous literature and the present data, I propose that cortico-amygdala activity is essential for social behavior, and it can be modulated in a bidirectional manner by PTEN expression levels.

The involvement of PTEN PDZ interactions for the control of social behavior is also intriguing. One interpretation is that PTEN location via interactions with its PDZ domain is essential for social behavior. Indeed, previous studies showed that altering PTEN nuclear/cytoplasmic localization affects social motivation differently from the *Pten* KO mouse (*Pten*^{m3/m4} mice (Tilot et al., 2014)). In the case of PTEN PDZ interactions, these have been shown to be particularly important for NMDAR-dependent LTD by controlling the synaptic localization of PTEN (Jurado et al., 2010). These results suggest that PTEN modification of sociability could be a consequence of LTD dysregulation. This interpretation is consistent with the fact that most of the ASD mouse models present impaired LTD (Piochon et al., 2016). In fact, I have also observed this correlation in a bidirectional manner with *Pten*^{tg} and PTEN-ΔPDZ mice. Thus, lack of PDZ motif results in impaired sociability and reduced cortico-LA LTD, whereas *Pten* overexpression leads to enhanced sociability and cortico-LA LTD. This observation suggests that there is a bidirectional modulation of sociability through PTEN PDZ-dependent regulation of NMDAR-dependent LTD in the cortical input of the amygdala. This hypothesis is also supported by the impairment in sociability and in LTD observed in VPA-induced ASD-like-model in the same circuit (Wu et al., 2016).

In conclusion, although it is challenging to relate mouse behavior to human behavior, at least I can confirm that *Pten* modification is sufficient to cause social deficits. Understanding the molecular basis for the bi-directional regulation of sociability could serve to develop therapeutic strategies for the treatment or prevention of ASD. Nevertheless, this will require a careful understanding of the mechanisms involved in the changes in sociability and cognition, and the definition of the time windows in which successful manipulations of sociability can be performed.

Conclusions





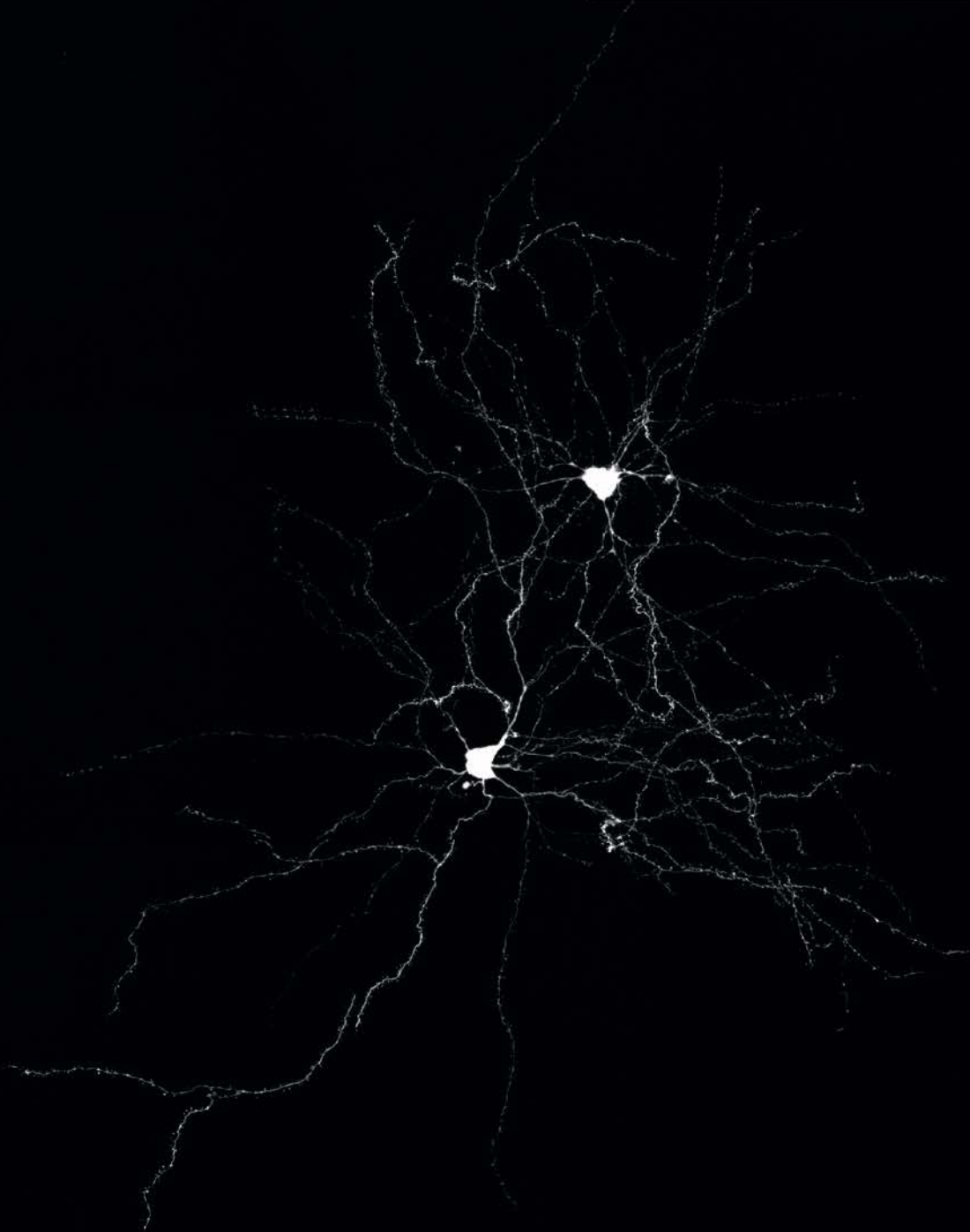
Conclusions:

1. PTEN expression level is a major factor to determine brain and hippocampal volume, with higher PTEN expression leading to smaller brain volume (microcephaly). PTEN interactions with PDZ proteins have a lower but significant influence. Impairment of these interactions leads to macrocephaly.
2. PTEN expression also determines overall neuronal growth, with higher expression leading to reduced dendritic arborization, synapse density and PSD size in lateral amygdala neurons. Synaptic density, but not PSD size, is also reduced in stratum radiatum of the hippocampus. Synapse density or PSD size are not strongly influenced by PTEN PDZ interactions.
3. PTEN expression levels and PDZ interactions have differential effects on synaptic transmission depending on the neuronal circuit considered. PTEN overexpression leads to depression of basal transmission in the CA3-CA1 and the thalamic-LA synapses, with no significant effect on cortico-LA synapses. Impairment of PDZ interactions does not affect basal transmission in the hippocampal or cortico-LA circuits, but depressed basal synaptic transmission of the thalamic-LA synapses.
4. As for synaptic plasticity, CA3-CA1 and cortico-LA synapses behave similarly, in the sense that increased PTEN levels impair LTP and PTEN PDZ interactions are required for NMDAR-dependent LTD. In addition, cortico-LA synapses displayed enhanced LTD upon PTEN overexpression. Synaptic plasticity is not altered by these manipulations in the thalamic-LA circuit.
5. PTEN overexpression impairs long-term spatial learning and memory in hippocampal-dependent tasks (Barnes maze) and reduces cued fear conditioning (amygdala-dependent).
6. Impaired fear memory consolidation upon PTEN overexpression is accompanied by hypoactivation of key brain regions during fear conditioning, as monitored by PET.
7. PTEN overexpression leads to impaired communication ability, with a decreased signal value of ultrasonic vocalizations. PTEN-PDZ interactions affect ultrasonic vocalizations depending on maternal genotype.
8. Anxiety is reduced by increased PTEN levels, independently from PDZ interactions.
9. Social interaction is enhanced by increased PTEN levels, and requires PTEN PDZ interactions.
10. Therefore, we can establish a bidirectional correlation between NMDAR-dependent LTD in cortico-LA synapses and social behavior. Thus, manipulations that reduce LTD (removal of PTEN-PDZ interactions) impair sociability. And conversely, manipulations that enhance LTD (PTEN overexpression) lead to enhanced sociability.

Conclusiones:

1. El nivel de expresión de PTEN es un factor importante para la determinación del volumen del cerebro y del hipocampo, observándose que la sobreexpresión de PTEN conduce a un menor volumen cerebral (microcefalia). La interacción de PTEN con proteínas PDZ tiene una menor pero significativa influencia en este aspecto, dado que la ausencia de estas interacciones da lugar a macrocefalia.
2. El nivel de expresión de PTEN también determina el crecimiento neuronal, dado que la sobreexpresión da lugar a la reducción del árbol dendrítico, de la densidad de las sinapsis y del tamaño de dichas sinapsis en las neuronas principales del núcleo lateral de la amígdala (AL). La densidad sináptica también se encuentra reducida en el hipocampo, pero no el tamaño de las sinapsis. Por otro lado, la modulación de la densidad de las sinapsis no depende de las interacciones PDZ, aunque sí tienen un pequeño efecto sobre el tamaño de dichas sinapsis.
3. Los niveles de expresión de PTEN y sus interacciones PDZ tienen un efecto diferencial en la transmisión sináptica, dependiendo del circuito neuronal considerado. La sobreexpresión de PTEN da lugar a una depresión de la transmisión sináptica en las sinapsis CA3-CA1 y talámico-AL, pero no afecta a las sinapsis establecidas entre la vía cortical y el núcleo lateral de la amígdala. La alteración de las interacciones PDZ sólo modifica la transmisión basal en la vía talámica de la AL.
4. En cuanto a la plasticidad sináptica, las sinapsis CA3-CA1 y cortico-LA se comportan de forma similar, en el sentido de que un aumento en los niveles de PTEN altera la LTP y que sus interacciones dependientes del motivo PDZ son necesarias para la LTD dependiente de receptores NMDA. Además, las sinapsis cortico-LA mostraron un aumento en la LTD debido a la sobreexpresión de PTEN. La plasticidad sináptica no se encuentra alterada por estas manipulaciones en el circuito talámico-LA.
5. La sobreexpresión de PTEN perjudica el aprendizaje espacial y la memoria a largo plazo en las tareas dependientes del hipocampo (laberinto de Barnes) y reduce el aprendizaje asociativo del condicionamiento del miedo, dependiente de la amígdala.
6. La consolidación de la memoria del miedo deteriorada por la sobreexpresión de PTEN se acompaña de una menor activación de las regiones cerebrales clave para el condicionamiento del miedo, monitorizado mediante PET.
7. La sobreexpresión de PTEN conduce al deterioro de la capacidad de comunicación de las crías, con una disminución general del valor de las vocalizaciones ultrasónicas. Las interacciones PDZ afectan las vocalizaciones ultrasónicas dependiendo del genotipo materno.
8. La ansiedad se encuentra reducida debido a los niveles de PTEN, y esta modulación resulta ser independientemente de las interacciones PDZ.
9. La interacción social se ve aumentada por el aumento de los niveles de PTEN, y requiere de las interacciones PDZ.
10. Por lo tanto, podemos establecer una correlación bidireccional entre la LTD dependiente de NMDAR en las sinapsis cortico-LA y el comportamiento social. De esta forma, las manipulaciones que reducen la LTD (eliminación de las interacciones PDZ) perjudican la sociabilidad, mientras que las manipulaciones que mejoran LTD (sobreexpresión de PTEN) conducen a una mayor sociabilidad.

Bibliography



A

- Adhikari, A. (2014). Distributed circuits underlying anxiety. *Front. Behav. Neurosci.* *8*, 112.
- Al-Khouri, A.M., Ma, Y., Togo, S.H., Williams, S., and Mustelin, T. (2005). Cooperative phosphorylation of the tumor suppressor phosphatase and tensin homologue (PTEN) by casein kinases and glycogen synthase kinase 3beta. *J. Biol. Chem.* *280*, 35195–35202.
- Alessi, D.R., Andjelkovic, M., Caudwell, B., Cron, P., Morrice, N., Cohen, P., and Hemmings, B.A. (1996). Mechanism of activation of protein kinase B by insulin and IGF-1. *EMBO J.* *15*, 6541–6551.
- Allsop, S.A., Vander Weele, C.M., Wichmann, R., Tye, K.M., Belzung, C., and Francois Rabelais, U. (2014). Optogenetic insights on the relationship between anxiety-related behaviors and social deficits.
- Amaral, D.G., Schumann, C.M., and Nordahl, C.W. (2008). Neuroanatomy of autism. *Trends Neurosci.* *31*, 137–145.
- Amiri, A., Cho, W., Zhou, J., Birnbaum, S.G., Sinton, C.M., McKay, R.M., and Parada, L.F. (2012). Pten Deletion in Adult Hippocampal Neural Stem/Progenitor Cells Causes Cellular Abnormalities and Alters Neurogenesis. *J. Neurosci.* *32*, 5880–5890.
- Andersen, P., Morris, R., Amaral, D., Bliss, T., and O’Keefe, J. (2007). *The Hippocampus Book* (Oxford University Press).
- Anderson, G.M. (2015). Autism biomarkers: challenges, pitfalls and possibilities. *J. Autism Dev. Disord.* *45*, 1103–1113.
- Angoa-Pérez, M., Kane, M.J., Briggs, D.I., Francescutti, D.M., and Kuhn, D.M. (2013). Marble Burying and Nestlet Shredding as Tests of Repetitive, Compulsive-like Behaviors in Mice. *J. Vis. Exp.* 50978.
- Arendt, K.L., Royo, M., Fernández-Monreal, M., Knafo, S., Petrok, C.N., Martens, J.R., and Esteban, J. a (2010). PIP3 controls synaptic function by maintaining AMPA receptor clustering at the postsynaptic membrane. *Nat. Neurosci.* *13*, 36–44.
- Arendt, K.L., Benoist, M., Lario, A., Draffin, J.E., Munoz, M., and Esteban, J.A. (2014). PTEN counteracts PIP3 upregulation in spines during NMDA-receptor-dependent long-term depression. *J. Cell Sci.* *127*, 5253–5260.
- Assini, F.L., Duzzioni, M., and Takahashi, R.N. (2009). Object location memory in mice: pharmacological validation and further evidence of hippocampal CA1 participation. *Behav. Brain Res.* *204*, 206–211.
- Auclair, N., Otani, S., Soubrie, P., and Crepel, F. (2000). Cannabinoids modulate synaptic strength and plasticity at glutamatergic synapses of rat prefrontal cortex pyramidal neurons. *J. Neurophysiol.* *83*, 3287–3293.

B

- Babiec, W.E., Guglietta, R., Jami, S.A., Morishita, W., Malenka, R.C., and O’Dell, T.J. (2014). Ionotropic NMDA receptor signaling is required for the induction of long-term depression in the mouse hippocampal CA1 region. *J. Neurosci.* *34*, 5285–5290.
- Bai, J., Trinh, T.L.H., Chuang, K.-H., and Qiu, A. (2012). Atlas-based automatic mouse brain image segmentation revisited: model complexity vs. image registration. *Magn. Reson. Imaging* *30*, 789–798.
- Bailey, A., Luthert, P., Dean, A., Harding, B., Janota, I., Montgomery, M., Rutter, M., and Lantos, P. (1998). A clinicopathological study of autism. *Brain* 889–905.

- Barnes, C.A. (1979). Memory deficits associated with senescence: a neurophysiological and behavioral study in the rat. *J. Comp. Physiol. Psychol.* *93*, 74–104.
- Baron-Cohen, S. (2002). The extreme male brain theory of autism. *Trends Cogn. Sci.* *6*, 248–254.
- Baron-Cohen, S., Ring, H.A., Bullmore, E.T., Wheelwright, S., Ashwin, C., and Williams, S.C. (2000). The amygdala theory of autism. *Neurosci. Biobehav. Rev.* *24*, 355–364.
- Benton, D., and Nastiti, K. (1988). The influence of psychotropic drugs on the ultrasonic calling of mouse pups. *Psychopharmacology (Berl)*. *95*, 99–102.
- Berridge, M.J. (2009). Inositol trisphosphate and calcium signalling mechanisms. *Biochim. Biophys. Acta - Mol. Cell Res.* *1793*, 933–940.
- Bishop, W.R., Pachter, J.A., and Pai, J.K. (1992). Regulation of phospholipid hydrolysis and second messenger formation by protein kinase C. *Adv. Enzyme Regul.* *32*, 177–192.
- Bleuler, E. (1951). *Organization and pathology of thought: Selected sources* (NY: Columbia University Press).
- Bliss, T. V, and Lomo, T. (1973). Long-lasting potentiation of synaptic transmission in the dentate area of the anaesthetized rabbit following stimulation of the perforant path. *J. Physiol.* *232*, 331–356.
- Blitzer, R.D. (2005). Teaching resources. Long-term potentiation: mechanisms of induction and maintenance. *Sci. STKE* *2005*, tr26.
- Bonifant, C.L., Kim, J.-S., and Waldman, T. (2007). NHERFs, NEP, MAGUKs, and more: interactions that regulate PTEN. *J. Cell. Biochem.* *102*, 878–885.
- Boosani, C.S., and Agrawal, D.K. (2013). PTEN modulators: a patent review. *Expert Opin. Ther. Pat.* *23*, 569–580.
- Bourgeron, T. (2009). A synaptic trek to autism. *Curr. Opin. Neurobiol.* *19*, 231–234.
- Bredt, D.S., and Nicoll, R.A. (2003). AMPA receptor trafficking at excitatory synapses. *Neuron* *40*, 361–379.
- Brose, N., O'Connor, V., and Skehel, P. (2010). Synaptopathy: dysfunction of synaptic function? *Biochem. Soc. Trans.* *38*, 443–444.
- Brown, R.E., and Milner, P.M. (2003). The legacy of Donald O. Hebb: more than the Hebb Synapse. *Nat. Rev. Neurosci.* *4*, 1013–1019.
- Brown, T.H., Chapman, P.F., Kairiss, E.W., and Keenan, C.L. (1988). Long-term synaptic potentiation. *Science* *242*, 724–728.
- de Bruin, J.P., Sánchez-Santed, F., Heinsbroek, R.P., Donker, A., and Postmes, P. (1994). A behavioural analysis of rats with damage to the medial prefrontal cortex using the Morris water maze: evidence for behavioural flexibility, but not for impaired spatial navigation. *Brain Res.* *652*, 323–333.
- Buxbaum, J.D., Cai, G., Chaste, P., Nygren, G., Goldsmith, J., Reichert, J., Anckarsäter, H., Rastam, M., Smith, C.J., Silverman, J.M., et al. (2007). Mutation screening of the PTEN gene in patients with autism spectrum disorders and macrocephaly. *Am. J. Med. Genet. B. Neuropsychiatr. Genet.* *144B*, 484–491.

C

- C. V. Howard, M.G.R. (1998). *Unbiased Stereology: Three-Dimensional Measurement in Microscopy*. By C. V. HOWARD and M. G. REID. (Pp. xviii+246; illustrated; f19.95 paperback; ISBN 1 85996 071 5.) Oxford: BIOS. 1998. (BIOS Scientific Publishers).

Campbell, R.B., Liu, F., and Ross, A.H. (2003). Allosteric Activation of PTEN Phosphatase by Phosphatidylinositol 4,5-Bisphosphate. *J. Biol. Chem.* *278*, 33617–33620.

Cantley, L.C. (2002). The Phosphoinositide 3-Kinase Pathway. *Science* (80-). *296*.

Caroni, P., Donato, F., and Muller, D. (2012). Structural plasticity upon learning: regulation and functions. *Nat. Rev. Neurosci.* *13*, 478–490.

Castellucci, V., Pinsker, H., Kupfermann, I., and Kandel, E.R. (1970). Neuronal mechanisms of habituation and dishabituation of the gill-withdrawal reflex in *Aplysia*. *Science* *167*, 1745–1748.

Chen, J., Yu, S., Fu, Y., and Li, X. (2014). Synaptic proteins and receptors defects in autism spectrum disorders. *Front. Cell. Neurosci.* *8*, 276.

Chen, Y., Huang, W.-C., Sejourne, J., Clipperton-Allen, A.E., and Page, D.T. (2015). Pten Mutations Alter Brain Growth Trajectory and Allocation of Cell Types through Elevated β -Catenin Signaling. *J. Neurosci.* *35*, 10252–10267.

Chow, D.K., Groszer, M., Pribadi, M., Machniki, M., Carmichael, S.T., Liu, X., and Trachtenberg, J.T. (2009). Laminar and compartmental regulation of dendritic growth in mature cortex. *Nat. Neurosci.* *12*, 116–118.

Clipperton-Allen, A.E., and Page, D.T. (2014). Pten haploinsufficient mice show broad brain overgrowth but selective impairments in autism-relevant behavioral tests. *Hum. Mol. Genet.* *23*, 3490–3505.

Clipperton-Allen, A.E., and Page, D.T. (2015). Decreased aggression and increased repetitive behavior in *Pten* haploinsufficient mice. *Genes, Brain Behav.* *14*, 145–157.

Cohen, P., Alessi, D.R., and Cross, D.A.. (1997). PDK1, one of the missing links in insulin signal transduction? ¹. *FEBS Lett.* *410*, 3–10.

Crawley, J.N. (2004a). Designing mouse behavioral tasks relevant to autistic-like behaviors. *Ment. Retard. Dev. Disabil. Res. Rev.* *10*, 248–258.

Crawley, J.N. (2004b). Designing mouse behavioral tasks relevant to autistic-like behaviors. *Ment. Retard. Dev. Disabil. Res. Rev.* *10*, 248–258.

D

Deacon, R. (2012). Assessing burrowing, nest construction, and hoarding in mice. *J. Vis. Exp.* e2607.

Deacon, R.M.J. (2006a). Assessing nest building in mice. *Nat. Protoc.* *1*, 1117–1119.

Deacon, R.M.J. (2006b). Assessing nest building in mice. *Nat. Protoc.* *1*, 1117–1119.

Domin, J., and Waterfield, M.D. (1997). Using structure to define the function of phosphoinositide 3-kinase family members. *FEBS Lett.* *410*, 91–95.

Dunwiddie, T., and Lynch, G. (1978). Long-term potentiation and depression of synaptic responses in the rat hippocampus: localization and frequency dependency. *J. Physiol.* *276*, 353–367.

E

Ecker, C., Bookheimer, S.Y., and Murphy, D.G.M. (2015). Neuroimaging in autism spectrum disorder: brain structure and function across the lifespan. *Lancet Neurol.* *14*, 1121–1134.

Ehret, G., and Haack, B. (1981). Categorical perception of mouse pup ultrasound by lactating females. *Naturwissenschaften* 68, 208–209.

Esteban, J.A. (2003). AMPA Receptor Trafficking: A Road Map for Synaptic Plasticity. *Mol. Interv.* 3, 375–385.

Ey, E., Leblond, C.S., and Bourgeron, T. (2011). Behavioral Profiles of Mouse Models for Autism Spectrum Disorders. 5–16.

F

Fanselow, M.S. (2010). From contextual fear to a dynamic view of memory systems. *Trends Cogn. Sci.* 14, 7–15.

Fanselow, M.S., and Dong, H.-W. (2010). Are the Dorsal and Ventral Hippocampus Functionally Distinct Structures? *Neuron* 65, 7–19.

Fanselow MS, G.G. (2003). Amygdala, Fear and Memory. *Ann N Y Acad Sci. Apr*, 125–134.

Fayard, E., Xue, G., Parcellier, A., Bozulic, L., and Hemmings, B.A. (2010). Protein Kinase B (PKB/Akt), a Key Mediator of the PI3K Signaling Pathway. In *Current Topics in Microbiology and Immunology*, pp. 31–56.

Felix-Ortiz, A.C., and Tye, K.M. (2014). Amygdala inputs to the ventral hippocampus bidirectionally modulate social behavior. *J. Neurosci.* 34, 586–595.

Felix-Ortiz, A.C., Beyeler, A., Seo, C., Leppla, C.A., Wildes, C.P., and Tye, K.M. (2013). BLA to vHPC inputs modulate anxiety-related behaviors. *Neuron* 79, 658–664.

Felix-Ortiz, A.C., Burgos-Robles, A., Bhagat, N.D., Leppla, C.A., and Tye, K.M. (2015). Bidirectional modulation of anxiety-related and social behaviors by amygdala projections to the medial prefrontal cortex. *Neuroscience*.

Fields, C., and Glazebrook, J.F. (2017). Disrupted development and imbalanced function in the global neuronal workspace: a positive-feedback mechanism for the emergence of ASD in early infancy. *Cogn. Neurodyn.* 11, 1–21.

Fox, G.B., Fan, L., Levasseur, R.A., and Faden, A.I. (1998). Effect of Traumatic Brain Injury on Mouse Spatial and Nonspatial Learning in the Barnes Circular Maze. *J. Neurotrauma* 15.

FOX, G.B., FAN, L., LeVASSEUR, R.A., and FADEN, A.I. (1998). Effect of Traumatic Brain Injury on Mouse Spatial and Nonspatial Learning in the Barnes Circular Maze. *J. Neurotrauma* 15, 1037–1046.

Fraser, M.M., Zhu, X., Kwon, C.-H., Uhlmann, E.J., Gutmann, D.H., and Baker, S.J. (2004). Pten loss causes hypertrophy and increased proliferation of astrocytes in vivo. *Cancer Res.* 64, 7773–7779.

Fraser, M.M., Bayazitov, I.T., Zakharenko, S.S., and Baker, S.J. (2008). Phosphatase and tensin homolog, deleted on chromosome 10 deficiency in brain causes defects in synaptic structure, transmission and plasticity, and myelination abnormalities. *Neuroscience* 151, 476–488.

Frazier, T.W., Youngstrom, E.A., Hardan, A.Y., Georgiades, S., Constantino, J.N., and Eng, C. (2015). Quantitative autism symptom patterns recapitulate differential mechanisms of genetic transmission in single and multiple incidence families. *Mol. Autism* 6, 58.

G

Gallagher, M., and Chiba, A.A. (1996). The amygdala and emotion. *Curr. Opin. Neurobiol.* 6, 221–227.

Garcia-Junco-Clemente, P., and Golshani, P. (2014). PTEN: A master regulator of neuronal structure, function, and plasticity. *Commun. Integr. Biol.* 7, e28358.

Gaskill, B.N., Karas, A.Z., Garner, J.P., and Pritchett-Corning, K.R. (2013). Nest Building as an Indicator of Health and Welfare in Laboratory Mice. *J. Vis. Exp.* 51012.

Georgescu, M.M., Kirsch, K.H., Akagi, T., Shishido, T., and Hanafusa, H. (1999). The tumor-suppressor activity of PTEN is regulated by its carboxyl-terminal region. *Proc. Natl. Acad. Sci. U. S. A.* 96, 10182–10187.

Goshen, I., Brodsky, M., Prakash, R., Wallace, J., Gradinaru, V., Ramakrishnan, C., and Deisseroth, K. (2011). Dynamics of Retrieval Strategies for Remote Memories. *Cell* 147, 678–689.

Gregorian, C., Nakashima, J., Dry, S.M., Nghiemphu, P.L., Smith, K.B., Ao, Y., Dang, J., Lawson, G., Mellinghoff, I.K., Mischel, P.S., et al. (2009). PTEN dosage is essential for neurofibroma development and malignant transformation. *Proc. Natl. Acad. Sci.* 106, 19479–19484.

Griffin, A.L. (2015). Role of the thalamic nucleus reuniens in mediating interactions between the hippocampus and medial prefrontal cortex during spatial working memory. *Front. Syst. Neurosci.* 9, 29.

Gross, C. (2016). Defective phosphoinositide metabolism in autism. *J. Neurosci. Res.*

Groszer, M., Erickson, R., Scripture-Adams, D.D., Lesche, R., Trumpp, A., Zack, J.A., Kornblum, H.I., Liu, X., and Wu, H. (2001). Negative Regulation of Neural Stem/Progenitor Cell Proliferation by the Pten Tumor Suppressor Gene in Vivo. *Science* (80-). 294, 2186–2189.

Gunaydin, L.A., Grosenick, L., Finkelstein, J.C., Kauvar, I.V., Fenno, L.E., Adhikari, A., Lammel, S., Mirzabekov, J.J., Airan, R.D., Zalocusky, K.A., et al. (2014). Natural Neural Projection Dynamics Underlying Social Behavior. *Cell* 157, 1535–1551.

Gundersen, H.J., Jensen, E.B., Kiêu, K., and Nielsen J (1999). The efficiency of systematic sampling in stereology--reconsidered. *J. Microsc.* 193, 199–211.

H

Harris, K.M., and Kirov, S.A. (1999). Dendrites are more spiny on mature hippocampal neurons when synapses are inactivated. *Nat. Neurosci.* 2, 878–883.

Harris, K.M., and Weinberg, R.J. (2012). Ultrastructure of Synapses in the Mammalian Brain. *Cold Spring Harb. Perspect. Biol.* 4, a005587–a005587.

Haws, M.E., Jaramillo, T.C., Espinosa, F., J. Widman, A., Stuber, G.D., Sparta, D.R., Tye, K.M., Russo, S.J., Parada, L.F., Stavarache, M., et al. (2014). PTEN knockdown alters dendritic spine/protrusion morphology, not density. *J. Comp. Neurol.* 522, 1171–1190.

Hazlett, H.C., Gu, H., Munsell, B.C., Kim, S.H., Styner, M., Wolff, J.J., Elison, J.T., Swanson, M.R., Zhu, H., Botteron, K.N., et al. (2017). Early brain development in infants at high risk for autism spectrum disorder. *Nature* 542, 348–351.

Hebb, D.O. (Donald O. (2002). *The organization of behavior : a neuropsychological theory* (L. Erlbaum Associates).

Hitti, F.L., and Siegelbaum, S.A. (2014a). The hippocampal CA2 region is essential for social memory. *Nature* 508, 88–92.

Hitti, F.L., and Siegelbaum, S.A. (2014b). The hippocampal CA2 region is essential for social memory. *Nature* 508, 88–92.

Hodakoski, C., Hopkins, B.D., Barrows, D., Mense, S.M., Keniry, M., Anderson, K.E., Kern, P.A., Hawkins, P.T., Stephens, L.R., and Parsons, R. (2014). Regulation of PTEN inhibition by the pleckstrin homology domain of P-REX2 during insulin signaling and glucose homeostasis. *Proc. Natl. Acad. Sci. U. S. A.* 111, 155–160.

Hoksbergen, R., ter Laak, J., Rijk, K., van Dijkum, C., and Stoutjesdijk, F. (2005). Post-Institutional Autistic Syndrome in Romanian adoptees. *J. Autism Dev. Disord.* 35, 615–623.

Holtmaat, A., and Svoboda, K. (2009). Experience-dependent structural synaptic plasticity in the mammalian brain. *Nat. Rev. Neurosci.* 10, 647–658.

Hooper, C., Markevich, V., Plattner, F., Killick, R., Schofield, E., Engel, T., Hernandez, F., Anderton, B., Rosenblum, K., Bliss, T., et al. (2007). Glycogen synthase kinase-3 inhibition is integral to long-term potentiation. *Eur. J. Neurosci.* 25, 81–86.

Hopkins, B.D., Hodakoski, C., Barrows, D., Mense, S.M., and Parsons, R.E. (2014). PTEN function: the long and the short of it. *Trends Biochem. Sci.* 39, 183–190.

Horne, E.A., and Dell'Acqua, M.L. (2007). Phospholipase C Is Required for Changes in Postsynaptic Structure and Function Associated with NMDA Receptor-Dependent Long-Term Depression. *J. Neurosci.* 27.

Huang, J., Yan, J., Zhang, J., Zhu, S., Wang, Y., Shi, T., Zhu, C., Chen, C., Liu, X., Cheng, J., et al. (2012). SUMO1 modification of PTEN regulates tumorigenesis by controlling its association with the plasma membrane. *Nat. Commun.* 3, 911.

Huang, W.-C., Chen, Y., and Page, D.T. (2016). Hyperconnectivity of prefrontal cortex to amygdala projections in a mouse model of macrocephaly/autism syndrome. *Nat. Commun.* 7, 13421.

Hulbert, S.W., and Jiang, Y. (2015). Monogenic Mouse Models of Autism Spectrum Disorders: Common Mechanisms and Missing Links. *Neuroscience*.

Hull, J. V., Jacokes, Z.J., Torgerson, C.M., Irimia, A., and Van Horn, J.D. (2017). Resting-State Functional Connectivity in Autism Spectrum Disorders: A Review. *Front. Psychiatry* 7, 205.

Humeau, Y., Herry, C., Kemp, N., Shaban, H., Fourcaudot, E., Bissière, S., and Lüthi, A. (2005). Dendritic Spine Heterogeneity Determines Afferent-Specific Hebbian Plasticity in the Amygdala. *Neuron* 45, 119–131.

Hutsler, J.J., and Zhang, H. (2010). Increased dendritic spine densities on cortical projection neurons in autism spectrum disorders. *Brain Res.* 1309, 83–94.

I

Ikenoue, T., Inoki, K., Zhao, B., and Guan, K.-L. (2008). PTEN Acetylation Modulates Its Interaction with PDZ Domain. *Cancer Res.* 68, 6908–6912.

Irwin, S. (1968). Comprehensive observational assessment: Ia. A systematic, quantitative procedure for assessing the behavioral and physiologic state of the mouse. *Psychopharmacologia* 13, 222–257.

J

Jamain, S., Radyushkin, K., Hammerschmidt, K., Granon, S., Boretius, S., Varoquaux, F., Ramanantsoa, N., Gallego, J., Ronnenberg, A., Winter, D., et al. (2008). Reduced social interaction and ultrasonic communication in a mouse model of monogenic heritable autism. *Proc. Natl. Acad. Sci. U. S. A.* 105, 1710–1715.

Janak, P.H., and Tye, K.M. (2015). From circuits to behaviour in the amygdala. *Nature* 517, 284–292.

Jenkinson, M., and Smith, S. (2001). A global optimisation method for robust affine registration of brain images. *Med. Image Anal.* 5, 143–156.

Jurado, S., Benoist, M., Lario, A., Knafo, S., Petrok, C.N., and Esteban, J. a (2010). PTEN is recruited to the postsynaptic terminal for NMDA receptor-dependent long-term depression. *EMBO J.* *29*, 2827–2840.

Juranek, J., Filipek, P.A., Berenji, G.R., Modahl, C., Osann, K., and Spence, M.A. (2006). Association between amygdala volume and anxiety level: magnetic resonance imaging (MRI) study in autistic children. *J. Child Neurol.* *21*, 1051–1058.

K

Kandel, E.R. (1997). Genes, synapses, and long-term memory. *J. Cell. Physiol.* *173*, 124–125.

Kanner, L. (1943). Autistic disturbances of affective contact. *Pathology*.

Kauer, J.A., and Malenka, R.C. (2007). Synaptic plasticity and addiction. *Nat. Rev. Neurosci.* *8*, 844–858.

Kim, E., and Sheng, M. (2004). PDZ domain proteins of synapses. *Nat. Rev. Neurosci.* *5*, 771–781.

Kim, J.J., and Jung, M.W. (2006). Neural circuits and mechanisms involved in Pavlovian fear conditioning: a critical review. *Neurosci. Biobehav. Rev.* *30*, 188–202.

Knafo, S., Venero, C., Merino-Serrais, P., Feraud-Espinosa, I., Gonzalez-Soriano, J., Ferrer, I., Santpere, G., and DeFelipe, J. (2009). Morphological alterations to neurons of the amygdala and impaired fear conditioning in a transgenic mouse model of Alzheimer's disease. *J. Pathol.* *219*, 41–51.

Knafo, S., Sánchez-Puelles, C., Palomer, E., Delgado, I., Draffin, J.E., Mingo, J., Wahle, T., Kaleka, K., Mou, L., Pereda-Perez, I., et al. (2016). PTEN recruitment controls synaptic and cognitive function in Alzheimer's models. *Nat. Neurosci.* *19*, 443–453.

Komada, M., Takao, K., and Miyakawa, T. (2008). Elevated Plus Maze for Mice. *J. Vis. Exp.* e1088–e1088.

Kwon, C.-H., Zhu, X., Zhang, J., Knoop, L.L., Tharp, R., Smeyne, R.J., Eberhart, C.G., Burger, P.C., and Baker, S.J. (2001). Pten regulates neuronal soma size: a mouse model of Lhermitte-Duclos disease. *Nat. Genet.* *29*, 404–411.

Kwon, C.-H., Luikart, B.W., Powell, C.M., Zhou, J., Matheny, S. a, Zhang, W., Li, Y., Baker, S.J., and Parada, L.F. (2006). Pten regulates neuronal arborization and social interaction in mice. *Neuron* *50*, 377–388.

L

Lázaro, M.T., and Golshani, P. (2015). The utility of rodent models of autism spectrum disorders. *Curr. Opin. Neurol.* *28*, 103–109.

LeDoux, J.E. (2000). Emotion circuits in the brain. *Annu. Rev. Neurosci.* *23*, 155–184.

Lee, J.O., Yang, H., Georgescu, M.M., Di Cristofano, A., Maehama, T., Shi, Y., Dixon, J.E., Pandolfi, P., and Pavletich, N.P. (1999). Crystal structure of the PTEN tumor suppressor: implications for its phosphoinositide phosphatase activity and membrane association. *Cell* *99*, 323–334.

Lee, J.T., Shan, J., Zhong, J., Li, M., Zhou, B., Zhou, A., Parsons, R., and Gu, W. (2013). RFP-mediated ubiquitination of PTEN modulates its effect on AKT activation. *Cell Res.* *23*, 552–564.

Lee, S.-R., Yang, K.-S., Kwon, J., Lee, C., Jeong, W., and Rhee, S.G. (2002). Reversible Inactivation of the Tumor Suppressor PTEN by H₂O₂. *J. Biol. Chem.* *277*, 20336–20342.

Leslie, N.R., and Longy, M. (2016). Inherited PTEN mutations and the prediction of phenotype. *Semin. Cell Dev. Biol.* *52*, 30–38.

- Leslie, N.R., Gray, A., Pass, I., Orchiston, E.A., and Downes, C.P. (2000). Analysis of the cellular functions of PTEN using catalytic domain and C-terminal mutations: differential effects of C-terminal deletion on signalling pathways downstream of phosphoinositide 3-kinase. *Biochem. J.* *346 Pt 3*, 827–833.
- Leslie, N.R., Bennett, D., Gray, A., Pass, I., Hoang-Xuan, K., and Downes, C.P. (2001). Targeting mutants of PTEN reveal distinct subsets of tumour suppressor functions. *Biochem. J.* *357*, 427–435.
- Leslie, N.R., Bennett, D., Lindsay, Y.E., Stewart, H., Gray, A., and Downes, C.P. (2003). Redox regulation of PI 3-kinase signalling via inactivation of PTEN. *EMBO J.* *22*, 5501–5510.
- Levy, S.E., Giarelli, E., Lee, L.-C., Schieve, L.A., Kirby, R.S., Cunniff, C., Nicholas, J., Reaven, J., and Rice, C.E. (2010). Autism spectrum disorder and co-occurring developmental, psychiatric, and medical conditions among children in multiple populations of the United States. *J. Dev. Behav. Pediatr.* *31*, 267–275.
- Li, J., Yen, C., Liaw, D., Podsypanina, K., Bose, S., Wang, S.I., Puc, J., Miliareisis, C., Rodgers, L., McCombie, R., et al. (1997). PTEN, a putative protein tyrosine phosphatase gene mutated in human brain, breast, and prostate cancer. *Science* *275*, 1943–1947.
- Li, X., Aggarwal, M., Hsu, J., Jiang, H., and Mori, S. (2013). AtlasGuide: software for stereotaxic guidance using 3D CT/MRI hybrid atlases of developing mouse brains. *J. Neurosci. Methods* *220*, 75–84.
- Li, Z., Dong, X., Wang, Z., Liu, W., Deng, N., Ding, Y., Tang, L., Hla, T., Zeng, R., Li, L., et al. (2005). Regulation of PTEN by Rho small GTPases. *Nat. Cell Biol.* *7*, 399–404.
- Lin, C.-H., Yeh, S.-H., Lin, C.-H., Lu, K.-T., Leu, T.-H., Chang, W.-C., and Gean, P.-W. (2001). A Role for the PI-3 Kinase Signaling Pathway in Fear Conditioning and Synaptic Plasticity in the Amygdala. *Neuron* *31*, 841–851.
- Lister, R.G. (1987). The use of a plus-maze to measure anxiety in the mouse. *Psychopharmacology (Berl.)* *92*, 180–185.
- London, E.B. (2014). Categorical diagnosis: a fatal flaw for autism research? *Trends Neurosci.* *37*, 683–686.
- Lugo, J.N., Smith, G.D., Morrison, J.B., and White, J. (2013). Deletion of PTEN produces deficits in conditioned fear and increases fragile X mental retardation protein. *Learn. Mem.* *20*, 670–673.
- Lugo, J.N., Smith, G.D., Arbuckle, E.P., White, J., Holley, A.J., Floruta, C.M., Ahmed, N., Gomez, M.C., and Okonkwo, O. (2014). Deletion of PTEN produces autism-like behavioral deficits and alterations in synaptic proteins. *Front. Mol. Neurosci.* *7*, 27.
- Luikart, B.W., Schnell, E., Washburn, E.K., Bensen, A.L., Tovar, K.R., and Westbrook, G.L. (2011). Pten knockdown in vivo increases excitatory drive onto dentate granule cells. *J. Neurosci.* *31*, 4345–4354.
- ## M
- Maclean, P.D. (1952). Some psychiatric implications of physiological studies on frontotemporal portion of limbic system (visceral brain). *Electroencephalogr. Clin. Neurophysiol.* *4*, 407–418.
- Madden, D.R. (2002). ION CHANNEL STRUCTURE THE STRUCTURE AND FUNCTION OF GLUTAMATE RECEPTOR ION CHANNELS. *Nat. Rev. Neurosci.* *3*, 91–101.
- Magistretti, P.J., and Pellerin, L. (1999). Cellular mechanisms of brain energy metabolism and their relevance to functional brain imaging. *Philos. Trans. R. Soc. B Biol. Sci.* *354*, 1155–1163.
- Malenka, R.C., and Bear, M.F. (2004). LTP and LTD: an embarrassment of riches. *Neuron* *44*, 5–21.
- Malinow, R., and Malenka, R.C. (2002). AMPA RECEPTOR TRAFFICKING AND SYNAPTIC PLASTICITY. *Annu. Rev. Neurosci.* *25*, 103–126.

- Marchese, M., Conti, V., Valvo, G., Moro, F., Muratori, F., Tancredi, R., Santorelli, F.M., Guerrini, R., and Sicca, F. (2014). Autism-epilepsy phenotype with macrocephaly suggests PTEN, but not GLIALCAM, genetic screening. *BMC Med. Genet.* *15*, 26.
- Mathis, D.M., Furman, J.L., and Norris, C.M. (2011). Preparation of acute hippocampal slices from rats and transgenic mice for the study of synaptic alterations during aging and amyloid pathology. *J. Vis. Exp.*
- Meng, Z., Jia, L.-F., and Gan, Y.-H. (2016). PTEN activation through K163 acetylation by inhibiting HDAC6 contributes to tumour inhibition. *Oncogene* *35*, 2333–2344.
- Miller, S.J., Lou, D.Y., Seldin, D.C., Lane, W.S., and Neel, B.G. (2002). Direct identification of PTEN phosphorylation sites. *FEBS Lett.* *528*, 145–153.
- Moorehead, R.A., Hojilla, C. V., De Belle, I., Wood, G.A., Fata, J.E., Adamson, E.D., Watson, K.L.M., Edwards, D.R., and Khokha, R. (2003). Insulin-like growth factor-II regulates PTEN expression in the mammary gland. *J. Biol. Chem.* *278*, 50422–50427.
- Moretti, P., Bouwknicht, J.A., Teague, R., Paylor, R., and Zoghbi, H.Y. (2005). Abnormalities of social interactions and home-cage behavior in a mouse model of Rett syndrome. *Hum. Mol. Genet.* *14*, 205–220.
- Morris, R. (1984). Developments of a water-maze procedure for studying spatial learning in the rat. *J. Neurosci. Methods* *11*, 47–60.
- Moser, M.B., and Moser, E.I. (1998). Functional differentiation in the hippocampus. *Hippocampus* *8*, 608–619.
- Mosienko, V., Beis, D., Alenina, N., and Wöhr, M. (2015). Reduced isolation-induced pup ultrasonic communication in mouse pups lacking brain serotonin. *Mol. Autism* *6*, 13.
- Moy, S.S., Nadler, J.J., Perez, A., Barbaro, R.P., Johns, J.M., Magnuson, T.R., Piven, J., and Crawley, J.N. (2004). Sociability and preference for social novelty in five inbred strains: an approach to assess autistic-like behavior in mice. *Genes, Brain Behav.* *3*, 287–302.
- Mukaddes, N.M., Kilincaslan, A., Kucukyazici, G., Sevketoglu, T., and Tuncer, S. (2007). Autism in visually impaired individuals. *Psychiatry Clin. Neurosci.* *61*, 39–44.
- Munson, J., Dawson, G., Abbott, R., Faja, S., Webb, S.J., Friedman, S.D., Shaw, D., Artru, A., and Dager, S.R. (2006). Amygdalar Volume and Behavioral Development in Autism. *Arch. Gen. Psychiatry* *63*, 686.
- Murai, T., Okuda, S., Tanaka, T., and Ohta, H. (2007). Characteristics of object location memory in mice: Behavioral and pharmacological studies. *Physiol. Behav.* *90*, 116–124.
- Murcia, C.L., Gulden, F., and Herrup, K. (2005). A question of balance: a proposal for new mouse models of autism. *Int. J. Dev. Neurosci.* *23*, 265–275.

N

- Nabavi, S., Kessels, H.W., Alfonso, S., Aow, J., Fox, R., and Malinow, R. (2013). Metabotropic NMDA receptor function is required for NMDA receptor-dependent long-term depression. *Proc. Natl. Acad. Sci.* *110*, 4027–4032.
- Nastiti, K., Benton, D., and Brain, P.F. (1991). The effects of compounds acting at the benzodiazepine receptor complex on the ultrasonic calling of mouse pups. *Behav. Pharmacol.* *2*, 121–128.
- Nicoll, R.A., and Malenka, R.C. (1995). Contrasting properties of two forms of long-term potentiation in the hippocampus. *Nature* *377*, 115–118.
- Nimchinsky, E.A., Sabatini, B.L., and Svoboda, K. (2002). Structure and Function of Dendritic Spines. *Annu. Rev. Physiol.* *64*, 313–353.

Ning, K., Pei, L., Liao, M., Liu, B., Zhang, Y., Jiang, W., Mielke, J.G., Li, L., Chen, Y., El-Hayek, Y.H., et al. (2004). Dual neuroprotective signaling mediated by downregulating two distinct phosphatase activities of PTEN. *J. Neurosci.* *24*, 4052–4060.

Niswender, C.M., and Conn, P.J. (2010). Metabotropic Glutamate Receptors: Physiology, Pharmacology, and Disease. *Annu. Rev. Pharmacol. Toxicol.* *50*, 295–322.

O

Odriezola, L., Singh, G., Hoang, T., and Chan, A.M. (2007). Regulation of PTEN activity by its carboxyl-terminal autoinhibitory domain. *J. Biol. Chem.* *282*, 23306–23315.

Okumura, K., Mendoza, M., Bachoo, R.M., DePinho, R.A., Cavenee, W.K., and Furnari, F.B. (2006). PCAF Modulates PTEN Activity. *J. Biol. Chem.* *281*, 26562–26568.

Okuyama, T., Kitamura, T., Roy, D.S., Itoharu, S., and Tonegawa, S. (2016). Ventral CA1 neurons store social memory. *Science* (80-). *353*, 1536–1541.

Opazo, P., Watabe, A.M., Grant, S.G.N., and O’Dell, T.J. (2003). Phosphatidylinositol 3-kinase regulates the induction of long-term potentiation through extracellular signal-related kinase-independent mechanisms. *J. Neurosci.* *23*, 3679–3688.

Orrico, a, Galli, L., Buoni, S., Orsi, a, Vonella, G., and Sorrentino, V. (2009). Novel PTEN mutations in neurodevelopmental disorders and macrocephaly. *Clin. Genet.* *75*, 195–198.

Ortega-Molina, A., Efeyan, A., Lopez-Guadamillas, E., Muñoz-Martin, M., Gómez-López, G., Cañamero, M., Mulero, F., Pastor, J., Martinez, S., Romanos, E., et al. (2012). Pten Positively Regulates Brown Adipose Function, Energy Expenditure, and Longevity. *Cell Metab.* *15*, 382–394.

P

Page, D.T., Kuti, O.J., Prestia, C., and Sur, M. (2009). Haploinsufficiency for Pten and Serotonin transporter cooperatively influences brain size and social behavior. *Proc. Natl. Acad. Sci. U. S. A.* *106*, 1989–1994.

Di Paolo, G., and De Camilli, P. (2006). Phosphoinositides in cell regulation and membrane dynamics. *Nature* *443*, 651–657.

Pape, H.-C., and Pare, D. (2010). Plastic Synaptic Networks of the Amygdala for the Acquisition, Expression, and Extinction of Conditioned Fear. *Physiol. Rev.* *90*.

Pardo, C.A., and Eberhart, C.G. (2007). The neurobiology of autism. *Brain Pathol.* *17*, 434–447.

Passafaro, M., Pièch, V., and Sheng, M. (2001). Subunit-specific temporal and spatial patterns of AMPA receptor exocytosis in hippocampal neurons. *Nat. Neurosci.* *4*, 917–926.

Patel, L., Pass, I., Coxon, P., Downes, C.P., Smith, S.A., and Macphee, C.H. (2001). Tumor suppressor and anti-inflammatory actions of PPAR γ agonists are mediated via upregulation of PTEN. *Curr. Biol.* *11*, 764–768.

Paul, C., Schöberl, F., Weinmeister, P., Micale, V., Wotjak, C.T., Hofmann, F., and Kleppisch, T. (2008). Signaling through cGMP-dependent protein kinase I in the amygdala is critical for auditory-cued fear memory and long-term potentiation. *J. Neurosci.* *28*, 14202–14212.

Pêgo, J.M., Morgado, P., Pinto, L.G., Cerqueira, J.J., Almeida, O.F.X., and Sousa, N. (2008). Dissociation of the morphological correlates of stress-induced anxiety and fear. *Eur. J. Neurosci.* *27*, 1503–1516.

Peineau, S., Nicolas, C.S., Bortolotto, Z.A., Bhat, R. V., Ryves, W.J., Harwood, A.J., Dournaud, P., Fitzjohn, S.M., and Collingridge, G.L. (2009a). A systematic investigation of the protein kinases involved in NMDA receptor-dependent LTD: evidence for a role of GSK-3 but not other serine/threonine kinases. *Mol. Brain* 2, 22.

Peineau, S., Bradley, C., Taghibiglou, C., Doherty, A., Bortolotto, Z.A., Wang, Y.T., and Collingridge, G.L. (2009b). The role of GSK-3 in synaptic plasticity. *Br. J. Pharmacol.* 153, S428–S437.

Pellow, S., and Sandra, E. (1986). Anxiolytic and Anxiogenic Drug Effects on Exploratory Activity in an Elevated Plus-Maze : a Novel Test of Anxiety in the Rat. 24.

Piochon, C., Kano, M., and Hansel, C. (2016). LTD-like molecular pathways in developmental synaptic pruning. *Nat. Neurosci.* 19, 1299–1310.

Pun, R.Y.K., Rolle, I.J., LaSarge, C.L., Hosford, B.E., Rosen, J.M., Uhl, J.D., Schmeltzer, S.N., Faulkner, C., Bronson, S.L., Murphy, B.L., et al. (2012). Excessive Activation of mTOR in Postnatally Generated Granule Cells Is Sufficient to Cause Epilepsy. *Neuron* 75, 1022–1034.

R

Rácz, B., Blanpied, T.A., Ehlers, M.D., and Weinberg, R.J. (2004). Lateral organization of endocytic machinery in dendritic spines. *Nat. Neurosci.* 7, 917–918.

Rahdar, M., Inoue, T., Meyer, T., Zhang, J., Vazquez, F., and Devreotes, P.N. (2009). A phosphorylation-dependent intramolecular interaction regulates the membrane association and activity of the tumor suppressor PTEN. *Proc. Natl. Acad. Sci. U. S. A.* 106, 480–485.

Ram Venkataraman, G., O’Connell, C., Egawa, F., Kashef-Haghighi, D., and Wall, D.P. (2016). De novo mutations in autism implicate the synaptic elimination network. *Pac. Symp. Biocomput.* 22, 521–532.

Ramón y Cajal, S. (1909). *Histologie du système nerveux de l’homme & des vertébrés* (Paris: Paris: Maloine).

Rogers, D.C., Fisher, E.M.C., Brown, S.D.M., Peters, J., Hunter, A.J., and Martin, J.E. (1997). Commentary Behavioral and functional analysis of mouse phenotype: SHIRPA, a proposed protocol for comprehensive phenotype assessment. *Mamm Genome* 8, 711–713.

Rosenhall, U., Nordin, V., Sandström, M., Ahlsén, G., and Gillberg, C. (1999). Autism and hearing loss. *J. Autism Dev. Disord.* 29, 349–357.

Rutter, M., Andersen-Wood, L., Beckett, C., Bredenkamp, D., Castle, J., Groothues, C., Kreppner, J., Keaveney, L., Lord, C., and O’Connor, T.G. (1999). Quasi-autistic patterns following severe early global privation. English and Romanian Adoptees (ERA) Study Team. *J. Child Psychol. Psychiatry.* 40, 537–549.

Rutter, M., Kreppner, J., Croft, C., Murin, M., Colvert, E., Beckett, C., Castle, J., and Sonuga-Barke, E. (2007). Early adolescent outcomes of institutionally deprived and non-deprived adoptees. III. Quasi-autism. *J. Child Psychol. Psychiatry.* 48, 1200–1207.

S

Sambrook, J., and Russel, D.W. (2001). *Molecular Cloning. A Laboratory Manual* (Cold Spring Harbor Laboratory Press, Cold Spring Harbor, New York).

Sampedro, M.N., Bussineau, C.M., and Cotman, C.W. (1981). Postsynaptic density antigens: preparation and characterization of an antiserum against postsynaptic densities. *J. Cell Biol.* 90, 675–686.

- Sanders, S.J., He, X., Willsey, A.J., Ercan-Sencicek, A.G., Samocha, K.E., Cicek, A.E., Murtha, M.T., Bal, V.H., Bishop, S.L., Dong, S., et al. (2015). Insights into Autism Spectrum Disorder Genomic Architecture and Biology from 71 Risk Loci. *Neuron* 87, 1215–1233.
- Schumann, C.M. (2004). The Amygdala Is Enlarged in Children But Not Adolescents with Autism; the Hippocampus Is Enlarged at All Ages. *J. Neurosci.* 24, 6392–6401.
- Schumann, C.M., and Amaral, D.G. (2006). Stereological analysis of amygdala neuron number in autism. *J. Neurosci.* 26, 7674–7679.
- Scoville, W.B., and Milner, B. (1957). Loss of recent memory after bilateral hippocampal lesions. *J. Neurol. Neurosurg. Psychiatry* 20, 11–21.
- Sewell, G.D. (1970). Ultrasonic communication in rodents. *Nature* 227, 410.
- Sherrington, C.S. (1906). *The integrative action of the nervous system* (New York : Scribner).
- Shi, S.H., Hayashi, Y., Petralia, R.S., Zaman, S.H., Wenthold, R.J., Svoboda, K., and Malinow, R. (1999). Rapid spine delivery and redistribution of AMPA receptors after synaptic NMDA receptor activation. *Science* 284, 1811–1816.
- Sigurdsson, T., Doyère, V., Cain, C.K., and LeDoux, J.E. (2007). Long-term potentiation in the amygdala: A cellular mechanism of fear learning and memory. *Neuropharmacology* 52, 215–227.
- Silverman, J.L., Yang, M., Lord, C., and Crawley, J.N. (2010). Behavioural phenotyping assays for mouse models of autism. *Nat. Rev. Neurosci.* 11, 490–502.
- Smith, J.C., and C., J. (1976). Responses of adult mice to models of infant calls. *J. Comp. Physiol. Psychol.* 90, 1105–1115.
- Song, M.S., Salmena, L., Carracedo, A., Egia, A., Lo-Coco, F., Teruya-Feldstein, J., and Pandolfi, P.P. (2008). The deubiquitylation and localization of PTEN are regulated by a HAUSP-PML network. *Nature* 455, 813–817.
- Sperow, M., Berry, R.B., Bayazitov, I.T., Zhu, G., Baker, S.J., and Zakharenko, S.S. (2012). Phosphatase and tensin homologue (PTEN) regulates synaptic plasticity independently of its effect on neuronal morphology and migration. *J. Physiol.* 590, 777–792.
- Spinelli, L., Black, F.M., Berg, J.N., Eickholt, B.J., and Leslie, N.R. (2015). Functionally distinct groups of inherited PTEN mutations in autism and tumour syndromes. *J. Med. Genet.* 52, 128–134.
- Stambolic, V., Suzuki, A., de la Pompa, J.L., Brothers, G.M., Mirtsos, C., Sasaki, T., Ruland, J., Penninger, J.M., Siderovski, D.P., and Mak, T.W. (1998). Negative regulation of PKB/Akt-dependent cell survival by the tumor suppressor PTEN. *Cell* 95, 29–39.
- Stephens, L., Anderson, K., Stokoe, D., Erdjument-Bromage, H., Painter, G.F., Holmes, A.B., Gaffney, P.R., Reese, C.B., McCormick, F., Tempst, P., et al. (1998). Protein kinase B kinases that mediate phosphatidylinositol 3,4,5-trisphosphate-dependent activation of protein kinase B. *Science* 279, 710–714.
- Stiles, B., Groszer, M., Wang, S., Jiao, J., and Wu, H. (2004). PTENless means more. *Dev. Biol.* 273, 175–184.
- Sungur, A.Ö., Schwarting, R.K.W., and Wöhr, M. (2016). Early communication deficits in the *Shank1* knockout mouse model for autism spectrum disorder: Developmental aspects and effects of social context. *Autism Res.* 9, 696–709.

T

- Takeuchi, K., Gertner, M.J., Zhou, J., Parada, L.F., Bennett, M.V.L., and Zukin, R.S. (2013). Dysregulation of synaptic plasticity precedes appearance of morphological defects in a *Pten* conditional knockout mouse model of

autism. *Proc. Natl. Acad. Sci. U. S. A.* *110*, 4738–4743.

Tamguney, T., and Stokoe, D. (2007). New insights into PTEN. *J. Cell Sci.* *120*.

Tibarewal, P., Zilidis, G., Spinelli, L., Schurch, N., Maccario, H., Gray, A., Perera, N.M., Davidson, L., Barton, G.J., and Leslie, N.R. (2012). PTEN protein phosphatase activity correlates with control of gene expression and invasion, a tumor-suppressing phenotype, but not with AKT activity. *Sci. Signal.* *5*, ra18.

Tilot, A.K., Gaugler, M.K., Yu, Q., Romigh, T., Yu, W., Miller, R.H., Frazier, T.W., and Eng, C. (2014). Germline disruption of Pten localization causes enhanced sex-dependent social motivation and increased glial production. *Hum. Mol. Genet.* *23*, 3212–3227.

Tilot, A.K., Frazier, T.W., and Eng, C. (2015). Balancing Proliferation and Connectivity in PTEN-associated Autism Spectrum Disorder. *Neurotherapeutics* *12*, 609–619.

Tilot, A.K., Bebek, G., Niazi, F., Altemus, J.B., Romigh, T., Frazier, T.W., and Eng, C. (2016). Neural transcriptome of constitutional Pten dysfunction in mice and its relevance to human idiopathic autism spectrum disorder. *Mol. Psychiatry* *21*, 118–125.

Ting, J.T., Daigle, T.L., Chen, Q., and Feng, G. (2014). Acute brain slice methods for adult and aging animals: application of targeted patch clamp analysis and optogenetics. *Methods Mol Biol.* *1183*, 221–242.

Tolkacheva, T., and Chan, A.M. (2000). Inhibition of H-Ras transformation by the PTEN/MMAC1/TEP1 tumor suppressor gene. *Oncogene* *19*, 680–689.

Tordjman, S., Cohen, D., Coulon, N., Anderson, G.M., Botbol, M., and Roubertoux, P.L. (2017). Reframing autism as a behavioral syndrome and not a specific mental disorder: Perspectives from a literature review. *Neurosci. Biobehav. Rev.*

Torres, J., and Pulido, R. (2001). The tumor suppressor PTEN is phosphorylated by the protein kinase CK2 at its C terminus. Implications for PTEN stability to proteasome-mediated degradation. *J. Biol. Chem.* *276*, 993–998.

Trotman, L.C., Wang, X., Alimonti, A., Chen, Z., Teruya-Feldstein, J., Yang, H., Pavletich, N.P., Carver, B.S., Cordon-Cardo, C., Erdjument-Bromage, H., et al. (2007). Ubiquitination regulates PTEN nuclear import and tumor suppression. *Cell* *128*, 141–156.

V

Valiente, M., Andrés-Pons, A., Gomar, B., Torres, J., Gil, A., Tapparel, C., Antonarakis, S.E., and Pulido, R. (2005). Binding of PTEN to specific PDZ domains contributes to PTEN protein stability and phosphorylation by microtubule-associated serine/threonine kinases. *J. Biol. Chem.* *280*, 28936–28943.

Vanderver, A., Tonduti, D., Kahn, I., Schmidt, J., Medne, L., Vento, J., Chapman, K.A., Lanpher, B., Pearl, P., Gropman, A., et al. (2014). Characteristic brain magnetic resonance imaging pattern in patients with macrocephaly and *PTEN* mutations. *Am. J. Med. Genet. Part A* *164*, 627–633.

Vazquez, F., Ramaswamy, S., Nakamura, N., and Sellers, W.R. (2000). Phosphorylation of the PTEN tail regulates protein stability and function. *Mol. Cell. Biol.* *20*, 5010–5018.

Vazquez, F., Grossman, S.R., Takahashi, Y., Rokas, M. V., Nakamura, N., and Sellers, W.R. (2001). Phosphorylation of the PTEN tail acts as an inhibitory switch by preventing its recruitment into a protein complex. *J. Biol. Chem.* *276*, 48627–48630.

Virolle, T., Adamson, E.D., Baron, V., Birle, D., Mercola, D., Mustelin, T., and de Belle, I. (2001). The Egr-1 transcription factor directly activates PTEN during irradiation-induced signalling. *Nat. Cell Biol.* *3*, 1124–1128.

Vogel-Ciernia, A., Wood, M.A., Vogel-Ciernia, A., and Wood, M.A. (2014). Examining Object Location and Object Recognition Memory in Mice. In *Current Protocols in Neuroscience*, (Hoboken, NJ, USA: John Wiley & Sons, Inc.), p. 8.31.1-8.31.17.

W

Wang, X., Trotman, L.C., Koppie, T., Alimonti, A., Chen, Z., Gao, Z., Wang, J., Erdjument-Bromage, H., Tempst, P., Cordon-Cardo, C., et al. (2007). NEDD4-1 is a proto-oncogenic ubiquitin ligase for PTEN. *Cell* *128*, 129–139.

Wang, Y., Cheng, A., and Mattson, M.P. (2006). The PTEN phosphatase is essential for long-term depression of hippocampal synapses. *Neuromolecular Med.* *8*, 329–336.

Wenk, M.R., and De Camilli, P. (2004). Protein-lipid interactions and phosphoinositide metabolism in membrane traffic: insights from vesicle recycling in nerve terminals. *Proc. Natl. Acad. Sci. U. S. A.* *101*, 8262–8269.

Weston, M.C., Chen, H., and Swann, J.W. (2012). Multiple roles for mammalian target of rapamycin signaling in both glutamatergic and GABAergic synaptic transmission. *J. Neurosci.* *32*, 11441–11452.

Williams, C.A., Dagli, A., and Battaglia, A. (2008). Genetic disorders associated with macrocephaly. *Am. J. Med. Genet. Part A* *146A*, 2023–2037.

Williams, M.R., DeSpensa, T., Li, M., Gullledge, A.T., and Luikart, B.W. (2015). Hyperactivity of Newborn Pten Knock-out Neurons Results from Increased Excitatory Synaptic Drive. *J. Neurosci.* *35*, 943–959.

Wöhr, M., and Schwarting, R.K.W. (2008). Maternal care, isolation-induced infant ultrasonic calling, and their relations to adult anxiety-related behavior in the rat. *Behav. Neurosci.* *122*, 310–330.

Wöhr, M., Dahlhoff, M., Wolf, E., Holsboer, F., Schwarting, R.K.W., and Wotjak, C.T. (2008a). Effects of genetic background, gender, and early environmental factors on isolation-induced ultrasonic calling in mouse pups: an embryo-transfer study. *Behav. Genet.* *38*, 579–595.

Wöhr, M., Dahlhoff, M., Wolf, E., Holsboer, F., Schwarting, R.K.W., and Wotjak, C.T. (2008b). Effects of Genetic Background, Gender, and Early Environmental Factors on Isolation-Induced Ultrasonic Calling in Mouse Pups: An Embryo-Transfer Study. *Behav. Genet.* *38*, 579–595.

Wöhr, M., Rouillet, F.I., Hung, A.Y., Sheng, M., and Crawley, J.N. (2011). Communication impairments in mice lacking Shank1: reduced levels of ultrasonic vocalizations and scent marking behavior. *PLoS One* *6*, e20631.

Won, H., Mah, W., and Kim, E. (2013). Autism spectrum disorder causes, mechanisms, and treatments: focus on neuronal synapses. *Front. Mol. Neurosci.* *6*, 19.

Wu, H.-F., Chen, P.S., Chen, Y.-J., Lee, C.-W., Chen, I.-T., and Lin, H.-C. (2016). Alleviation of N-Methyl-d-Aspartate Receptor-Dependent Long-Term Depression via Regulation of the Glycogen Synthase Kinase-3 β Pathway in the Amygdala of a Valproic Acid-Induced Animal Model of Autism. *Mol. Neurobiol.*

X

Xia, D., Srinivas, H., Ahn, Y.-H., Sethi, G., Sheng, X., Yung, W.K.A., Xia, Q., Chiao, P.J., Kim, H., Brown, P.H., et al. (2007). Mitogen-activated protein kinase kinase-4 promotes cell survival by decreasing PTEN expression through an NF kappa B-dependent pathway. *J. Biol. Chem.* *282*, 3507–3519.

Xiong, Q., Oviedo, H. V, Trotman, L.C., and Zador, A.M. (2012). PTEN regulation of local and long-range connections in mouse auditory cortex. *J. Neurosci.* *32*, 1643–1652.

Y

Yang, E.-J., Ahn, S., Lee, K., Mahmood, U., and Kim, H.-S. (2016). Early Behavioral Abnormalities and Perinatal Alterations of PTEN/AKT Pathway in Valproic Acid Autism Model Mice. *PLoS One* *11*, e0153298.

Young, D.M., Schenk, A.K., Yang, S.-B., Jan, Y.N., and Jan, L.Y. (2010). Altered ultrasonic vocalizations in a tuberous sclerosis mouse model of autism. *Proc. Natl. Acad. Sci. U. S. A.* *107*, 11074–11079.

Yuste, R., Denk, W., Petralia, R.S., Zaman, S.H., Wenthold, R.J., Svoboda, K., and Malinow, R. (1995). Dendritic spines as basic functional units of neuronal integration. *Nature* *375*, 682–684.

Z

Zhang, X.C., Piccini, A., Myers, M.P., Van Aelst, L., and Tonks, N.K. (2012). Functional analysis of the protein phosphatase activity of PTEN. *Biochem. J.* *444*, 457–464.

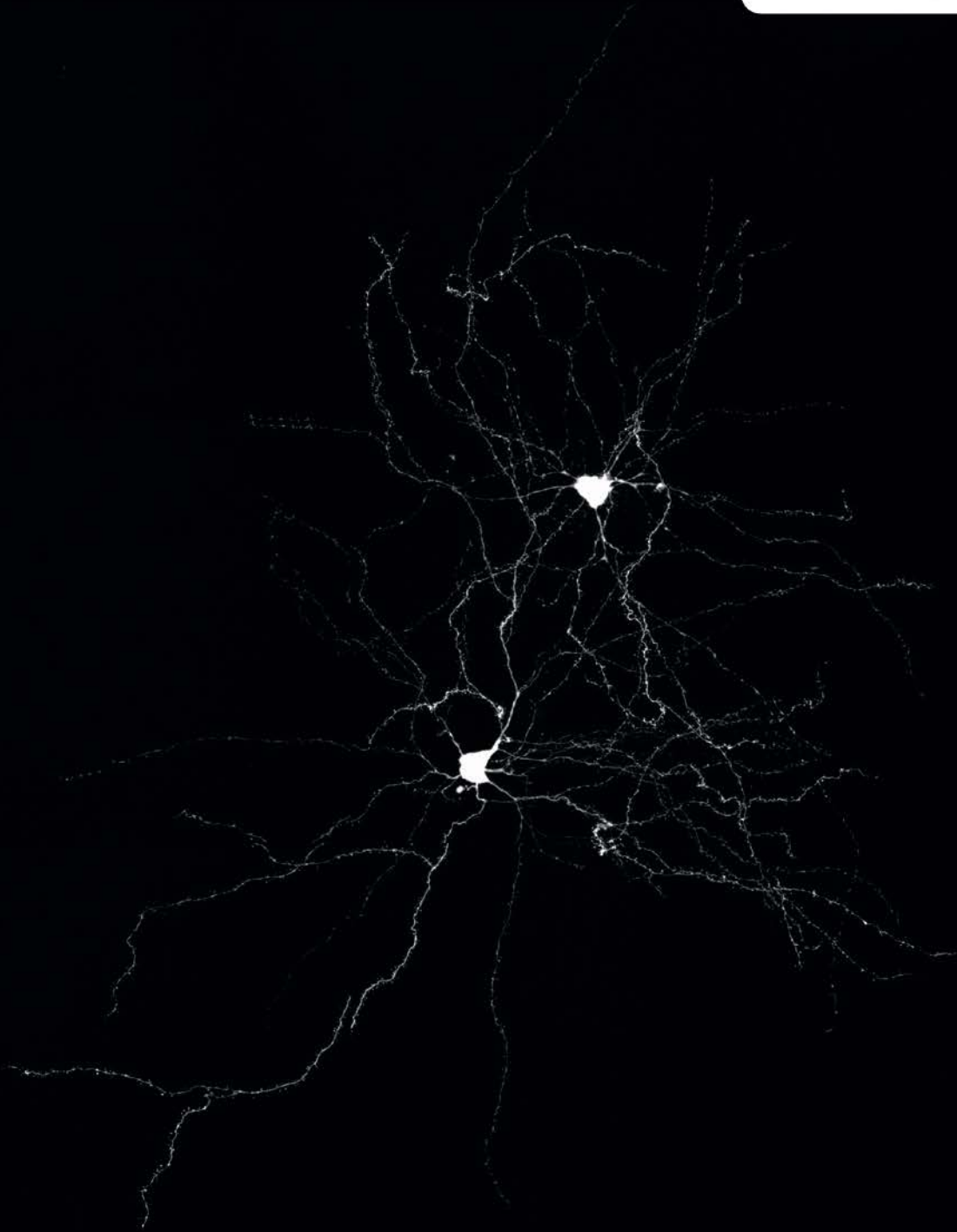
Zhou, J., and Parada, L.F. (2012). PTEN signaling in autism spectrum disorders. *Curr. Opin. Neurobiol.* 1–7.

Zhou, J., Blundell, J., Ogawa, S., Kwon, C.-H., Zhang, W., Sinton, C., Powell, C.M., and Parada, L.F. (2009). Pharmacological Inhibition of mTORC1 Suppresses Anatomical, Cellular, and Behavioral Abnormalities in Neural-Specific Pten Knock-Out Mice. *J. Neurosci.* *29*, 1773–1783.

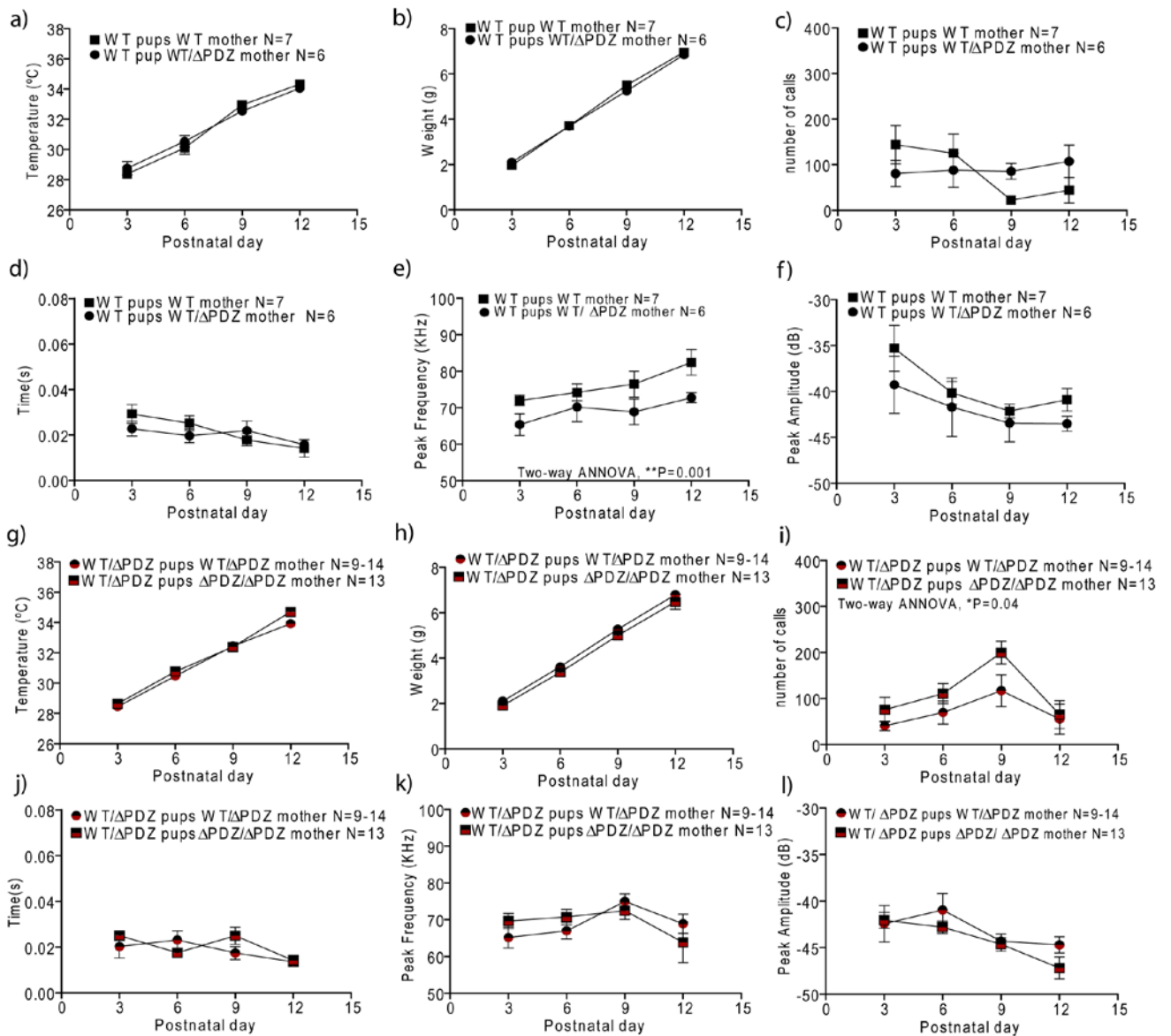
Zola-Morgan, S.M., and Squire, L.R. (1990). The primate hippocampal formation: evidence for a time-limited role in memory storage. *Science* *250*, 288–290.

Zschenderlein, C., Gebhardt, C., von Bohlen und Halbach, O., Kulisch, C., and Albrecht, D. (2011). Capsaicin-Induced Changes in LTP in the Lateral Amygdala Are Mediated by TRPV1. *PLoS One* *6*, e16116.

Annex I



Supplementary information



[Supplementary figure 1] Isolated induced ultrasonic vocalization (USV) from WT pups from WT and heterozygous WT/ΔPDZ mothers and heterozygous WT/ΔPDZ pups from heterozygous WT/ΔPDZ and homozygous ΔPDZ/ΔPDZ mothers. (a) Representation of the temperature of WT (a) and WT/ΔPDZ (g) pups right after the vocalization assessment was done. Weight of WT (b) and WT/ΔPDZ (h) pups observed each experimental day. Total number of USV emitted by WT (c) and WT/ΔPDZ (i) pups. Mean duration of USV emitted by WT (d) and WT/ΔPDZ (j) pups. Mean peak frequency of USV emitted by WT (e) and WT/ΔPDZ (k) pups. Mean peak amplitude of USV emitted by pups from WT (f) and WT/ΔPDZ (l) pups.

Table 1: Pten-ASD mouse models.

Mouse model	Genetic characteristics	Structural phenotype	Functional phenotype	Behavioral phenotype
Nse-Cre; Pten^{loxP/loxP}	Conditional Pten deletion in mature neurons from cortex and hippocampus (Kwon et al., 2006b)	Macrocephaly (Kwon et al., 2006a) Soma hypertrophy (Kwon et al., 2006a) Abnormal polarity (Kwon et al., 2006a) Axonal hypertrophy (Kwon et al., 2006a) ↑presynaptic vesicle number (Kwon et al., 2006a) Enlarge presynaptic terminals (Kwon et al., 2006a) Dendritic hypertrophy (Kwon et al., 2006a) ↑ Spine density (Kwon et al., 2006a) ↑ mushroom spine density (Williams et al., 2015) ↑ synapse proximity (Williams et al., 2015)	Electrophysiology: DG: 8-12 wks: ≈ BST, ≈ PPR, ↑LTP (TBS), no mGluR LTD (Takeuchi et al., 2013). 14-19 wks: ↑ BST, ↓ PPR, ↓LTP (TBS), no mGluR LTD (Takeuchi et al., 2013). 20-30 wks: ≈ BST, ≈ PPR, ↓LTP (TBS), no mGluR LTD (Takeuchi et al., 2013). CA3-CA1: 8-12 wks: ≈ BST, ≈ PPR, ↓ LTP (TBS), ↓ LTP (HFS), ≈ mGluR LTD (Takeuchi et al., 2013). 14-19 wks: ≈ BST, ≈ PPR, ↓LTP (TBS), ↓ LTP (HFS), ≈ mGluR LTD (Takeuchi et al., 2013). Seizures(Kwon et al., 2006a) ↑firing threshold(Williams et al., 2015) ↑action potentials peak frequencies and amplitude(Williams et al., 2015) ≈ IPSC(Williams et al., 2015) ↑EPSC amplitude(Williams et al., 2015) ↑ mEPSC amplitude and frequency(Williams et al., 2015)	↓sociability (Kwon et al., 2006a) ↓social memory (Kwon et al., 2006a) ↓ nest-building activity (Kwon et al., 2006a) ↓maternal care (Kwon et al., 2006a) ↓ sexual behavior (Kwon et al., 2006a) ↑ anxiety (Kwon et al., 2006a) ↓ Hippocampal-dependent learning (MWM) (Kwon et al., 2006a) ≈ Fear conditioning(Kwon et al., 2006a) ≈ Locomotion (Kwon et al., 2006a) ≈ Motor coordination (Kwon et al., 2006a) ↑Response to stimuli(Kwon et al., 2006a)
Pten^{+/-}	Pten haploinsufficiency. Deletion of exon 5 (core catalytic phosphatase domain) (Podsypanina et al., 1999)	Macrocephaly (Page et al., 2009)(Clipperton-Allen and Page, 2014) Soma hypertrophy (Layer V, somatosensory cortex) (Huang et al., 2016) Dendritic hypertrophy (Layer V, somatosensory cortex) (Huang et al., 2016) Hypertrophic neurons (mPFC) (Huang et al., 2016) CA1: ↓LTP, ↓NMDA-LTD mPFC-BLA axons ↑branching&synaptic boutons (Huang et al., 2016) ↑ Cell number but normal density in cerebral cortex(Chen et al., 2015)	mPFC-BLA hyperactivity in response to novel social stimulus (Huang et al., 2016) Electrophysiology: CA3-CA1: ≈BST, ↓PPF, ↓LTP(HFS), no NMDA-LTD (Wang et al., 2006). Low sociability (females)	↓ sociability and social memory(Clipperton-Allen and Page, 2014; Huang et al., 2016; Page et al., 2009) ↑ Repetitive behavior (Clipperton-Allen and Page, 2014, 2015) ↑ Depression-like behavior (males) (Clipperton-Allen and Page, 2014) ↓ Anxiety (Clipperton-Allen and Page, 2014) ↓ Fear conditioning (females) (Clipperton-Allen and Page, 2014) ≈ Locomotion (Clipperton-Allen and Page, 2014) ≈ Nociception (Clipperton-Allen and Page, 2014) ≈ Spatial working memory (Huang et al., 2016) ↓ Aggressive behavior (Clipperton-Allen and Page, 2015)

Mouse model	Genetic characteristics	Structural phenotype	Functional phenotype	Behavioral phenotype
Gfap-Cre; Pten^{loxP/loxP}	Conditional deletion in postmitotic cortical neurons, cerebellar granule cells and DG neurons (catalytic domain) (Backman et al., 2001; Fraser et al., 2004, 2008; Suzuki et al., 2001)	Macrocephaly (Backman et al., 2001; Fraser et al., 2004) Cerebellum displasia (Backman et al., 2001) ↑ astrocyte proliferation (Fraser et al., 2004) Celular hypertrophy (Fraser et al., 2004) ↑nuclear size (Fraser et al., 2008) ↑soma size (Backman et al., 2001; Fraser et al., 2008; Kwon et al., 2001) ↑dendritic size (Fraser et al., 2008) ↑axon size (Fraser et al., 2008) ↑spine density (Fraser et al., 2008) ↑PSD and presynaptic terminal size (Fraser et al., 2008) ↑number of presynaptic vesicles (Fraser et al., 2008) ↑mitochondria size (Fraser et al., 2008) ↑ribosomes number (Fraser et al., 2008)	Seizures, ataxia(Backman et al., 2001) Electrophysiology: CA3-CA1: ↓BST, ≈PPR, ↓LTP (HFS)(Fraser et al., 2008)	↓ sociability (Lugo et al., 2014a) ↓ repetitive behavior(Lugo et al., 2014a) Hyperactivity (Lugo et al., 2014a) ↓Anxiety (Lugo et al., 2014a) ≈ USV (Lugo et al., 2014a) ↓ Contextual fear conditioning (Lugo et al., 2013) ≈ Cued fear conditioning (Lugo et al., 2013) ≈ Novel odor discrimination (Lugo et al., 2014a)
Nestin-Cre;Pten^{loxP/loxP}	Pten deletion in hippocampal neural/stem progenitor cells (Amiri et al., 2012)	Macrocephaly (Amiri et al., 2012) Neuronal hypertrophy (GCL) (Amiri et al., 2012) Abnormal polarity (Amiri et al., 2012) Enlarge dendrites and axons (Amiri et al., 2012) ↑Neuronal proliferation and differentiation rate (Amiri et al., 2012)	Seizures (Amiri et al., 2012)	↓ sociability (Amiri et al., 2012) ≈ Locomotion (Amiri et al., 2012) ≈ Social olfactory behavior (Amiri et al., 2012) ≈ Reaction to sensory stimuli (Amiri et al., 2012) ≈ Anxiety (Amiri et al., 2012)
Pten^{m3m4}	Knock-in missense mutations in the exon 7 of Pten gene (affecting nuclear localization sequence-like) (Mester et al., 2011; Tilot et al., 2014)	Macrocephaly (Mester et al., 2011) ≈ neuron number (Tilot et al., 2014) ↑astrocytes and oligodendrocytes number (Tilot et al., 2014) ↑proliferation rate (Tilot et al., 2014) Neuron hypertrophy (Tilot et al., 2014) ≈dendritic diameter (Tilot et al., 2014) ↑neuroinflammatory response (reactive astrogliosis and microglial activation) (Tilot et al., 2014)		↑sociability (Tilot et al., 2014) ≈ social memory (Tilot et al., 2014) ≈ recognition memory (Tilot et al., 2014) ≈ locomotion (Tilot et al., 2014) ↓ balance (Tilot et al., 2014) ≈ motor learning (Tilot et al., 2014) ≈ anxiety (Tilot et al., 2014) ≈ nociception (Tilot et al., 2014)

Mouse model	Genetic characteristics	Structural phenotype	Functional phenotype	Behavioral phenotype
CamKIIα-Cre; Pten^{loxP/loxP}	Pten postnatal deletion in excitatory forebrain pyramidal neurons (Sperow et al., 2012; Tsien et al., 1996).	No changes (Sperow et al., 2012).	Electrophysiology: CA3-CA1: \approx AMPA/NMDAR, \approx mEPSCs, \approx BST, \approx PPR, \downarrow LTP(HFS), no NMDA-LTD (7-8 wks) (Sperow et al., 2012).	\downarrow Hippocampal-dependent learning (MWM) (Sperow et al., 2012).
CamKIIα-Cre; Pten^{loxP/+} (7 or 8 weeks)	Conditional forebrain pyramidal neurons deletion of Pten loxP/ loxP allele flanking exon 5 (encodes Pten's phosphatase domain) (Chow et al., 2009)	Dendritic hypertrophy (Pten ^{-/-}) (Chow et al., 2009) \approx spine density hypertrophy (Chow et al., 2009)	L2/3 pyramidal neurons in the mouse primary visual cortex: \downarrow intrinsic excitability (Garcia-Junco-Clemente et al., 2013) \uparrow SK _{Ca} conductance (Garcia-Junco-Clemente et al., 2013) \downarrow gain of visually evoked spike output (Garcia-Junco-Clemente et al., 2013)	

